Experimental Scrapie: Comparison of Pathology Following Oral and Other Parenteral Routes of Infection.

by
Barry Stewart

Submitted for the degree of
Doctor of Philosophy
in the faculty of Medicine, The University of Edinburgh.

December 1999.

for my family.

Declaration.

I declare that this thesis was composed by myself. The contributions of others to this work are clearly indicated.

Barry Stewart.

Acknowledgements

I would like to thank my supervisors, Drs Jan Fraser and James Ironside, not only for the opportunity to work on this project but for their unwavering support, patience and confidence throughout. They have both been a great source of motivation especially in the dark days of writing up where nothing seemed to flow and the end seemed a very long way off..

I am very grateful for the technical help I received from many quarters. In particular Bill Halliday, Bill Naillon and Ken Sutherland deserve my gratitude for their guidence in the often murky field of computerised image processing. Thanks also go to many of the staff at the Neuropathogenesis Unit for technical and social support. I would like to thank Dawn Drummond and Irene McConnell for their help and patience with regards to the animal work. Irene's ability to generate a population of mice in next to no time is a marvel of modern science.

Several people outwith the Neuropathogenesis Unit have always been willing to make themselves available for discussion or technical help. In particular thanks go to Martin Jeffery, for useful discussions and terrible jokes during this project and Chris Carter for technical advice, discussion and general support.

I owe my sanity to many of the friends I made in Edinburgh and to those people I would just like to say thank you. You know who you are. However, special mentions must go to Stephanie Collishaw, a valued friend and one time landlady, Neil Mabbott, owner of probably the strangest sense of humour I've ever come across, don't worry I'll keep an eye out for the flying lizards and to Aileen Chree who afforded me the opportunity of making a complete fool of myself in front of my colleagues on a regular basis around Christmas time. I wouldn't have missed it, though I fear I will.

I couldn't possibly have undertaken this project without the support of my family; mum, dad and David and Angela who seemed to make it all worthwhile. I am grateful for their help, support and for leaving well alone when the mood dictated.

Finally I have to thank the MRC for funding the project and Professor Moira Brown for allowing me the time to complete this manuscript.

Table Of Contents.

Abstract:

The aim of this project was to determine the effect that route of infection has on the incubation period and terminal pathology of experimental scrapie. Infection was established either by injection into the peritoneum or the *biceps femoralis* of the leg, or orally by administration of the agent with food. As a secondary study an experiment was devised to investigate the possible transport of scrapie infectivity in the central nervous system (CNS) of mice lacking a functional *prn-p* gene. The primary study was carried out using a combination of immunohistochemistry, histopathology and computerised image analysis. The study of agent transport was done by bioassay for reasons of sensitivity.

C57Bl mice were infected with ME7 scrapie by the routes described above and groups of animals were serially sacrificed at between 5 and 7 timepoints during the course of the disease. The timepoints were chosen so that tissues representative of early, mid and late/terminal infection could be collected for study. Specific antibodies were used to detect the presence of PrP and GFAP whilst vacuolation was detected by standard haematoxylin and eosin staining.

The results of this study indicate that the oral route of infection in experimental scrapie can be used to establish an infection with much more efficiency than has previously been reported. It is possible that the technique used to introduce the infection, by admixture with food as opposed to the more traditional gavage method is a significant factor in this increased efficiency.

Other important observations relate to the distribution and intensity of lesions in the brain following infection by each of the three routes examined. The distribution of vacuolation, PrP and GFAP following both muscular and peritoneal injection of infectivity are very similar; there are differences in the severity of the pathology such that intramuscular infection results in an advanced lesion but the distribution is almost identical. This is interesting considering how close together the

incubation periods for these two routes are. These observations are in stark contrast to the results seen following oral infection. Not only is the incubation period extended, the lesions are much more severe throughout the brain and the pattern of distribution is completely dissimilar from that seen in the animals infected by the other routes.

In the experiment to study the transport of infectivity in mice devoid of endogenous PrP the results suggest that some limited transport is possible. This is the result of a study using the projections of the optic nerve as a controlled system for assessing the transport of infectivity along defined neuroanatomical pathways.

In conclusion, the results of the work described in this thesis show that oral infection, at least in experimental systems, is a highly efficient route of infection that results in significantly more severe pathology than either the intramuscular or intraperitoneal routes. The efficiency of oral infection may have implications for human disease with reference to new variant CJD (nvCJD). Other results show that a limited degree of transport of infectivity may be possible in mice lacking a functional *prn-p* gene. This is the first time that this has been demonstrated.

Introduction.

1. Introduction.

Scrapie, a naturally occurring disease of sheep, and more rarely goats (MacKay and Smith, 1961), is the oldest member of a group of diseases known as the spongiform encephalopathies. This disease is endemic in Britain where its presence has been documented for over two hundred years (Comber as cited by McGowan, 1914). Scrapie has been reported in many other countries and has recently been found in countries that were earlier thought to be free of the disease such as Cyprus (Toumazos, 1988) and the former Yugoslavia (Knezevic and Jovanovic, 1986). It had been previously reported in the Antipodes (Parry, 1964) although these countries are now thought to be scrapie free (Foster and Hunter, 1998). Scrapie gets its name from the characteristic pruritus which results in the scraping that affected sheep display.

Other diseases of this group have been identified in a variety of animal species and in man. They share a characteristic spectrum of pathology that is the result of infection with a common type of agent. Pathology will be discussed in greater detail in section 1.3. Table 1 lists these scrapie-like diseases and the species affected by them.

1.1 History of Scrapie and the TSEs

Scrapie is transmissible: this was first demonstrated by Cuillé and Chelle and reported in works published between 1936 and 1942, reviewed by Pattison, 1988. Their studies involved the passage of spinal cord homogenate, obtained from scrapie affected sheep, to unaffected sheep by the intraocular (i.o.) route. Of nine animals experimentally infected two eventually succumbed to the disease after unusually long incubation periods of 16 and 23 months. This extended period between infection and onset of illness is now a recognised feature of this class of diseases. There was initially scepticism that, because of the long incubation period, transmission of the scrapie agent had occurred. However, this observation was inadvertently confirmed when several hundred sheep acquired the disease after being injected with a contaminated louping ill vaccine.

Disease.	Species Affected.	Reference.
Scrapie	sheep/goats	McGowan, 1922.
Transmissible Mink Encephalopathy (TME)	farmed mink	Hartsough and Burger, 1965.
Chronic Wasting Disease (CWD)	mule deer, elk, white tailed deer	Williams and Young, 1980.
Bovine Spongiform Encephalopathy (BSE)'	cattle	Wells et al., 1987.
Feline Spongiform Encephalopathy (FSE)[H]	cats (domestic and zoo species)	Wyatt et al., 1990.
Spongiform Encephalopathy[H]	exotic ungulates (nyala, gemsbok, oryx, kudu)	Jeffrey and Wells, 1988 Bradley, R. 1997
Kuru	man	Gadjusek and Zigas, 1957.
Creutzfeldt-Jakob Disease (CJD)*.	man	Creutzfeldt, 1920. Jakob, 1921 &1923.
Gerstmann-Sträussler-Scheinker syndrome (GSS)	man	Gerstmann, 1928.
Fatal familial Insomnia (FFI)	man	Medori et. al., 1992
New variant CJD[H]' (vCJD)	man	Will et al., 1996.

Table1. The spectrum of spongiform diseases and the species that they affect

H There is epidemiological and strain typing evidence to suggest that these diseases are related to the advent of BSE (Bruce et. al., 1994). ' There is recent evidence to suggest that these two diseases are caused by a common agent (Bruce et. al., 1997; Hill et. al., 1997). * CJD can be classified as sporadic, iatrogenic or familial. (Collinge and Palmer, 1997 for review).

The vaccine had been prepared from formalin treated sheep brains and it is thought that at least one of the sheep used was incubating scrapie without displaying clinical signs (Gordon, 1946). Subsequent studies by others in the field confirmed that the disease transmitted with an unusually long incubation period (reviewed by Kimberlin 1981). The successful transmission of disease from affected to healthy animals suggested that scrapie occurred as the result of infection with a causitive agent. Serial passage of the disease through nine generations of sheep provided confirmation that there was a transmissible agent, (reviewed by Pattison 1988). It was considered likely that a virus was responsible for scrapie (Wilson et. al., 1950). The source of infectivity in these cases was brain homogenate prepared from affected animals. The protracted incubation period which is a feature of infection by the scrapie (and scrapie-like) agents led to its description as an unconventional slow virus by Sigurdsson (1954). The belief that the agent responsible for scrapie was a virus were based on the observations that the diseases are transmissible and the agent had a very small size (Stamp et. al, 1959), although even now, almost 45 years later, a scrapie specific virus has still to be isolated. The lack of an identifiable specific virus caused some to consider that there was another cause of scrapie. The possibility that scrapie was a genetic disease was postulated (Parry, 1962; 1964), but whilst host genetics are acknowledged to exert an influence on the susceptibility to and the progression of the disease, scrapie (and the associated diseases) are not considered to be true genetic diseases.

A major milestone in scrapie research was reached in the early 1960s when the first successful transmission of scrapie to rodents was achieved (Chandler, 1961; Zlotnik and Rennie, 1962). Experimental infection of mice by the intracerebral (i.c.) route produced a practical model with relatively short incubation periods, making it much easier to study the disease. The availability of a reliable rodent model for scrapie has greatly advanced study in the field of this and other associated diseases. The associated conditions, including BSE and CJD share common pathological

features and are commonly referred to as members of a group of diseases known as transmissible spongiform encephalopathies (TSEs).

The demonstration of scrapie as a transmissible disease led to speculation that the naturally occurring disease was caused by vertical (ewe-to-lamb) transmission in the womb (Dickinson et al., 1965). It has been noted that the eventual scrapie status of a lamb depends more on the status of the ewe than it does of the ram (Dickinson, 1976) however, there is evidence to suggest that vertical transmission is not the only way in which the disease is spread. Instances of what can only be described as 'contact transmission' have been reported between sheep and goats (MacKay and Smith, 1961) and there is even a report of transmission between laboratory rodents (Dickinson et. al, 1964) although this has not been reported in any of the literature since. Contagious spread of this nature is not completely understood but it seems likely that the oral route of infection is important (Pattison and Millson, 1961; Gordon, 1966). Placental material from scrapie affected ewes has been demonstrated to contain high levels of scrapie infectivity (Pattison et al., 1974), this raises the possibility that grazing sheep on pasture land contaminated with infective ovine placentae can lead to transmission of the disease.

Since the first successful laboratory transmissions of the disease there have been around 20 distinct strains of mouse adapted scrapie identified. Of these 20 or so strains the present investigation is being carried out using the ME7 strain of the scrapie agent (Zlotnik and Rennie, 1962 and 1963). Strains are separated on the basis of incubation period and specific patterns of pathology on passage in certain strains of mouse (Outram et. al., 1973). Incubation periods for the various strains of mouse adapted scrapie can range from around 150 days up to and exceeding the lifespan of a mouse.

Incubation period in murine scrapie is influenced by the *Sinc* genotype of the affected mouse (Dickinson et. al., 1968). *Sinc*, for Scrapie INCubation, which is found on chromosome 2 in mouse, is functionally similar to the *Sip* gene in sheep.

The *Sinc* gene is also known as *Prn-i*. The gene has two alleles designated s7 and p7. These alleles determine whether or not the incubation period of the ME7 scrapie strain is short or long respectively. It is now accepted that the *Sinc* designation reflects the function of the gene. The product of the gene is the host-encoded sialoglycoprotein PrP, and it has been shown that the *Sinc* gene and the gene that codes for PrP, *Prn-p*, are in fact the same gene and the influence that the gene has over incubation period is controlled by PrP dimorphisms at codon 108 (L108F) and /or codon 189 (T189V; Hunter et. al., 1992; Moore et. al, 1998).

The exact nature of the scrapie agent is a matter of some controversy and will be discussed in section 1.2, then pathogenesis of the disease will be considered. The popular view now is that the infective agent is a prion (Prusiner, 1982). Prions - which are an abnormal isoform of a host-encoded protein, prion protein (PrP)- will be discussed in greater detail in section 1.2 but basically a prion is postulated to be a self-replicating pathogenic protein devoid of a nucleic acid informational molecule. However, the prion theory struggles to explain scrapie strain diversity and stability upon passage and there are still those who advocate the possibility that the agent is a virus (Diringer et. al, 1994; Diringer et. al., 1997; Manuelidis, 1997; Murdoch et. al, 1990). The suggestion is that due to its very small size and unusual physico-chemical properties (Stamp et. al, 1959; Alper et. al, 1966) a virus has not yet been isolated. The exact nature of the agent is still a matter of some controversy. What is irrefutable about the nature of the disease and can be considered here are its very unusual physical and chemical characteristics. The agent displays a very high stability under conditions that would be detrimental to most conventional viral and bacterial agents. Furthermore, infection fails to induce a specific cell mediated immune or inflammatory response (Kimberlin, 1976) but other inflammatory reactions involving microglia and cytokines may occur (Williams et. al., 1994; Williams et. al., 1995) within the CNS.

1.2 The nature of the agent.

Despite what is often recorded in textbooks, the exact nature of the agents responsible for TSE infections is still an unresolved issue. There are several hypotheses as to the aetiology of these diseases. These include the possibility that the TSEs are genetic diseases (in familial cases), are caused by an unconventional virus or are the result of infection with a novel type of agent composed solely of protein (Griffith, 1967; Prusiner, 1982).

Until recently most of the experimental information on these agents has come from studies of experimentally transmitted scrapie in laboratory rodents (mice and hamsters). Early studies of the scrapie agent demonstrated that the infectious agent displayed unusual physical and chemical properties. These include a resistance to heating; the agent survived prolonged heating at temperatures in excess of 120^0C in the absence of water. There was even evidence to suggest that some infectivity could survive prolonged boiling (Gordon, 1946). Other unusual properties included the partial protease resistance of the agent and the resistance of infectivity to ionising radiation, a treatment that normally degrades nucleic acids (Alper et. al., 1966). These observations, and the inherent suggestion that the agent was devoid of DNA or RNA led some to postulate that the agent may be composed mostly or entirely of protein (Griffiths, 1967; Pattison and Jones, 1967; Alper et. al., 1967).

Other groups maintain faith in the dogma that biological information such as that pertaining to propagation/replication of infectivity and faithful replication of strain characteristics can only come from a nucleic acid. These groups (see Braig and Diringer, 1985; Manuelidis et. al., 1995 for examples) believe that the agent is a virus or possibly a virino. A virino is described as a molecule composed mostly of protein but with a small nucleic acid element (Dickinson and Outram, 1988; Somerville, 1991). However, to date no TSE specific nucleic acid has been isolated. Furthermore it has been demonstrated that, while infectivity was selectively

decreased by treatment with proteases there was no appreciable loss of infectivity titre following treatment with nucleases, lipases or glycosidases (see Millson et. al., 1976 for review). These observations argued against the agent being a conventional virus and suggested that a protein was critical for infectivity.

The idea that the agent may be a new type of infectious agent, one that replicates without a conventional informational molecule led Professor Stanley Prusiner to coin the term 'prion' (adapted from *pro*teinaceous *in*fectious agent; Prusiner, 1982). Bolton and colleagues were the first to identify a protein which co-purified with scrapie infectivity (Bolton et. al., 1982). The candidate protein was identified as PrP –also known as protease resistant protein or the 'prion' protein (Bolton et. al., 1982). This protein is the constituent element of the amyloid plaques seen in many cases of TSE infection (Merz et. al., 1981; Prusiner et. al., 1983). PrP is a highly conserved protein expressed by mammalian species, primarily in the CNS where it is expressed in astrocytes and at the neuronal cell surface where it is anchored by a GPI-moeity (Collinge et. al., 1994; Moser et. al., 1995). PrP exists primarily in one of two forms (although there are postulated transient intermediaries, see Harris, 1999 for a review of the molecular nature of the PrP^{C} conversion to PrP^{Sc}). The native form of PrP (known as PrP^{C}), which is expressed in normal CNS tissue, has a molecular weight of 33-35 kilodaltons (kDa), is a mainly alpha-helical protein (Approximately 40% alpha-helix, little or no beta-sheet). This form of PrP is sensitive to digestion by proteolytic enzymes. The disease associated form of the protein, known as PrP^{SC} has a far higher beta-sheet content than the native form (60% beta-sheet and 20 % alpha-helix; Martins, 1999) and is formed as a result of post-translational modifications. PrP^{SC} undergoes limited proteolysis and the product of the reaction is a protein core, designated PrP27-30, which can polymerise to form amyloid rods (Prusiner, 1993). The conformational change from PrP^{C} to PrP^{SC} is autocatalytic with PrP^{SC} propogating itself by facilitating the conversion, the exact mechanism of this conversion is not clear (Nixon, 1999).

Although primarily a CNS protein PrP can be found in other tissues (Kubo et. al., 1995; Horiuchi et. al., 1995; Doi, 1991). The high degree of sequence conservation seen between PrP proteins from various species and its expression early in development (Manson et. al., 1992) tends to suggest that the protein must have an important function. However, to date no definitive function for the protein has been identified (Estibeiro, 1996) although several possibilities have been mooted such as the regulation of diurnal rhythms (Tobler at. al., 1996) or involvement in the regulation of copper/zinc superoxide dismutase (SOD), suggesting a role for PrP^{C} in cellular resistance to oxidative stress (Brown et. al., 1997). One of the more puzzling facts with respect to the function of the protein is that ablation of the gene which controls production of the protein is not a lethal event. (Büeler et. al., 1992; Manson et. al., 1994).

What is not in dispute with regard to the infectious agent is that the presence of the PrP protein is essential for disease propagation. This has been evidenced by studies involving mice where the PrP gene has been ablated or otherwise disrupted. Animals which have this knockout mutation are resistant to infection by the scrapie agent (Büeler et. al., 1992; Büeler et. al., 1993;). It has been shown that expression of PrP^{C} is required for replication of the infectivity in the CNS (Sailer et. al., 1994), for neurodegeneration to occur (Brandner et. al., 1996a) and for the transfer of infectivity from the periphery to the CNS (Blättler et. al., 1997). However in these experiments the transfer of infectivity has been related to the accumulation of disease specific PrP in neural grafts which over-express normal PrP. Sakaguchi and colleagues (1993) have demonstrated that levels of infectivity in lymphoid tissues of mice infected with the human CJD agent do not correlate with the levels of disease specific protein detected. Work by Somerville and Dunn (1996) concludes that at least some of the PrP^{SC} in the brain is not directly associated with infectivity, recent work by Hill et. al. (1999) using *in vitro* conversion assays supports this. These studies suggest that while PrP^{SC} accumulation is associated with replication of the infective agent it is not clear that the protein itself is the agent.

Experiments designed to detect infectivity were carried out by bioassay of tissues from the visual system of mutant mice that did not produce PrP protein and their wild-type counterparts which did. The visual system is a well-characterised system and has proven useful to study the neural spread of the scrapie agent (Fraser, 1982a,b; Scott and Fraser, 1987). Bioassays are a method of detecting infectivity alone and do not relate the deposition of PrP^{SC} in the CNS to the activity or the identity of the infectious agent. It was felt that this approach was valid given the concerns surrounding the exact nature of PrP's role in the pathogenesis of these diseases and the questions that still surround the exact nature of the agent.

1.3 Pathology and Pathological Markers of TSE infection.

In the murine model of scrapie, onset of clinical disease is difficult to detect as there is a long asymptomatic period following experimental infection. During this period the agent replicates and accumulates in the organs of the lymphoreticular system; spleen, lymph nodes, Peyers patches and the brain (Outram 1976; Race and Ernst, 1992). The early signs are generally subtle and there is a spectrum of clinical signs that might suggest a diagnosis of TSE infection. These can include altered gait, pruritus (in the case of scrapie at least) and hyperexcitibility in response to a range of stimuli, for example, sound, touch and movement (Bradley, 1997). There is, as has been previously mentioned no specific host mediated immune response. A definite diagnosis can, at present, only be made following post mortem pathological examination of the brain although there is currently much interest in the development of reliable antemortem diagnostic tests.

The first signature lesion to be identified in natural scrapie was a vacuolation of the perikaryon in the ventral horn of the spinal cord; this was described by Besnoit and Morel in the 19^{th} century (reviewed by Bradley, 1997). Subsequent intraneuronal vacuolation in the brain was also found (Zlotnik and Rennie, 1962).

All the identified TSEs share a common type of pathology. In general this is characterised by spongiform degeneration, mainly of the grey matter neuropil in murine scrapie, and the deposition throughout the CNS of an abnormal, disease associated, form of a host encoded amyloidogenic protein known as PrP or the prion protein (Prusiner, 1982). The disease-associated form of this protein is known as PrP^{SC}, or PrP-scrapie, and is formed from a normally present precursor PrP^{C}, or cellular-PrP as discussed previously.

In contrast with transmissible spongiform encephalopathies of man, the neuropathology of scrapie in sheep and goats often includes vacuolation of neuronal cell bodies. This and the frequently vacuolation of the neuropil is readily detected in paraffin sections of brain stained with haematoxylin and eosin (H&E, Figure 1 illustrates vacuolation of the neuropil as seen in an H&E stained section). This disease specific vacuolation of the neuropil is caused by the loss of organelles and swelling in the dendrites and axonal terminals (Jeffrey et. al., 1992) and is discernible from non-specific damage by the presence of membrane and granular debris (Chou et. al., 1980; Sato et. al., 1980).

It is possible to detect amyloid plaques in H&E stained paraffin sections due to the eosinophilic nature of the amyloid; this is readily confirmed by the use of dyes such as Congo Red or Thioflavin-T which selectively stain amyloid deposits (Vasser and Culling, 1959; Puchtler et. al., 1962). The availability of specific anti-PrP antibodies has made the detection and visualisation of plaques and the less aggregated, non-amyloid, forms of the protein involved in TSE infections easier (Zanusso et. al., 1998; Farquhar et. al., 1989).

Amyloid forms of PrP^{SC} have not been observed in all cases of the natural disease (Gilmour et. al., 1986). PrP^{SC} aggregations have a variety of appearances this includes plaques as well as more diffuse deposits (Fig 2a and 2b). Although it is widely thought that PrP^{SC} is the pathological agent it is unclear how it effects damage.

It is possible that the abnormal protein is neurotoxic, there is evidence, from *in vitro* studies that at least a portion of the prion protein, the fragment represented by amino-acid residues 106-123, can be directly neurotoxic (Selvaggini et. al., 1993; Forloni et. al., 1996). This PrP neurotoxicity possibly occurs by a microglia associated mechanism (Brandner et. al., 1998). Alternatively, the withdrawal of PrP^{C}, the precursor molecule, could be detrimental to neuronal survival (Brandner et. al., 1996b; Aguzzi et. al., 1997).

Other pathological features include astrocytic hypertrophy and hyperplasia and, in some models, neuronal loss, which may occur by an apoptotic mechanism (Giese et. al., 1995; Kretzschmar et. al., 1997) which may account for the lack of inflammation in the central nervous system. The astrocytic hypertrophy is marked by an upregulation of glial fibrillary acidic protein (GFAP). The role of astrocytes in the disease process is unclear but it may involve trafficking of the abnormal protein; astrocytes have been demonstrated to accumulate PrP^{SC} prior to the development of the other neuropathological changes (Diedrich et. al., 1991a). The importance of this observation with respect to the pathogenesis of disease is not clear. It had been suggested that the astrocytosis was the primary lesion in TSE infection and that the nerve cell vacuolation was a secondary change initiated by faulty metabolism of astrocytes (Field and Raine, 1964). However, there are others who believe that astrocytic hypertrophy is a reactive change (Fraser, 1979a). The upregulation of GFAP (Diedrich et. al., 1991b) can occur late in the incubation period of certain scrapie models, after the appearance of vacuolation or PrP, this seems to suggest that astrocytic hypertrophy and hyperplasia is a secondary lesion.

Figures 1-3 illustrate the types of pathology that are seen in scrapie and other TSE infections. Where the pathology shown is from sources other than experimental ME7 scrapie, the sources are noted. These are accepted as the defining features of pathology, which are common to all diseases of this type. The lesions seemingly arise without activating the host immune system. Exactly how these pathological features translate into the clinical phenotypes that occur in cases of these diseases is unclear, especially as the clinical presentation is not always the same (particularly in cases of human spongiform encephalopathy; Collinge et. al., 1992). It is also worth

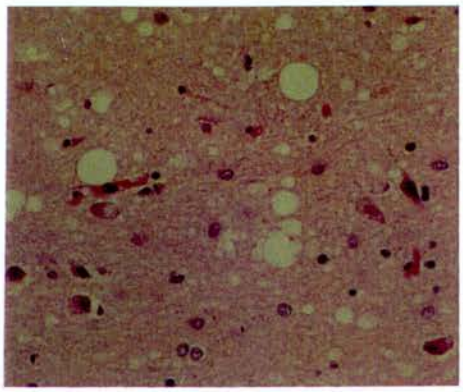

Figure1.

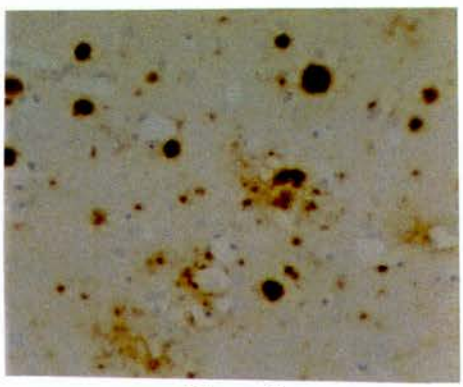

Figure 2a.

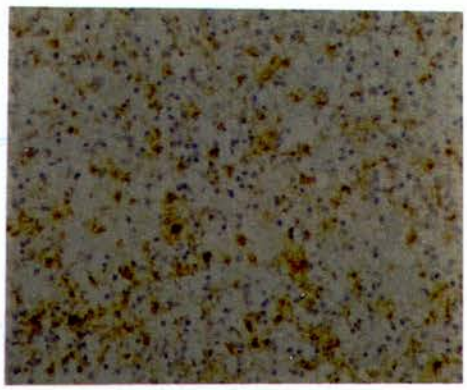

Figure 2b.

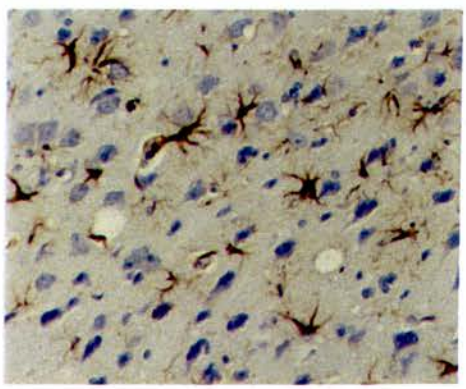

Figure 3.

Figures 1-3. Illustration of the three major pathological markers observed in cases of transmissible spongiform encephalopathy infection. **Figure 1** shows vacuolar degeneration of the neuropil often referred to as spongiform change. **Figure 2a** PrP in the form of plaques. **Figure 2b** shows a more diffuse form of PrP that can be found in TSE infections. **Figure 3** shows reactive astrocytes, identified by immunohistochemical detection of glial fibrillary acidic protein (GFAP).
(Figures 1-3, x200 magnification).

noting that although these are characteristic brain lesions, there exists a broad spectrum of human neuropathology in terms of the severity of lesion and the distribution of damage throughout the brain (Lantos, 1992). Under experimental conditions the distribution and severity of the lesion can be faithfully reproduced in rodent models where host strain, with particular emphasis on the *Sinc/Prn-i* genotype, the agent strain and the route of exposure are kept constant (Fraser and Dickinson, 1976; Fraser, 1979b). The recognition of these characteristic features of scrapie infection made it possible to develop a tool for identifying scrapie strains in defined mouse models. The method relies on simple measurement of disease characteristics. The major features that are measured are the incubation period and the degree of vacuolar pathology in specific regions of the scrapie-affected murine brain (the lesion profile) where agent strains show faithfully reproducible differences in the severity and distribution of vacuolation in the neuropil of genetically identical animals (Bruce, 1986).

1.4 Assessment and Quantification of Pathology

Different strains of the scrapie agent will produce distinctive patterns of pathology in certain strains of laboratory mice. These differences include variation in spatial distribution and severity of lesions in the CNS and can include differences in the type of PrP^{SC} that can be detected, as defined in terms of its aggregated or more widely dispersed state. In some cases the protein is deposited as plaques whereas in others there may be less structure to the protein deposits. It is notoriously difficult to objectively measure/quantify the degree of pathology that is present in cases of TSE infection. The most important lesion in the TSEs is vacuolation of the grey matter; it is this feature which forms the basis of a semiquantitative method of strain discrimination, the lesion profile (Fraser and Dickinson, 1973). This is a means of assessing the amount of pathology in the brain of a mouse at the late clinical, or terminal, stages of the disease, it is not a tool that lends itself to the sequential mapping and quantification of pathology during the incubation period. It is however very useful in determining the causative strain of agent in a given strain of mouse. To assess the degree of vacuolation, the severity of the lesion is scored in nine grey matter areas and three white matter areas, grey matter vacuolation is scored from 0-5 where 5 is the most

severe and white matter vacuolar change is scored on a scale from 0-3 (Bruce, 1996). There are verbal definitions of each score which aid consistency between examiners and representative photographs are available (Fraser, 1970). Each animal in a given experimental scrapie transmission group is scored according to these criteria. The mean scores for each of the twelve areas is calculated and a lesion profile can be constructed. Lesion profiles are signatures for a given strain of agent in a given mouse strain (Figure 4 illustrates this point) and are dictated by the combination of agent strain and mouse genotype (Bruce et. al., 1991). The shape of the lesion profile produced is independent of the initial infecting dose and can also be used to determine the fatal strain if an animal is infected with a mixture of strains. It was lesion profiling that led to the discovery that BSE and new variant CJD were caused by the same agent (Bruce et. al., 1997), and that BSE was caused by a single stable strain of agent (Bruce et. al.., 1994).

Lesion profiling is a time consuming and labour intensive procedure that is prone to examiner fatigue, this is a potential source of error and inconsistency. Each examiner has to be trained in the same way, to the same standard so as to maintain a level of uniformity between examiners. Because of these requirements there are generally very few people who are actually able to produce these profiles. Although lesion profiling was designed as a semiquantitative tool it is limited to the examination of the mouse brain in the 12 defined areas and is used only at the terminal stage of the disease. It is not a suitable tool for measurement of pathology through the course of disease incubation, and as such is not suitable for tempero-spatial investigations of pathogenesis. This is because, certainly in some models, during the early stages of infection the distribution of vacuolation is influenced by the spread of the infectious agent, which is likely to be the same for other strains that are inoculated in the same way, and does not necessarily reflect the eventual lesion profile that is found at the terminal stage (Cole and Kimberlin, 1984). In such studies a more quantifiable and thorough, in terms of the number of regions that can easily be examined, method of measuring pathology is desirable.

(a)

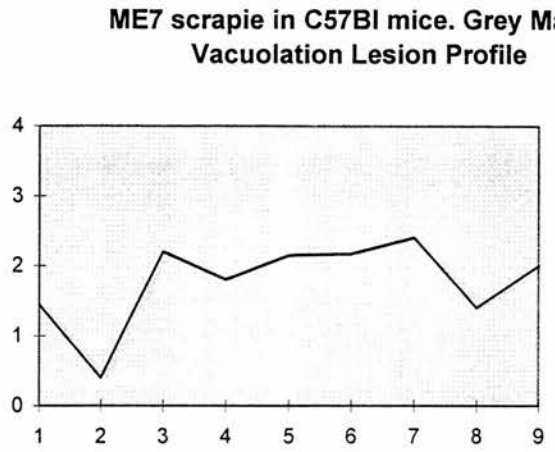

(b)

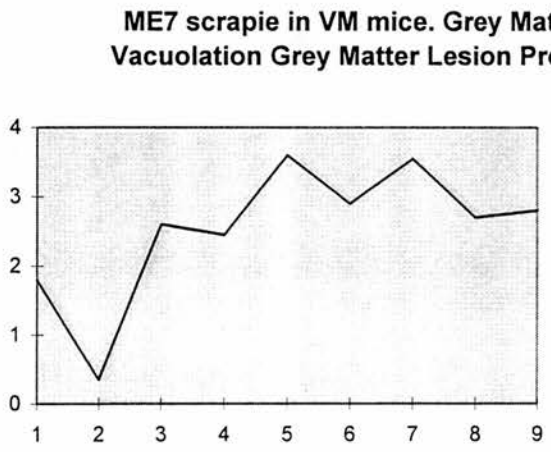

Figure 4: Shows a representation of the grey matter portion of two complete lesion profiles. C57Bl mice (4a) produce different lesions that VM mice (4b) when they are both infected with the same strain of the scrapie agent -ME7. This illustrates to some degree the effect that host genetics exerts on pathology and pathogenesis of disease. In both plots the X-axis represents the nine grey matter regions that are examined as standard and the Y-axis denotes the pathological 'score'.

Although invaluable in discriminating between strains, the lesion profile does not allow for a complete picture of pathology and pathogenesis to be produced. Vacuolation is the major lesion in the TSEs but there are other pathological indices that should be considered in order to understand more fully the disease process. It has been demonstrated that the distribution of vacuolar change in the neuropil correlates closely with the accumulation of PrP (Bruce et. al., 1989; Bruce et. al., 1991). However, the distribution and accumulation of PrP is not considered in terms of the lesion profile. The other major pathological features, astrocytosis and neuronal loss are not incorporated into the lesion profile either. A time course study of the disease, involving the computer aided mapping and measurement of the major pathological features, vacuolation, astrocytosis and PrP deposition, would help to expand the understanding of disease pathogenesis and serve to illustrate the potential use of computers in a routine pathological context.

By using a computerised system, measurements of vacuolation, PrP deposition and astrocytosis can be made in a reliable and semi-objective way. The visualisation of PrP and GFAP (the astrocyte marker) is made possible due to the availability of specific antisera and effective immunohistochemistry protocols. GFAP is a cytoskeletal protein found in mature astrocytes. Levels of GFAP are regulated under pathological conditions and upregulation of GFAP is one of the main characteristics of the astrocytic reaction that is commonly seen following CNS insult (Gomes et. al., 1999). Vacuolation is assessed in routine/H&E sections.

1.5 The BSE Epidemic and vCJD.

The most widely reported animal spongiform encephalopathy of the past ten years has been bovine spongiform encephalopathy (BSE). The first report of BSE or "mad cow disease" was made in 1987 (Wells et. al.) following confirmation in November of 1986 at the Central Veterinary Laboratory in Weybridge (Bradley, 1997). It is likely that the affected cattle were infected as calves in 1981-82

(Wilesmith, 1991). The neurohistological lesions observed in these cases were scrapie-like, that is characterised by spongiform change in the central nervous system. Subsequent epidemiological studies confirmed that BSE was a new disease and the first clinical case probably occurred as early as April of 1985 (Wilesmith et. al., 1988; Taylor 1992). The peak incidence of cases occurred in late 1992 and early 1993 (Anderson et. al., 1996). Since then there has been a progressive reduction in the number of cases seen annually. By the end of January 1998 there had been 170259 confirmed cases of BSE in the mainland UK (Ferguson et. al., 1998). The greatest number of cases reported from outside the UK was Switzerland with 234 (Collee and Bradley, 1997a).

Epidemiology suggests that BSE is an orally acquired disease resulting from contaminated animals feed. It appears that the epidemic was initiated by the inadvertent transmission of the scrapie agent from sheep to cattle. Sheep carcasses were commonly rendered to produce meat and bone meal (MBM) as a protein supplement for cattle. As mentioned, the first infections probably occurred in 1981-82, this coincides with changes to the rendering process by which the MBM was produced. It was at this time that most rendering plants abandoned the use of organic solvents in the preparation of MBM (Nathanson et. al., 1997). BSE is thought to have been caused by scrapie infectivity which was able to survive this modified process (Taylor, 1992). Recent evidence (Taylor et. al., 1998), however, has suggested that the abandonment of solvent extraction was not the sole key factor that allowed BSE to emerge, although it may still have played a part.

A major concern that was voiced during the BSE epidemic was that there might be a risk of infection to humans from the consumption of tainted beef and beef products. Studies of the tissue distribution of infectivity in bovine tissues have been carried out. The purpose of these studies was to identify the possible risk to humans from consumption of meat/meat product from potentially infected animals (Collee and Bradley, 1997b). In general the BSE agent is not as widely detectable in a range of bovine tissues as the scrapie agent is in ovine tissues (Kimberlin, 1994). BSE

infectivity is generally limited to the central nervous system: brain and spinal cord. These offal were banned from human consumption in 1989 (Anderson et. al., 1996). What is important from a human health aspect is that there is no detectable infectivity in either milk or skeletal muscle (Bradley, 1994). However, it was recognised that the population of the UK had possibly been exposed to the BSE agent through the food chain before the offal ban was put in place.

In 1994 and 1995 two cases of the human TSE Creutzfeldt-Jakob disease (CJD) were identified in unusually young patients (Britton et. al., 1995; Bateman et. al., 1995). At this time there had only been four previous cases reported in this age group (Almond, 1995). In 1996 it was reported that these two cases as well as eight others had suffered from a new form of CJD. This new variant of CJD (vCJD) was distinguished from sporadic, familial and iatrogenic CJD on the basis of atypical electroencephalogram features, young age of the cases, unusual clinical presentation and a new and distinct neuropathological profile (Will et. al., 1996; Zeidler et. al, 1997a; Zeidler et. al., 1997b). It was suggested that this new disease was the result of infection with the BSE agent, the most likely route of infection was the oral route. There is evidence for the oral transmission of human TSEs in the case of Kuru. Kuru is the archetypal acquired human TSE. It is associated with the ritualistic cannibalism that was practised by the Fore people of Papua New Guinea (Zigas and Gadjusek, 1957; Alpers, 1968), however, the neuropathology which has been described for Kuru is markedly different from that seen in vCJD (McLean et. al., 1998). This suggests that if vCJD is transmitted by the oral route that the strain of agent being passed is different. Epidemiological studies of vCJD incidence indicate the existence of a link between this disease and BSE. Of 28 confirmed cases of vCJD only one has occurred outside of the UK (Delsys et. al., 1997). Recent studies have all but confirmed that the strain of agent responsible for BSE in cattle is the same strain that causes vCJD in humans (Bruce et. al., 1997; Hill et. al., 1997).

Kuru and vCJD are not the only examples of acquired TSEs in humans. Iatrogenic infection with the TSE agent has been demonstrated. These cases are

usually referred to as CJD although the cases arising from peripheral infection, such as growth hormone injections, present with a clinical picture that is more similar to Kuru than to sporadic CJD (Collinge and Palmer, 1997). Iatrogenic transmission of CJD has occurred in a number of cases as the result of medical procedures. These accidental infections have occurred by a number of routes (Brown et. al., 1992) and include the use of inadequately decontaminated neurosurgical instruments (Bernoulli et. al., 1977), dura mater and corneal grafts (Duffy et. al., 1974; Thadani et. al., 1988) and the use of human cadaveric pituitary derived growth hormone (Koch et. al., 1985). It appears that the route of infection affects the clinical syndrome. Intracerebral (from neurosurgical instruments) and ocular (corneal grafts) inoculation present as classical CJD whereas infection by a peripheral route, as in the growth hormone cases, presents more like a kuru type infection with more severe lesions in the cerebellum and basal ganglia (deVillemeur et. al., 1996; Weller et. al., 1986).

The three major factors that influence disease phenotype in experimental TSE infections are agent strain, host genetics and route of infection. Recent evidence suggests differences in the neuropathology of kuru and vCJD are more a function of agent strain than of host genetics (McLean et. al., 1998). The work presented in this thesis attempts to determine whether route of infection has an appreciable effect on developing and eventual neuropathology when host genotype and agent strain are kept constant.

1.6 Objectives of Study.

This body of work described in this thesis outlines an experiment to test the hypothesis that the early stage pathology observed in the CNS of a constant scrapie strain/mouse strain combination is influenced by the route of infection. This involved the use of computerised image analysis techniques to map and measure the major pathological features of TSE infection, vacuolation, GFAP accumulation and PrP accumulation. The information gathered from this experiment will be used to examine the kinetics of disease. In the case of this thesis the model of infection is

C57BL mice infected with the ME7 strain of scrapie. Details of the system are described below but it is broadly similar to the system in use at the National CJD Surveillance Unit in Edinburgh (Sutherland et. al., 1996; MacDonald et. al., 1996). The experiments were designed to make it possible to examine the pathogenesis of the disease following parenteral and peripheral infection. Initially this was to involve spinal cord pathogenesis, but due to unforeseen problems, as outlined in Chapters 3 and 4, was eventually restricted to the brain.

A further objective of this work was an attempt to determine whether or not transportation of scrapie infectivity can occur in animals (mice) that do not possess a functional copy of the PrP gene and subsequently cannot produce the PrP protein. The approach adopted in this study is significantly different from that chosen by previous groups (Brandner et. al., 1996b; Blättler et. al., 1997). Instead of working with PrP null mice (Büeler et. al., 1992) grafted with neuroectoderm from *tga20* (PrP over-expressing) mice (Fischer et. al., 1996) the work described in this thesis relates to a bioassay experiment using a different strain of PrP null mice (129Ola mice with a disrupted ability to produce PrP protein). These mice were generated in-house at the Neuropathogenesis Unit (Manson et. al., 1994).

A final objective of this thesis is a qualitative comparison of the appearance of vacuolar and PrP pathology in murine and human acquired TSE infection. This was considered potentially interesting in light of the putative oral route of acquisition for vCJD in humans. This study was intended to investigate the extent to which pathology in human disease is influenced by route of acquisition by comparing the pathological phenotypes seen in different types of human CJD with the animal model of scrapie used elswhere in this thesis. Of course the route of infection is not the sole influencing factor on the eventual pathological profile of a TSE infection, there are other factors which are acknowledged as being very important but were not considered in this attempted study. This highlights the major shortcoming of this study and the susbsequent value of any observations is diminished as a result.

Materials and Methods.

2. Materials and Methods.

2.1 Experimental mice.

All experimental animals were taken from the specified-pathogen free (SPF) colony maintained at the Neuropathogenesis Unit. Further information regarding the excluded pathogens is in Appendix I. Details of the mouse strains used are given below. The generation of the particular PrP null mice used in this study is described by Manson et. al. (1994).

Most of the experimental work was carried out on C57BL/FaBtDk (referred to in the text as C57BL) mice. This was for two main reasons. Firstly, the combination of ME7 scrapie and C57BL host has been well studied, especially in the case of intracerebral infection; secondly, the number of C57BL mice that were available was sufficiently high where those for other inbred mouse strains were not. This allowed reliable sentinels to be included in the experimental group to indicate effective transmission of disease at an early stage and calculation of infectivity titres from a standard dose response curve (Appendix II). It was not possible to carry out all of the experimental work in a single sex group of mice. Although this would have been preferable in terms of experimental control, it has been reported that the gender effect that is often seen with some scrapie strain/host combinations (where the incubation time for the disease is longer in females), is not observed when ME7 scrapie is used (Outram, 1976). The other strains of mice used in this work were the 129/Ola mice (Hooper et al., 1987) and a genetically modified strain of 129 that has an interrupted PrP gene which results in a complete loss of mRNA production and subsequent protein translation (Manson et al., 1994). These mice are referred to as 129 and PrPnull mice (or $PrP^{-/-}$) respectively. All these strains of mice carry the s7 allele of the gene *Sinc*. This gene controls the length of the incubation period and has two alleles, s7 or p7 (Dickinson et. al., 1968). The effects of the *Sinc* gene are described in Chapter 1.

2.2 Mouse Husbandry.

Mice are kept in groups of not more than six. They are given food and water ad libitum, drinking water is acidified to a pH in the range 2.3-3.0. Food pellets (Teklad extruded lab diet, Harlan) are irradiated. All animal bedding (Illico gold range, dust free) is autoclaved prior to use in the animal colony. The animals are checked twice weekly at cleaning by experienced animal technicians for signs of illness. In the period from 30 to 60 days before the predicted end-point of the disease the mice are also scored once a week for clinical signs of disease. Mice in the animal unit are maintained in a controlled environment. This is a 12-hour light/dark cycle. Intensity of the light in the animal rooms varied from 50 to 200 lux (Foster et al., 1986). Temperature in the animal colony is thermostatically controlled within the range 19-23°C

2.3 Strains of Scrapie.

There are over twenty discrete strains of scrapie but for the work outlined in this thesis only one, the ME7 strain, was used. The ME7 strain has been widely studied and faithfully produces precise and regular incubation periods in all mouse strains. ME7 was the strain used in the early scrapie genetic experiments when the *Sinc* gene was identified, and the s7 (shortening) or p7 (prolonged) refer to the influence on the incubation of ME7 in certain strains of mice. ME7 was originally isolated from the spleen of a Suffolk sheep affected with natural scrapie (Zlotnik and Rennie, 1963). Passage into mice was via intragastric challenge of Moredun random bred mice. The agent was then passaged intracerebrally (i.c.) once more into the Moredun mice, then nine times through inbred C57BL mice (Fraser and Dickinson, 1973).

2.4 Inoculum Preparation.

Inocula for use in oral, intramuscular and intraperitoneal infection were all prepared using standard methods employed at the Neuropathogenesis unit. These methods are unpublished but are described, briefly, below.

The sources of infectivity for most experimental murine scrapie work are the brains of terminally infected mice. These are removed using aseptic techniques and stored at -30^{0}C until they are needed. Full and detailed records of the source and destination of each tissue are maintained. When required tissues are thawed, weighed and then transferred to a new, sterile Griffith tube. This is a glass tube with a close fitting glass pestle for grinding. The tissues are homogenised in sterile saline to give either a 1% or 10% wet weight concentration. All the inocula used in these studies, with the exception of the bioassay material from the null mice (detailed below) were prepared at the 1% concentration. In some instances the resultant homogenate is centrifuged to remove large particulate matter and the supernatant used as the inoculum source. However, it has been shown previously at the Neuropathogenesis Unit that this centrifugation can result in up to a 10-fold reduction in the infectivity titre (Jan Fraser, personal communication). For this reason the inocula for these experiments was used unspun and care was taken to ensure that the maceration of the tissue was sufficient not to result in a suspension containing large fragments of tissue. Care was taken at every stage of the preparation to avoid cross-contamination of the inocula with other scrapie strains. Due to the extreme resistance of certain strains to conventional sterilisation techniques all new glass wear was autoclave sterilised before use and disposed of after a single use. All inocula were prepared in a safety cabinet.

For the bioassay experiment the preparation of inocula was slightly different. Bioassay can be defined as the inoculation of tissue from one animal into another in order to determine the presence of infectivity. The tissues used as inocula for this

experiment, optic nerve, superior colliculus and dorsal lateral geniculate nucleus were taken serially, at six different time points, over a period of 117 days from both 129 and PrPnull mice. These mice had been infected with 1μl of standard ME7 scrapie inoculum (prepared as described above) by the intraocular route. Injection was into the right eye. Consequently when the tissues were harvested the optic nerve from the right side was taken while the superior colliculus and dorsal lateral geniculate nucleus was taken from the left side of the brain. This is due to the almost complete crossover of nerve fibres at the optic chiasm (Sefton and Dreher, 1985). *Since* the amount of tissue that can be harvested from the visual system of an individual animal is very small it was necessary to pool the tissues from six animals at each of the six time points to ensure sufficient inoculum for the bioassay experiment. The concentration of these inocula (w\v) was calculated using figures for the mean weight of 10 samples. The tissues were homogenised in 300μl of sterile saline, the minimum volume that could be used to ensure sufficient inoculum to inject a group of nine animals. Details of these weights and the inoculum concentrations are given in table 2.

Tissue	Mean Weight of 10 samples (mg)	Working Dilution
Optic Nerve	0.72 ± 0.044	1%
Superior Colliculus	5.62 ± 0.33	10%
Dorsal Lateral Geniculate	22.45 ± 1.40	10%

Table 2: Standard weights and dilutions for assayed tissues (adapted from Jan Fraser, Ph.D. Thesis 1988).

When the tissues were harvested for assay, care was taken to sample approximately equal quantities of tissue from each time point. Pools of tissue were stored in sealed eppendorf tubes at -30^{0}C until animals became available for assay. These tissues were harvested using methods of sampling which were similar to those used by Jan Fraser (Ph.D. Thesis, 1988) and are described in Fig 5. Optic nerves

were cut at the chiasm prior to extraction of the globe from the orbit. The nerve was then cut away from the caudal aspect of the globe.

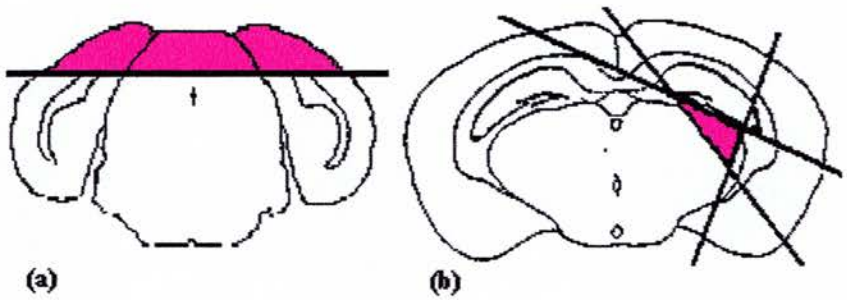

Figure 5: The red regions denote superior colliculus (a) and dorsal lateral geniculate nucleus (b). The heavy black lines illustrate the incisions that must be made in order to harvest these tissues.

When required for injection the pools of tissue are removed from the freezer, one at a time, and the frozen tissue is ground in situ using 300µl of saline and a disposable sterile teflon Eppendorf grinder (Fisher Scientific). Because the agent responsible for scrapie and the associated diseases has not been categorically isolated bioassay is the only truly effective way of measuring "the amount of disease causing agent" - this is commonly referred to as infectivity. There is a demonstrable inverse relationship between incubation period (the time from infection to death) and the dilution/concentration (which controls the amount of infectivity) of the inoculum (Eklund et. al., 1963; Kimberlin and Walker, 1979; Prusiner et. al., 1980).The regular increase in incubation times with increasing dilution (reduced concentration) of the inoculum forms the basis of an assay which is at least as accurate as quantal endpoint titration in determining the amount of infectivity in an inoculum source (Prusiner et. al., 1980).

By infecting groups of animals with inoculum of known dilution/concentration (in the form of a serially diluted, titration experiment) and measuring the respective incubation periods it has been possible to construct dose-response curves for a series of agent-strain, mouse strain combinations. These curves can be presented in the form, dilution of inoculum against incubation period.

Alternatively the amount of infectivity in the infecting dose of inoculum can be calculated by the method of Kärber (Parker, 1959) and this can be plotted as the number of infectious units against incubation period. By using these curves the amount of infectivity in the inocula used in the bioassays described in this thesis can be calculated (at least in terms of i.c. equivalent doses) without the need to perform a full endpoint titration.

Since the purpose of the bioassay is to detect infectivity, and the quantities of tissue being assayed were very small, none of the samples were centrifuged prior to injection as this is known to reduce the infectivity titre, as previously mentioned.

2.5 Inoculation Procedure.

All of the animal work carried out in the course of this study was conducted under the terms of a Home Office Licence and was subject to scrutiny by the in-house ethical approval committee at the Neuropathogensis Unit.

The procedures used for different inoculation routes are described below:

2.5.1 Intracerebral (i.c.)

Intracerebral injections were given under halothane anaesthesia (fluothane). Injection volume for the i.c. route was 20µl. The injections were given with a 27G needle with a needle guard that prevents more than 2mm of the needle penetrating the brain. This limits the injection site to the cerebral cortex. i.c. injections were made to the right of the midline of the skull through the parietal bone. Some i.c. injections were performed for me by Dawn Drummond, as I did not have the necessary experience at the time when the animals were available. However by the time I was ready to inject the bioassay animals I was sufficiently competent to do my own i.c. injections.

2.5.2 Intraocular (i.o.)

Intraocular injections were performed under halothane anaesthesia, using a combination of anaesthetic chamber and a mask to maintain anaesthesia whilst the injection was being given. Injection was into the globe of the right eye. To achieve this the globe was exposed by applying pressure above and below the orbit. A 27G needle was used and the injection made at the scleral margin. The needle was inserted until the tip could be seen through the lens. injection volume for these experiments was 1µl. In the event of a poor injection, usually the result of a mouse "twitching" on the needle, the animal was replaced. On recovery from anaesthetic the mice appeared normal and did not exhibit any ill effects. Ocular pressure in the injected eye was low for at least the first 24 hours after injection; this was observed when the first group of animals were sacrificed for bioassay tissue, but appeared to have returned to normal at time points after this.

2.5.3 Intraperitoneal (i.p.)

Mice were injected by Dawn Drummond into the ventral abdominal cavity using a 27G needle. Injection volume was 20µl.

2.5.4 Intramuscular (i.m.)

Under anaesthesia mice were injected in to the large muscle of the thigh, the *biceps femoralis*, of the right leg. Injection was with a 27G needle and the injection volume was 20µl. A needle guard was used for these injections to limit the depth of penetration to 4mm, this was to prevent damage to the bones of the leg and helped avoid damage to blood vessels in the leg. It was found that extending the leg slightly made it easier to inject into the muscle and avoid scratching the bone. In order to ensure consistent injection site, a group of test mice were injected with a small amount of trypan blue immediately before being sacrificed by rapid cervical dislocation, and the location of the dye in the muscle of the leg was noted. Only

when consistency was achieved did the experimental animals receive their injections. On recovery from anaesthesia the animals appeared to reluctant to place weight on the injected limb but this behaviour disappeared after 1-2 days, otherwise the animals showed no ill-effects.

2.5.5 Oral

Successful oral dosing was achieved by adsorption of the inoculum to food pellets. 100µl of inoculum was dropped onto a single food pellet. The mice were then put into individual cages. Usual bedding was replaced with torn tissue paper which made it easier to determine that the whole dosed pellet had been ingested and not merely broken up and camouflaged by the standard bedding material. Water was given ad libitum and food was withdrawn except for two mouse pellets, the dosed one and an undosed one. The mice were observed until they had eaten both pellets, in all cases within 48 hours of dosing, and then they were recaged in groups of six as before with unrestricted food and water.

Previous attempts at oral dosing by dropping brain homogenate directly into the open mouth of each mouse were felt to be too variable. In this case the intended volume of inoculum to be administered was 100µl. However, in many cases the mice were uncooperative and best estimates are that on average between 60-70µl of the inoculum were actually ingested. Because individual animals received different amounts of inoculum it was decided that the value of information gathered from these animals might be reduced. For this reason a second group of animals were dosed via food pellets as described above, this gave more control of dosing. The animals from the initial experiment were maintained until they succumbed to disease. The incubation period data from this set of animals will be presented and discussed later in this thesis.

2.6 Harvest of Murine Tissues.

All of the animals used in the work described in this thesis were sacrificed in a serial fashion. The method of sacrifice, number of animals per group and the number and spacing of serial sacrifice time points in an experiment were determined in order to best suit the needs of the given experiment.

In the case of the study of the effect that route of infection has on the development of pathology in the murine CNS Following infection with the scrapie agent groups of animals were selected at various times after infection and sacrificed by carbon dioxide inhalation so that the brains and spinal cords might be removed intact. In the case of the animals involved in the investigation of possible transport of infectivity in $PrP^{-/-}$ mice rapid cervical dislocation was the method of euthanasia employed; in all cases euthanasia of animals was carried out in accordance with home office regulations.

Serial sacrifice time points were selected to ensure that the best possible chance of detecting early, middle and late pathological changes could be identified. Although the numbers of mice employed for the route study were quite high the necessity of harvesting tissues from each of the three groups (i.m. infected , i.p. infected and orally infected) at a sufficient number of time points such that the entire incubation period was covered, meant that the number of animals available for sacrifice from any given group at any given time point was small; in this case each serial sacrifice group consisted of four animals.

For this experiment animals were sacrificed at either six (i.m. and i.p.) or seven (oral) time points. These time points were assigned arbitrarily by the author and were selected with the intention that the last time point would coincide with the terminal stage of the disease. In all cases the first serial kill was made at a time point relating to a point approximately halfway through the expected incubation period. Estimation of the incubation periods were made for the i.m. and oral route based on

previous experiments conducted at the Neuropathogenesis Unit using similar, though not the same, model systems. Following sacrifice of the animal the spinal column and brain were removed and stored in 10% formal saline until processing. The length of fixation was approximately one week for the brain and two weeks for the spinal column.

In the case of the animals for the infectivity transport study animals were not sacrificed by CO_2 inhalation because the spinal cord was not required for this experiment. In this experiment two parallel groups of $PrP^{-/-}$ and PrP wild-type mice, 36 mice in each group, were infected intraocularly with ME7 scrapie. At each of six time points six animals from each group were sacrificed and the brain and injected eye removed. The superior colliculus and dorsal lateral geniculate nucleus from the side of the brain contralateral to the injected eye, and the optic nerve attached to the injected eye were dissected and used to produce inoculum for bioassay as detailed above. The time points ranged from 24 hours post injection up to 72 days post injection. This window was selected based on published information regarding the movement of scrapie infectivity through the visual system of C57BL mice that have normal PrP expression (Scott and Fraser, 1987). A larger number of animals were sacrificed at each timepoint than in the larger, route of infection, study in order to produce sufficient tissue, especially optic nerve, for the subsequent inoculation into the bioassay C57BL mice.

For the bioassay individual groups of nine C57BL mice were injected intracerebrally with inoculum produced from pools of each of the tissues harvested at each individual time point from either the $PrP^{-/-}$ mice or the wild-type 129 mice. Therefore for each serial sacrifice point 54 bioassay animals were injected. Unlike the larger study into route of infection where tissues were harvested, processed and analysed as they became available all of the tissues for bioassay were stored, frozen, until the end of the serial sacrifice schedule and all the bioassay animals were injecetd on the same day. Bioassay animals were monitored twice weekly for signs of neurodegenerative disease.

2.7 Determination of Incubation Period.

Incubation period is defined as the time elapsed, in days, between the day of infection and the clinical end point of the disease (Dickinson et al., 1968). In the case of the orally challenged mice the day of infection is taken to be the day of dosing although it is acknowledged that the mice could take up to two days to consume the full dose given (as mentioned above).

Infected mice are assessed by experienced animal technicians and each mouse (as identified by ear-punch and experimental number) is given a rating of 'unaffected', 'possibly affected' or 'definitely affected'. Calculation of incubation period is determined by the end-point which is defined in one of four ways: (1) end-point is the day on which the mouse receives a third consecutive weekly 'definite' rating. (2) The day on which a fourth 'definite' rating is given within five consecutive weeks. (3) The day on which the animal is killed in extremis, or (4) the animal is found dead in the cage having received a 'definite' rating at time of scoring in the previous week. In Chapter 3, unless otherwise stated, the incubation periods referred to are means. These are the mean incubation periods for a group of mice, (± the standard error of that mean).

2.8 Histological Preparation.

Mice were generally sacrificed by carbon dioxide inhalation as this made recovery of the whole spinal cord easier than if cervical dislocation was used. All tissues taken for histological examination were immersion fixed in 10% formal saline at room temperature prior to trimming and processing. In the case of brains and spleens this was for between 24 and 48 hours. For spinal cords the initial fixation was from 10 to 14 days. This was considered sufficient to ensure complete penetration of the fixative through the bone of the spinal column.

Fixed brains were trimmed sagittally, into two pieces. The bisection was made just to the left of midline at a level corresponding to sagittal level 107 in Sidmans mouse brain atlas (see figure 6 for line of incision). This ensured that it was possible to retrieve the maximum sagittal area of the brain. If the brain had been bisected along the midline then the areas exposed at the cut face would be lost when the tissue was trimmed on the microtome prior to cutting of tissue sections for immunocytochemistry and haematoxylin and eosin (H&E) staining. Saggital sections were chosen for use so that mapping of the spread of pathology from the brainstem to the forebrain could be conducted as far as possible given the limitations of an investigation in a single planar section.

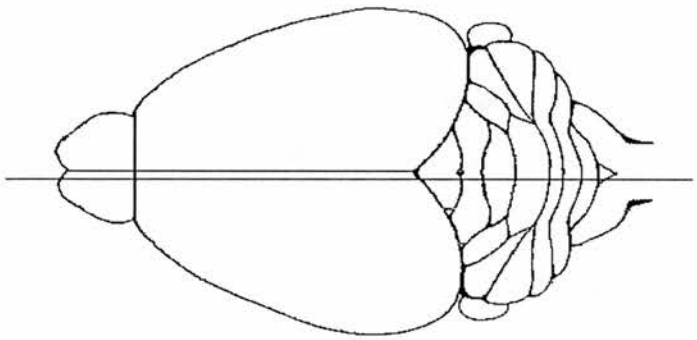

Figure 6. Illustrates the line of bisection made in the brain prior to processing and embedding. This corresponds to level 107 Sidman's mouse brain atlas.

Spinal columns were removed after the brains although it should be noted that all tissues were removed as soon after death as possible to minimise any autolytic damage. Following euthanasia with CO_2, the skin and muscle on the back of the mouse's neck was pared back to expose the cisterna magna. Decapitation was performed with scissors along the line of the cisterna magnum, this made it possible to retrieve the cervical sections of the spinal cord. The spinal cord was fixed and trimmed in situ within the spinal column. It is possible to remove the cord from the column following fixation of the tissue; however, initial trials of this procedure

determined that there was a likelihood of damage being caused to the cord in some cases during removal. Following fixation of the spinal cord it was necessary to decalcify the columns, this was done by incubating the column for 12 hours in Rapid Decal solution. Following decalcification the columns were returned to fixative for a further 24 hours before trimming and processing.

Each spinal cord was trimmed into nine transverse sections; 2 cervical, 4 thoracic and 3 lumbar. One side of each trimmed section of spinal cord was marked with Indian ink to enable accurate orientation of the sections for embedding. The spinal cord blocks were embedded with the rostral face down and marked on the caudal face so as to ensure uniform orientation prior to immunohistochemical staining..

Spleens were taken from some animals at a late stage in the disease incubation time, these were also fixed in 10% formal saline solution. These spleens were embedded whole with the exception of a small transverse section taken from one end of the organ, the standard practice for routine embedding of mouse spleens at the Neuropathogenesis Unit.

All tissues were processed into paraffin wax. This was done on one of the Neuropathogenesis' Units two processing centres, either a Shandon Hypercentre II (Shandon) or the TP 1050 (Reichart Jung/Leica). Although the reagents used for processing the tissues were the same as would be used for the routine work carried out at the Neuropathogenesis Unit it was necessary to increase the time of the processing in most cases (spleens could be processed using routine programs). This is because the saggital sections chosen for this study are thicker than the coronal sections used for routine diagnosis and study at the Neuropathogenesis Unit. This routine sectioning is necessary so that lesion profiling/scoring may be carried out at specific levels (as described in Chapter 1) however, this study is not concerned with the production of classical lesion profiles. Instead the brains that were used in these studies were cut on the sagittal plane for reasons described above. Trimming the

brain into five coronal pieces means that there is a quicker penetration of the processing reagents through the tissue than occurs when there are two large pieces of brain (the sagittal sections) as were used for this investigation, for this reason processing times were increased. The spinal cord sections, although not especially thick, take longer to process due to the presence of residual spinal column material. The general program that was used for tissue processing is given below in Table 3; the stages at which differences were necessary have been noted.

Reagent	Time	Temp/Pressure
10% Formal Saline	5 minutes	Amb/Amb
70% Alcohol (Ethanol)	45 minutes[1]	Amb/P
80% Alcohol	45 minutes[1]	Amb/P
95% Alcohol	45 minutes[1]	Amb/P
99% Alcohol	45 minutes[1]	Amb/P
99% Alcohol	45 minutes[1]	Amb/P
Xyl/Abs	45 minutes[2]	Amb/P
Xyl/Abs	45 minutes[2]	Amb/P
Xylene	45 minutes[2]	Amb/P
Xylene	45 minutes[2]	Amb/P
Paraffin Wax	25 minutes[3]	62^0C/Vac
Paraffin Wax	25 minutes[3]	62^0C/Vac
Paraffin Wax	25 minutes[3]	62^0C/Vac

Table 3: Tissue Embedding Program (Routine; suitable for coronal sections of brain and spleen) Key. Xyl/Abs - Equal parts xylene and absolute alcohol; 1These steps take 50 minutes when processing spinal cord and sagittal brain sections; 2These steps take 35 minutes when processing spinal cord and sagittal brain sections; 3 These steps take 30 minutes when processing spinal cord and sagittal brain sections; Amb - ambient temperature/pressure; P - processed under positive pressure; Vac - processed under vacuum.

Once processed the tissues are embedded in paraffin wax into metal moulds (Tissue Tek). The embedded tissues are then cut into 6μm thick sections on a microtome. The cut sections are floated out on a water bath and picked up onto electrostatically charged microscope slides (SuperFrost*/Plus, Menzel-Glaser).

These slides were chosen in preference to conventional glass slides as the tissues adhere more strongly to them, this makes them especially suitable for immunocytochemistry. Seven serial sections were taken from each tissue. These sections were numbered 1- 7. Section number 1 from each tissue was stained with H&E, automatically on a Jung Autostainer XL (Leica) with the other six sections being set aside for immunocytochemistry.

2.9 Immunocytochemical Techniques.

Brain and spinal cord were immunostained using antibodies raised against the prion protein (PrP) and glial fibrillary acidic protein. Spleens, when they were taken, were immunostained using only anti-PrP antibodies.

The identity, specificity, source and working concentration of the primary antibodies used are given in table 4

Antibody.	Specificity.	Source.	Working Dilution.
1A8	Rabbit Anti-PrP	C.F. Farquhar (NPU) (Farquhar et al., 1994)	1:1500
α-GFAP	Rabbit Anti-cow glial fibrillary acidic protein	Dako (cat= No. Z0334)	1:400

Table 4: Source and specificity of primary antibodies used in this project.

As mentioned above, the tissues were fixed in a solution of 10% formal saline. The fixative works by denaturing and then cross-linking protein chains within the tissue. Because of this mode of action it is a good fixative to use when preservation of tissue morphology is a concern, as is the case in histopathological

scoring. However, this type of fixation can in some cases reduce antigenicity of a tissue by masking certain epitopes. This is the case with PrP immunostaining, and so certain methods of antigen retrieval must be employed to ensure effective immunostaining. To this end there are a variety of methods which can be used. In the case of the work described in this thesis the tissues were autoclaved in distilled water and then treated with formic (methanoic) acid (Haritani et. al., 1994). On the basis of this work, autoclaving has now become a routine step in PrP immunostaining at the Neuropathogenesis Unit.

These antigen retrieval steps are not necessary in the case of GFAP immunostaining, facilitating the automation of the process in these cases. A Cadenza Automated Immunostainer (Shandon) was programmed to immunostain tissue sections with antibodies against GFAP. This ensured consistency of immunostaining and kept between run differences to a minimum. The Cadenza can be used for PrP immunostaining but previous experience [of poor results] and a reluctance to expose the machine to formic acid meant that all PrP immunostaining was done on the bench following the protocol below. The protocol employed by the Cadenza is virtually identical from step 5 onwards. Any differences are noted:

1). Sections are dewaxed and rehydrated through a series of alcohols into water. (Xylene; 99% alcohol; 94% alcohol; 70% alcohol; Water)

2). Sections are autoclaved (Little Sister2 benchtop autoclave, SES) for 15 minutes at 121oC. Sections are cooled rapidly in buffer or more distilled water.

3). Sections are incubated in 98% formic acid for 10 minutes, then washed in distilled water.

4). Sections are incubated in 3% Hydrogen Peroxide/Methanol for a further 10 minutes. This step blocks the action of endogenous peroxidases.

5). Wash sections in buffer, 3 x 5 minutes. Buffer is PBS/BSA (5g BSA/2500ml PBS).

6). Block sections with normal donkey serum (NDS) 1:20 for 30 minutes.

7). Apply primary antibody to sections at required working dilution (see table). Incubate at room temperature overnight. (One hour on the Cadenza).

8). Wash sections in buffer, 3 x 5 minutes.

9). Incubate sections with secondary antibody, donkey anti-rabbit IgG for 1 hour. Working dilution of secondary antibody is 1:40.

10). Wash sections in buffer, 3 x 5 minutes.

11). Incubate sections with rabbit PAP (peroxidase-anti-peroxidase) for 30 minutes. Working dilution of PAP is 1:100.

12). Wash sections in buffer, 3 x 5 minutes.

13). Incubate sections with chromagen, DAB (BDH, Poole, Dorset), for 6 minutes.

14). Wash sections in water; counterstain with haematoxylin (2 minutes); wash in water; "Blue" sections in Scott's Tap Water solution; dehydrate, clear and mount.

Step 14 cannot be performed by the Cadenza and must be done by hand. When immunostaining spleens a different chromagen is used. DAB gives a brown precipitate and this can be confused with haemosiderin, a brown pigment found in the spleen derived from damaged blood cells. For this reason a red chromagen (Vector Red, Vector Laboratories) is used when looking at spleen sections. This

chromagen does not react with peroxidase enzymes and requires an alkaline phosphatase molecule for the precipitate to form. It is therefore necessary to use a secondary antibody that is conjugated to alkaline phosphatase. Alternatively it is possible to take advantage of streptavidin's (or avidin) affinity for the vitamin molecule biotin by using a biotinylated secondary antibody. This can then be linked to a streptavidin-alkaline phosphatase conjugate before addition of the chromagen. When using this system a Tris based buffer (TBS) is used instead of PBS. This prevents interference with the phosphatase reaction of the chromagen.

2.9.1 Immunohistochemical Controls.

Due to the long incubation period associated with TSE infections, which accounts for the protracted nature of the experiments described in this thesis, and the large number of tissue to be immunostained and examined it was not possible to carry out all the immunostaining in a single run. For this reason certain controls had to be put in place to ensure that the quality of immunostaining observed from one run to the next was maintained.

Prior to the outset of the serial kill schedule for this project a mouse, from the Neuropathogenesis Unit general use animal population and infected with the 87V strain of scrapie was sacrificed and it's brain was taken. This mouse brain was trimmed at four coronal levels as is the normal procedure at the Neuropathogenesis Unit to produce the five standard brain segments mentioned above. This material was processed and embedded in paraffin wax as described previously. 6μm sections were cut from this block and these sections were then used as a source of positive control material. By including sections from this single animal in all the susequent immunohistochemical analyses of the experiemtnal tissues and comparing the staining seen in the equivalent material used between runs it was possible to determine that the staining seen in the experimental tissues was result of genuine antibody/antigen interactions and not a consequence of non-specific reactions. The use of this control material also served as a means of monitoring the between run

quality of the immunostaining. In an attempt to minimise the variation of the quality of staining between immunoruns as many variables as possible were controlled and kept constant. Most significantly this meant that single batches of the primary and secondary antibodies were used for all the immunohistochemistry. Other aspects of the immunostaining that were fairly easily controlled were the chromagen and the third stage, peroxidase-anti-peroxidase, reagents were also from a single batch or kit. Despite these controls it is however, inevitable that there will be some variation in the quality and intensity of the immunostaining seen between runs. The reasons for this are unclear but may be influenced by factors such as the quality of the tissue fixation or processing or the quality of the counterstain. These were outwith the control of the author as the equipment used to fix and process the material and the counterstain are communal resources that are heavily used and consequently the reagents involved have to be changed regularly.

Because there was observed variation between immunoruns it was apparent that some form of operator intervention would be required in order to produce the most meaningful results from the image analysis system (described below). The degree of inter run variation, whilst not suggestive of false results, was sufficient to mean that a single set of parameters regarding the appearance of immunopositivity to the computer system would not be adequate to carry out a full and detailed analysis. The nature of this operator intervention is described below.

2.10 Image Analysis.

Within the bounds of this thesis image analysis can be defined as the extraction of quantitative information from an image. In the terms of a conventional computer system the image merely represents a set of data like a number set in a statistical program. In this thesis the purpose of extracting the data is to allow for an objective (or minimally subjective) and reproducible interpretation of the content of an image.

2.10.1 Elements of the system.

Image analysis systems comprise four general elements:

1. Image capture (Input)
2. Image storage
3. Image manipulation (Processing capability)
4. Image display (output)

A JVC KY-F55B 3-CCD (Charge Coupled Device) colour video camera, with an RM-LP55U remote control unit, connected via a C-mount to a Nikon E400 light microscope,was used for the image input stage, this allows real time capture of images. The captured image has to be converted from an analogue signal to a digital one; this is done using a frame grabber, Snapper-24 (Active Imaging (UK) Ltd). It is the frame grabber that produces an image that is suitable for analysis. This image capture stage is also referred to as image acquisition.

2.10.2 Image manipulation.

A commercially available image analysis package, Image-Pro Plus v3.0 (Media Cybernetics, Maryland, USA), was used for all analyses. This is run under WindowsNT Workstation 4 (Microsoft) on a Viglen Genie 2/266 PC (Viglen Ltd, Middlesex) with 64Mb RAM and 4Gb SCSI hard disk. The PC also has a 2Mb graphics card. This level of specification is sufficient for rapid analysis of images.

The capacity of the hard disk makes it possible to store images on the computer. However, because storing colour images requires so much memory, in practice images were stored on the hard disk for a short time whilst the analyses were carried out. The images were then transferred to Zip Disk (Iomega) for long term storage. Each Zip Disk can hold up to 70 full colour images and these form the basis of an image archive.

Images are displayed on a 17-inch Viglen Envy colour monitor. The images captured by the camera and frame grabber are displayed at a resolution of 568 x 768 picture elements (Pixels) this is a suitable level of resolution for histological work (Wootton, 1995).

2.10.3 Processing of Images.

A standard protocol was devised to ensure minimal variation between samples. This standard analysis is described below.

Image capture has been described previously under the banner of image input. Image preparation involved processes of background correction and conversion of the colour image to a greyscale or black and white image. Processing of a black and white image is quicker than in colour and background correction eliminates aberrant illumination that may occur between sections although this should be minimal due to a stabilised light source. In order to accurately assess the degree of vacuolar pathology within a tissue section it is necessary to firstly define a vacuole in terms that the computer can interpret. This enables the system to differentiate between pathological vacuolation and non disease specific tissue cavitation which may occur as a result of the collapse of blood vessels or general tissue damage that occurs as a result of knife 'chatter' when sectioning. For the purposes of this study this meant that the shape (roundness; determined by the ratio of the two longest perpindicular diameters so that a perfect circle has a roundness value of 1), size (area) and transparancy of a vacuole (a measurement of the amount of transmitted light that passes through the section) had to be defined in such a way that these non-specific tissue aberrations were not included in any measurements. The values for these parameterswere determined with the assistance of experienced histopathology technicians and a series of archive tissues that exhibited varying degrees of vacuolation. When satsfactory identification of vacuolation could be assured the experimental tissues were assessed for pathological damage.

The experimental tissues were examined at nine distinct regions these were:- **1**. Frontal cortex, **2**.Caudate Putamen, **3**. Hippocampus (especially CA4), **4**. Thalamus (including laterodorsal, angular, lateral posterior and anteroventral) nuclei, **5**. Retrorubral fields, **6**. Superior/inferior colliculi, **7**. Parietal cortex, **8**. Parvocellular reticular nucleus/motor trigeminal nucleus and **9**. Interposed cerbellar nuclei. These regions were chosen because they represent the whole of the sagittal plane from the region of the olfactory system to the brainstem area thus providing a complete, though planar, series of results. It is extremely important that the nature of the measurements being made is understood.

For the quantitative analysis of vacuolation and PrP and GFAP accumulation what is actually being measured is the area of a given region of the brain that is occupied by the lesion or by the marker. Because the measurement is of an area within an area; it is critical that all the measurements are done at a single magnification or the parameters defining pathology are re-calibrated for each different magnification used in the study. Calibration of the image analysis system is done with an internal 'line-measure' tool which is a feature of the software and a microscopic scale. To calibrate the system for distance, and consequently area, a line of known length is drawn between two points and the details of the line are stored by the computer. This provides the computer with the necessary reference measurement to calculate areas in the experimental sections. As mentioned above, calibration must be carried out for each different power of magnification that is to be used.

Having determined the parameters for a vacuole and decided upon the areas that are to be examined the actual measurements were made by capturing an image of the brain area of interest and using a series of operations to optimise the image and extract the information that is of interest to this study. In order to ensure uniform treatment of the sections during the count a macro, a short program containing a set of instructions that can be carried out automatically, was written. This overcame potential problems that may have otherwise arisen on account of the analyses being performed over a period of weeks and not all at the same time.

The instructions contained in the macro were designed to make the analysis as quick and as constant as possible. However, the macro could not locate the initial area of interest on a tissue section, this required operator input. Having located the area of interest and acquired the image the macro instructs the computer to convert the image from full colour into a greyscale. The net result of this conversion is a black and white version of the initial image which is approximately one-third of the size (in terms of computer file size, not physical size) of the starting image. This makes the image easier to work with and subsequently the analyses proceed more quickly.

The next step of the analysis is the application of visual filters, in this case the images are sharpened to enhance the edges of the vacuoles. This edge enhancement is achieved by the application of the paradoxically named 'unsharpen' filter. This filter, and others, are features of the image analysis software. They work by performing complex calculations based on the grayscale value of any given pixel and the values of those immediately surrounding it further details of filter function can be found in the manual accompanying the image analysis software.

Having sharpened the image the macro then uses the predetermined parameters to threshold the image, that is identify regions of the image that are occupied by vacuolation, and isolate them from the surrounding tissue. The system then measures the area of each of these vacuoles and displays the cumulative total of these areas. This operation is performed for each of the tissues harvested from each serial kill timepoint and a mean value and standard error are calculated.

In the case of the immunostained slides, those for GFAP and PrP analyses, it became apparent that differences in staining quality that occur between runs and the types of staining that are produced meant that a single set of instructions such as those contained in a macro were not going to be sufficient to perform an accurate analysis. Consequently it was decided that it was necessary to manually threshold

each image in order to extract the maximum information from each section. This operation was carried out on colour images, not grayscale, and the immunostained product was isolated from the image background by using a pixel selection tool that is a feature of the image analysis software. This tool allows the operator to select a pixel which corresponds to an area of positive immunostaining, the computer will determine the value of this pixel and isolate all of the other pixels of that value in the image. In this way it is possible to separate the pixels that represent the chromagen from the rest of the image. The area occupied by the immunostaining is then determined by summing the areas of the individual pixels. As in the case of the vacuolation assessment this operation is performed on equivalent sections from the other animals sacrificed at the same timepoint and a mean value and standard errors are calculated for each of the nine brain regions in the study.

Although this manual thresholding of the immunostained sections is acknowledged as a source of bias and error the fact that all the thresholding operations were carried out by a single operator ensures that the bias across the range of sections is uniform and therefore does not affect the overall result.

The standard analysis protocol can be divided into four principal steps, as summarised in Table 5.

Step	Operation	Considerations	Tools Employed
1	Image Capture	Variability of Lighting. Camera/I.R. Response.	Stable Light Source. I.R. cut filter.
2	Image Preparation	Edge Definition. Speed of Operation.	Sharpening Filters. Greyscale Conversion.
3	Segmentation	Defined features of interest.	Thresholds. Roundness. Area. P2A.
4	Measurements	Defined area of Interest	AOI tool. Measure tool

Table 5. Outlines the principal steps involved in semi-quantitative image analysis and details some of the procedures employed.

2.10.4 Validation Image Analysis System.

In order to qualify the use of a computerised system of pathological measurement it was necessary to assess its accuracy when compared to experienced histopathology screeners. As described above, routine scrapie histopathology is scored on a scale of 0-5 depending on the severity of the lesion. The method of validating the computerised system is detailed in Chapter 2. Briefly, a series of pathological specimens, representing all categories of severity, were captured and transformed into digital (computerised) images. These images were then scored from 0-5 by three independent screeners. The averages were calculated and assigned to the respective image. The degree of vacuolation was then measured in each of the images using the system and macro outlined above. The extent of vacuolation in each section was measure as an area (μm^2). These measurements were then assigned a score of between 0-5 depending on the assessment of the screener. An average area of vacuolation for each score was calculated and a graph of 'average area of vacuolation' against 'pathological score' was plotted in order to demonstrate how well the computerised system could differentiate between different degrees of pathology.

2.11 Kinetics of Pathology.

In an attempt to make a meaningful comparison between the different experimental groups a method of examining the way in which the pathology in a given region changes with time was developed. In order to do this a way of standardising the non-uniform incubation periods had to be devised. This was done by converting the incubation period in to a linear scale of 100 divisions for each model. The day of injection is day zero (0) and the terminal stage is 100. In this way percentages of incubation periods and the amount of pathology present at the times relating to those percentages can be directly compared. Three regions were chosen for this examination, the thalamus, the hippocampus and the frontal cortex and 'kinetic curves' for each region were constructed.

2.12 Comparison with Human Tissue.

In conjunction with the National CJD Surveillance Unit it has been possible to study examples of sporadic, iatrogenic (as a result of growth hormone therapy) and new variant CJD. A qualitative study of similarities and differences in the patterns of lesion distribution and type of lesion (especially in the case of PrP deposits) that are seen in these different human diseases and the animal models under investigation was carried out. The human tissues were obtained from the National CJD Surveillance Unit in Edinburgh where the sections are routinely stained with haematoxylin and eosin and immunohistochemically for PrP (Bell and Ironside, 1993).

Results.

3. Results.

The results of this work are presented in such a way as to make comparisons between different routes of infection more straightforward. For this reason each of the three pathological markers of TSE infection that are under investigation (vacuolation, PrP accumulation and GFAP accumulation) will be dealt with individually. The significance of the results and the profiles they form as a whole will be discussed in Chapter 4. Unfortunately no valuable information could be extracted from the spinal cords of these animals. Because the cords were fixed, processed *in situ* (that is still enclosed in the spinal column) it was necessary to decalcify in order to make the sectioning easier. It appears that the decalcification agent used damaged the tissue as well as demineralising the bony column. The result was that all the spinal cord sections exhibited high levels of background making the detection of PrP by immunohistochemistry impossible. This was unfortunate and with hindsight it is now apparent that removal of the cord from the column, prior to processing, thus negating the need for decalcification, would have been a better course of action.

3.1 Examination of the Role of Route of Infection on Disease Pathogenesis.

3.1.1 Incubation Periods.

The main purpose of the work described in this thesis was to determine the influence that route of infection has on the eventual disease phenotype. For the purposes of presenting the data generated by these experiments, phenotype can be described as the combination of incubation period, degree of vacuolar degeneration, hypertrophy/hyperplasia of astrocytes (as indicated by increased GFAP production) and accumulation of the PrP protein. These four indices of pathogenesis and pathology will be considered below. Each of the four markers will be presented separately so that any route dependant differences can be more readily determined. The results from each section will be combined to provide a more complete picture. This will be discussed in Chapter 4.

The simplest of these indices to measure is the incubation period. In Table 6 the incubation periods for each of the chosen routes of infection are given. These are expressed as 'Mean ± Standard Error' number of days. The number of animals in each group that the means are calculated from is also given.

Route of Infection	Incubation Period(Mean±S.E.)	Number of Animals Affected	Dose(µl)/Dilution
Intracerebral (i.c.)	160±2	10/10	$20/10^{-2}$
Intraperitoneal (i.p.)	251±9	13/13	$20/10^{-2}$
Intramuscular (i.m.)	238±10	10/10	$20/10^{-2}$
Oral	307±2	15/15	$100/10^{-2}$

Table 6 : Incubation period data from experiment 531B-1C
The animals used in this study were C57BL mice there were approximately equal numbers of male and female mice.

Of particular interest in this case is the very small standard error associated with the incubation period of those animals which were infected by the oral route. This is especially interesting when considered next to the data from the intraperitoneally infected series. The data from these experiments suggests that the oral route of infection is potentially as efficient at establishing disease as the other routes under investigation and may provide a more 'natural' model for examining acquired disease in cattle and humans. This is discussed in further detail in Chapter 4.

Prior to the experiment described above, a similar project was undertaken using SV mice. This experiment had to be disregarded at the time due to fears of accidental contamination of the animals with the 301V (mouse-passaged BSE) strain of scrapie. The possibility of a contaminating event came to light when two of the animals in the experimental group developed signs of neurological illness shortly, within 21 days, of being injected with ME7 scrapie. The histopathology on the brains of these animals showed signs of TSE infection and the distribution of lesions indicated that the infecting strain was 301V. It appears that an error in the animal unit led to the introduction of previously infected animals into the population that was

used in this study. Because of this error there was no way to be sure that some or all of the other animals might also have been infected with 301V. Therefore, it was felt that the result of this study may be compromised and the experiment should be restarted with a population of animals that could not have been accidentally infected. The remaining animals in the original experimental group were allowed to develop disease and progress to the terminal stages without any serial culling for tissues. Post-mortem examination of the brains from these animals, including lesion profiling, determined that there had been no contamination and that the animals had succumbed to ME7 scrapie and not 301V. Although this experiment was not valuable in terms of a complete pathogenesis study, the incubation period data gained from it support the contention that the oral route of infection is more efficient than was once thought and may be worth considering as a routine method of establishing a 'natural-experimental' disease. The incubation period data from that experiment, designated 531B-1B are shown in Table 7.

Route of Infection	Incubation Period (Mean±S.E.)	Number of Animals Affected	Dose(µl)/Dilution
Intracerebral (i.c.)	213±21	4/4	$20/10^{-2}$
Intraperitoneal (i.p.)	287±4	42/42	$20/10^{-2}$
Intramuscular (i.m.)	245±6	37/37	$20/10^{-2}$
Oral	312±9	36/36	$100/10^{-2}$

Table 7: Incubation period data from experiment 531B-1B
The animals used in this experiment were SV mice. These have the same *Sinc* genotype (s7) as the C57BL mice used in experiment 531B-1C.

A number of intercurrent deaths in the intracerebral group has restricted the population size and possibly skewed the statistic. It is interesting that that the Oral incubation period does not differ greatly between the two experiments as in experiment 531B-1B the orally challenged mice were dosed with a chilled brain homogenate which was dropped from a syringe into their mouths. This is in contrast to experiment 531B-1C where the mice were dosed with inoculum that had been absorbed onto the surface of a standard mouse food pellet. In the case of experiment 531B-1B it was not possible to ensure that each animals received an identical dose of

scrapie infectivity, this was due to some animals refusing to drink the full amount (100μl) of inoculum. The implications of this will be discussed later.

3.1.2 Sequence of Appearance of Pathological Markers.

It has been shown that the terminal stage signature of pathological lesions for a given agent/rodent strain model is effectively preserved upon passage to mice of the same strain as long as the route of infection is kept constant. It is therefore possible to determine the strain of agent if the strain of mouse infected and the route of infection are known it is worth noting that generally this type of analysis is done in mice infected by the intracerebral (i.c.) route.

One of the noted features of the lesion profile system is that the signature profile is only found at times close to the clinical phase of the infection. Before this time the dynamics of vacuolar degeneration are different in different parts of the brain. This may be a result of the length of time that the lesion has to develop prior to onset of the clinical phase. This in turn is a function of the distribution of infectivity which can be affected by the route of infection (Cole and Kimberlin, 1984).

What is often evident where different routes of infection are employed to infect a uniform strain of mouse with a uniform strain of scrapie are differences in the height and shape of the lesion profiles. For example, a given strain of mouse that is infected by the i.c. route exhibits more pronounced pathology than a mouse that is infected by the i.p. route. Furthermore the profile of the pathological lesion in the i.c. infected animal is stable from approximately halfway through the incubation period (Fraser and Dickinson, 1968) with no significant changes in the shape of the profile between that point and the clinical phase. This is thought to be due to the extended duration of agent replication in the brain (as a result of direct injection) and the consequent widespread infectivity. In an i.p. system the lesion profile will be different to the i.c. profile and will be dynamic for longer as the infectivity spreads. In these cases the shapes of the terminal lesion profiles are generally similar but the preterminal profiles are not. It was the intention of this project to examine these

preterminal events in order to determine the extent that the route of infection can influence the early pathological events.

It was thought that these route dependant differences would be most apparent early in the incubation period of the disease, therefore, with the aim of identifying any route-dependant early pathological changes, a sequential identification and mapping of PrP deposition and GFAP upregulation was undertaken. These two markers were used as they traditionally appear prior to the first vacuolar changes (at least in the case of ME7 scrapie), and there are good immunohistochemical protocols in place to specifically identify them.

Table 8 below shows when the first detection of these markers was made for each of the routes under investigation and how this timepoint related to the eventual incubation period for that particular model.

Route of Infection	First PrP(dpi)	% incubation	First GFAP(dpi)	% incubation
intramuscular	140	58	166	70
intraperitoneal	140	56	140	56
oral	221	72	221	72

Table 8: Details of when the first pathological markers (PrP and GFAP) can be detected following peripheral infection with ME7 scrapie. Information displayed as time post injection and percentage of total incubation period. Percentages based on incubation periods displayed in table 6 above.

Figures 10-15 below illustrate the sequential appearance of PrP and GFAP in each of these cases. These figures are representations of the appearance and subsequent accumulation of PrP and GFAP in the CNS following experimental infection. Lists of brain areas affected are given in Appendix III. Although these maps are accurate, based on experimental observations, due to the constraints of the experimental design they cannot be assumed to be totally comprehensive. There is no doubt that other nuclei in the brain are affected. However, constraints of time did not allow for a more detailed investigation of the whole of the central nervous system. It

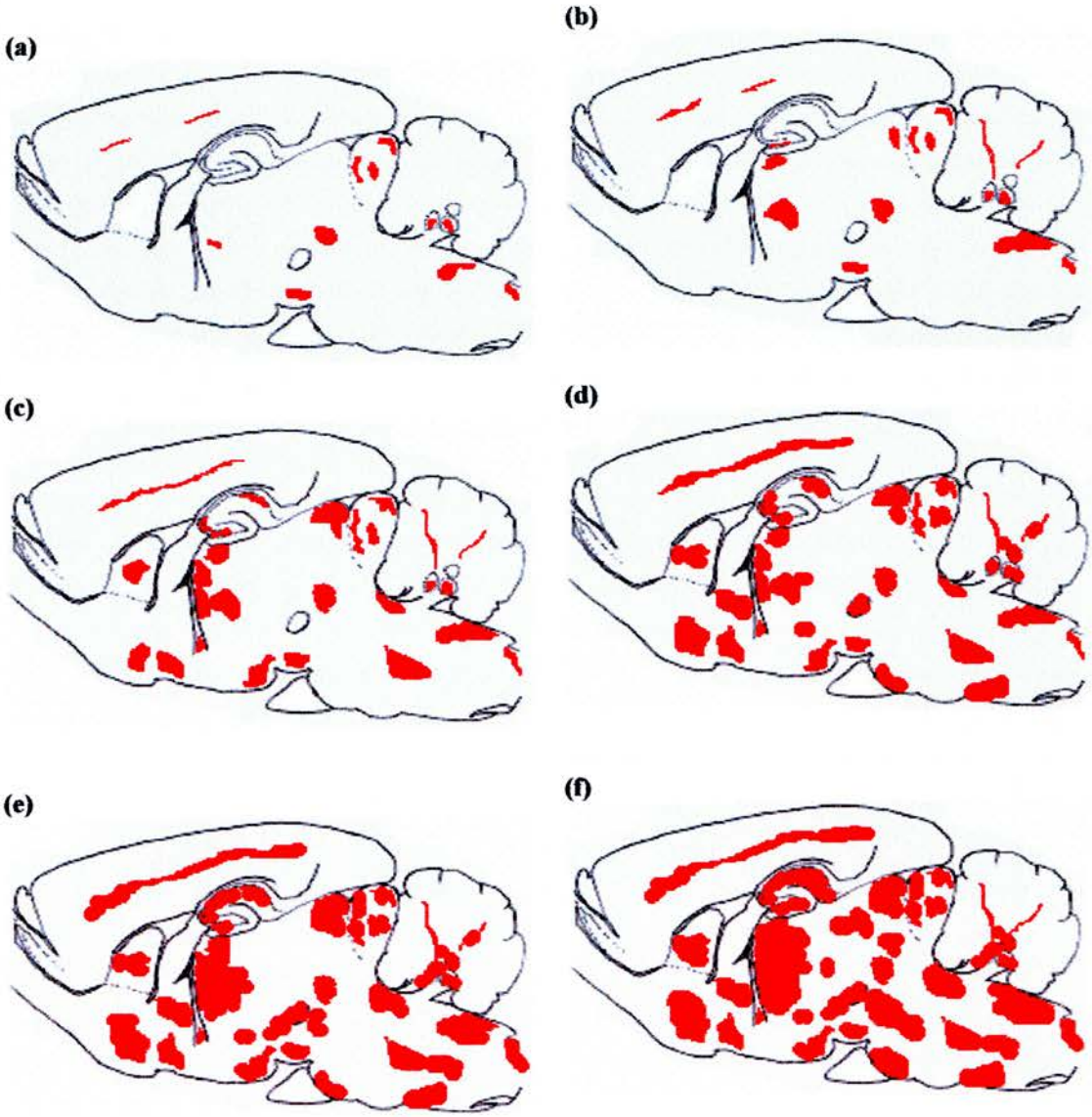

Figure 10(a-f): Sequential deposition of PrP in the brains of mice infected by the i.p. route.
(a) 140 days post injection (dpi)
(b) 166 dpi; (c) 189 dpi; (d) 221 dpi
(e) 231 dpi; (f) 246 dpi.

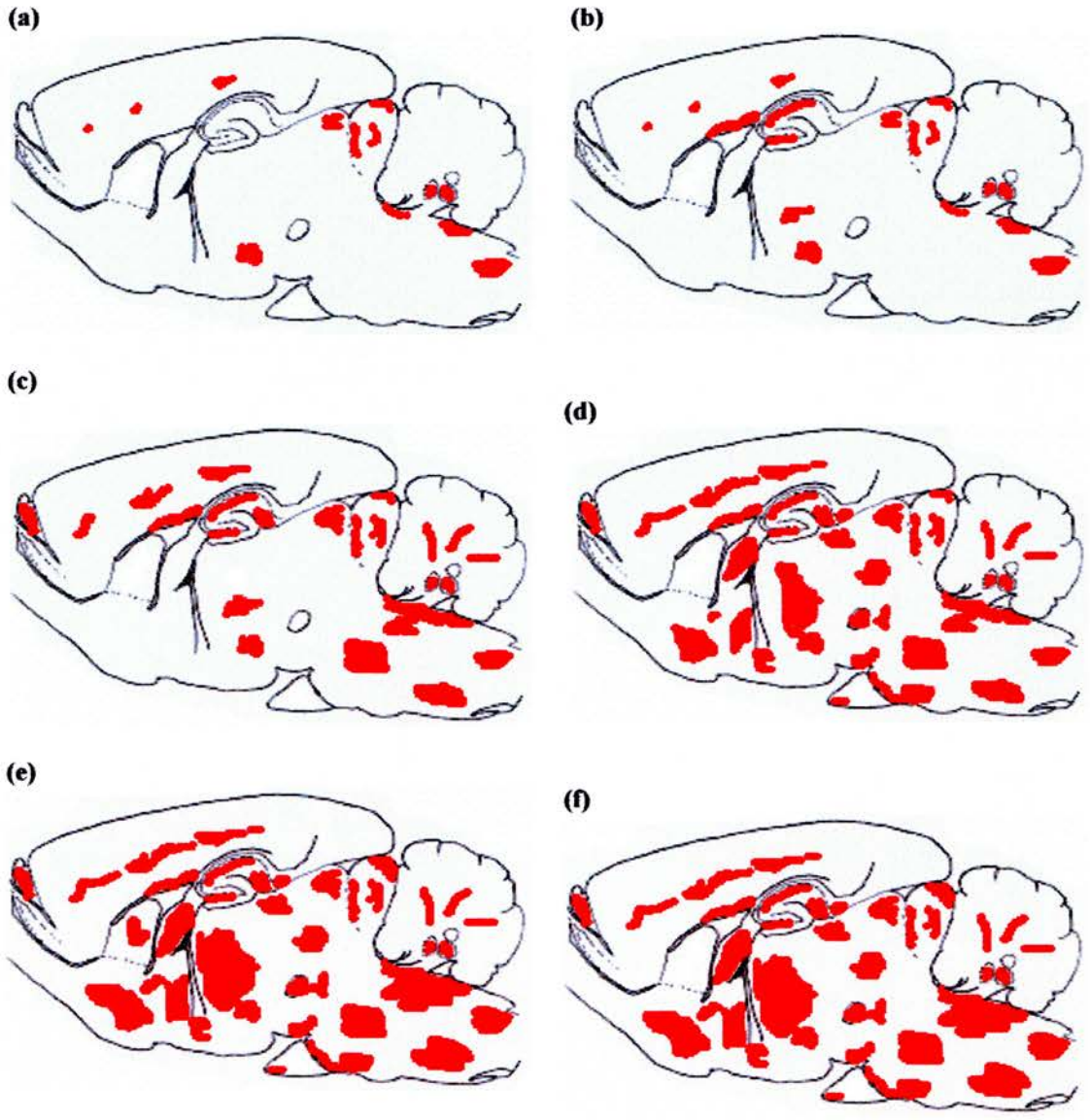

Figure 11(a-f): Sequential deposition of GFAP in the brains of mice infected by the i.p. route.
(a) 140 days post injection (dpi)
(b) 166 dpi; (c) 189 dpi; (d) 221 dpi
(e) 231 dpi; (f) 246 dpi.

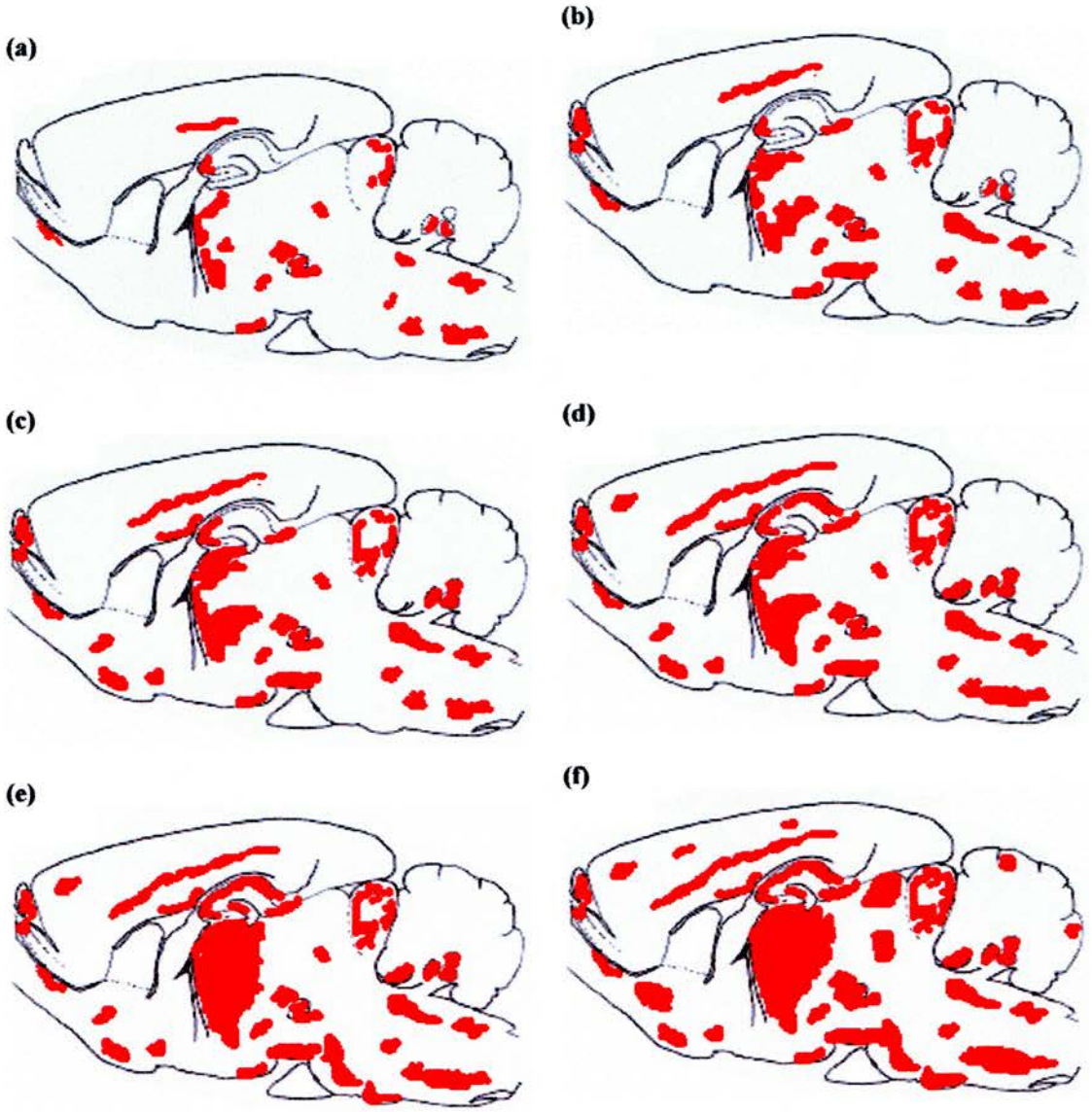

Figure 12 (a-f): Sequential deposition of PrP in the brains of mice infected by the i.m. route.
(a) 140 days post injection (dpi)
(b) 166 dpi; (c) 189 dpi; (d) 221 dpi
(e) 231 dpi; (f) 250 dpi.

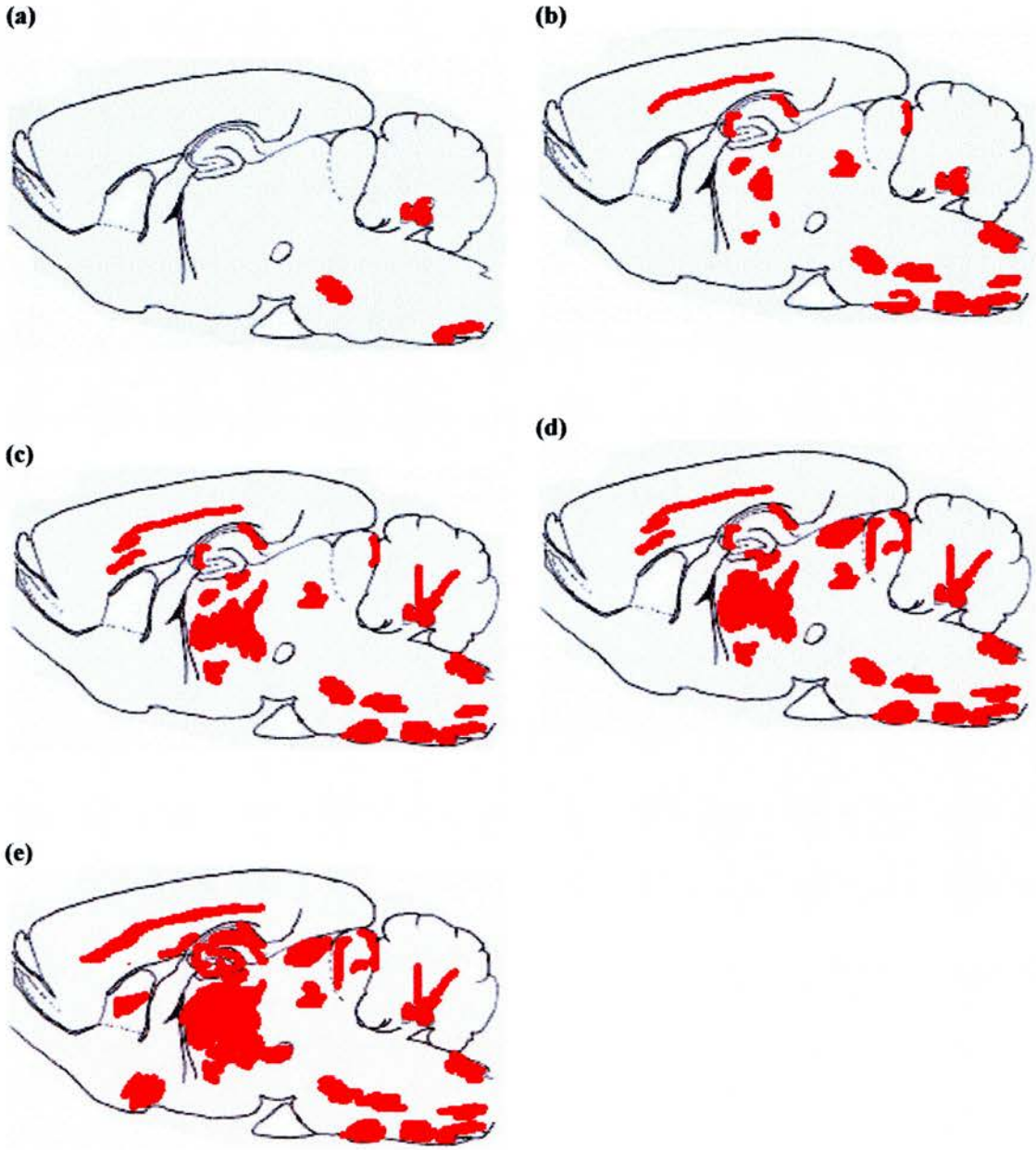

Figure 13(a-e): Sequential deposition of GFAP in the brains of mice infected by the i.m. route.
(a) 166 days post injection (dpi)
(b) 189 dpi; (c) 221 dpi; (d) 231 dpi
(e) 250 dpi.

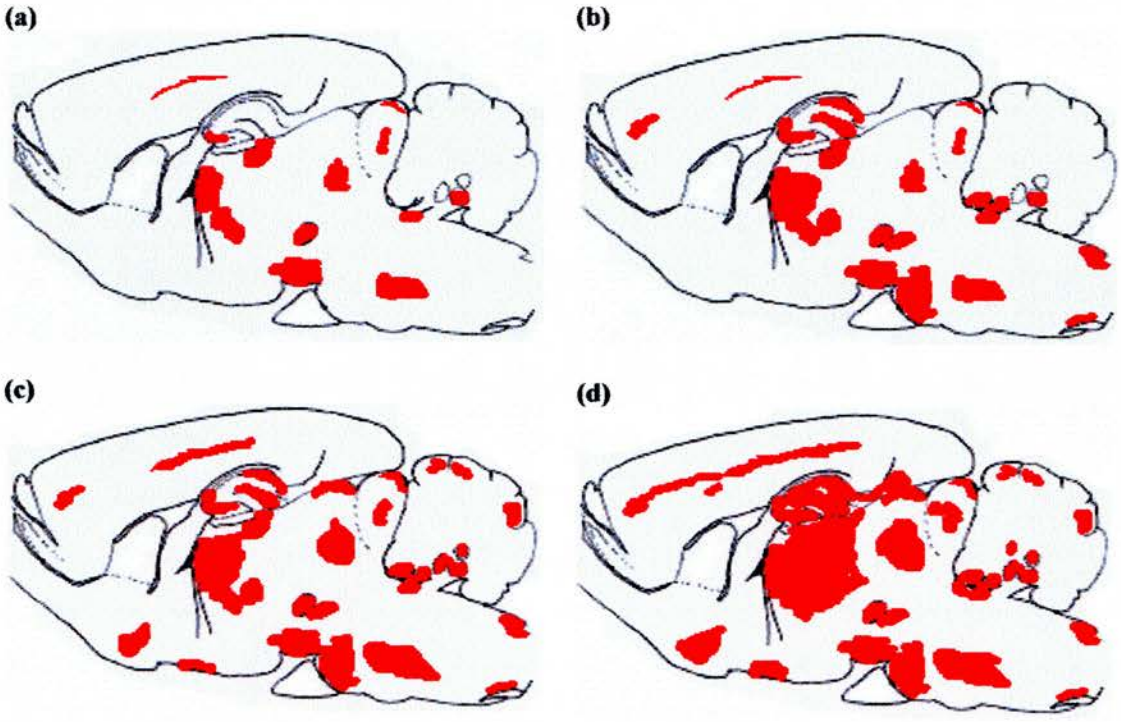

Figure 14 (a-d): Sequential deposition of PrP in the brains of mice infected by the oral route.
(a) 221 days post injection (dpi)
(b) 250 dpi; (c) 279 dpi; (d) 302 dpi/terminal stage.

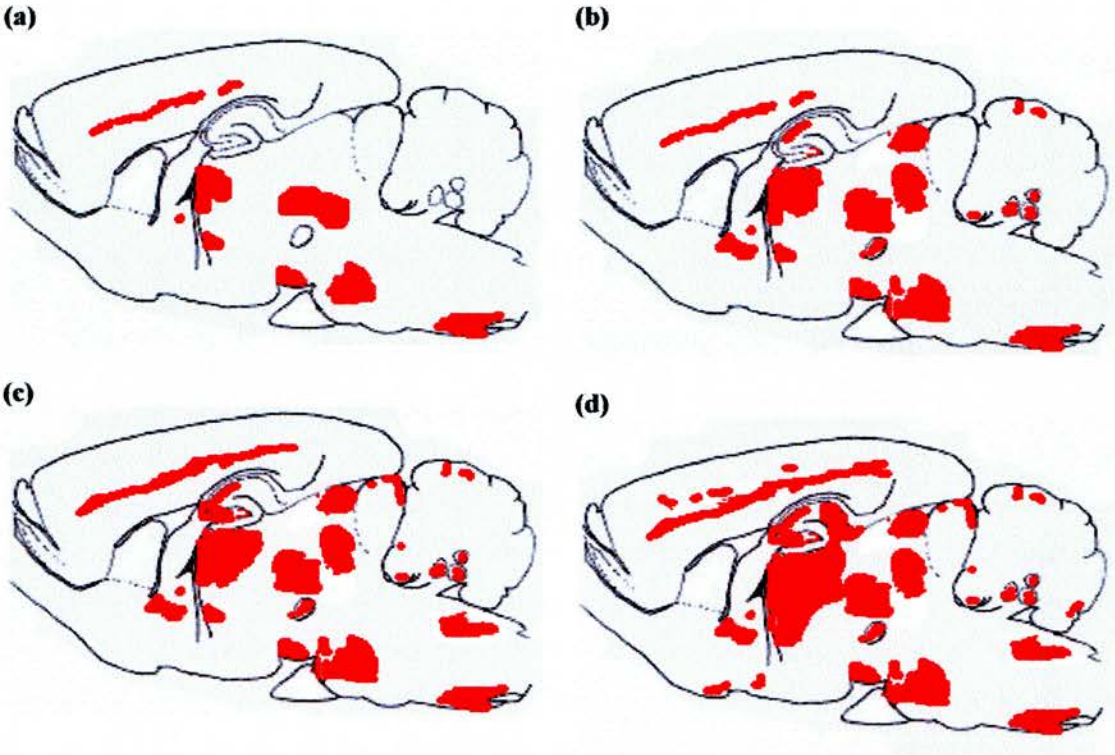

Figure 15 (a-d): Sequential deposition of GFAP in the brains of mice infected by the oral route.
(a) 221 days post injection (dpi)
(b) 250 dpi; (c) 279 dpi; (d) 302 dpi/terminal stage.

is assumed that the results and trends observed in the regions of the brain that were examined can be broadly applied to the CNS as a whole.

3.1.3 Assessment and Comparison of Vacuolar Pathology using Computerised Image Analysis.

In an attempt to identify specific pathological differences between experimental groups that could be attributed to route of infection, computerised image analysis was employed to measure the amount of 'pathology' in nine predetermined areas of the mouse brain. Details of the procedure employed to make these measurements can be found in Chapter 2. The results for each experimental group could then be compared and any route specific differences isolated. Figure 16 shows that the system can be used to detect varying degrees of vacuolar pathology in the validation images and that these differences correspond with the pathological scores given by experienced screeners.

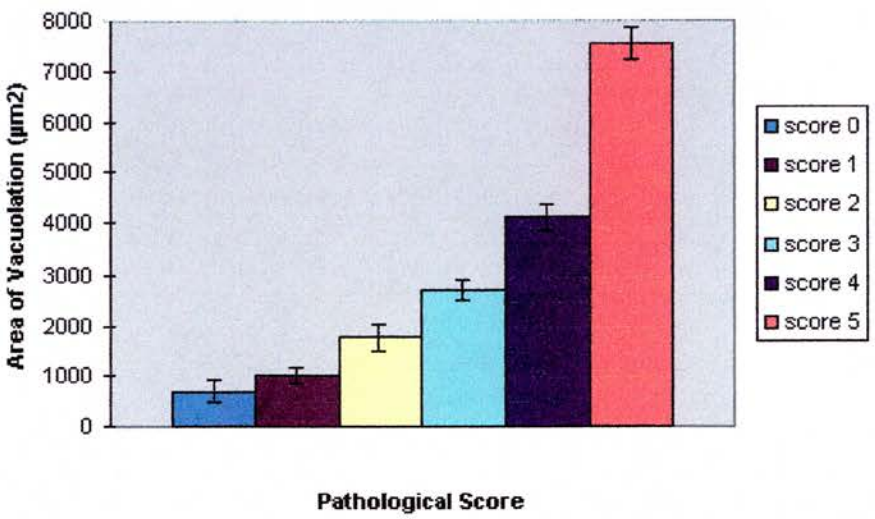

Figure 16: Demonstration that computerised image analysis can clearly differentiate between different severity's of vacuolar pathology.

The graph illustrates clearly the ability of the computerised image analysis system to differentiate between differing severity of vacuolar pathology. There no overlap anywhere on the graph with the exception of scores 0 and 1. This however is

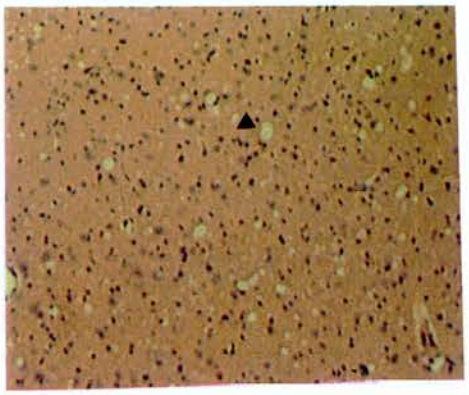

Figure17.

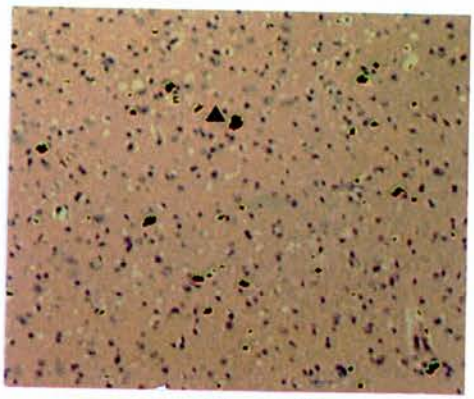

Figure 18.

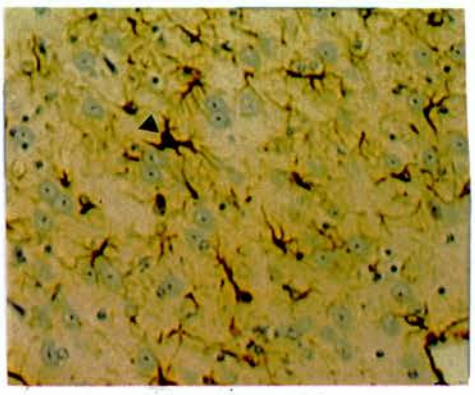

Figure 19.

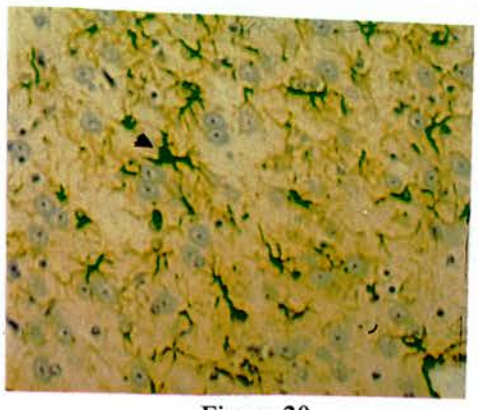

Figure 20.

Figures 17-20. These figures illustrate the capacity of the computerised image analysis system to recognise and measure markers of pathology in scrapie infected mouse brains. **Figures 17** and **18** show how vacuolation in the neuropil is detected. Figure 17 is a brain section before the image analysis system is employed. Figure 18 shows the detection of vacuolation in the same section by overlaying the image with black. Arrow heads indicate the same vacuole in both sections. **(x100 magnification). Figures 19** and **20** show the system being used to measure immunohistochemical product in a section stained for reactive astrocytes. Arrow heads indicate the same astrocyte in both figures. This method of detecting immunohistochemical product can also be used to measure PrP in scrapie infected brains. **(x200 magnification).**

almost inconsequential as a score of 1 is not considered sufficient to deliver a diagnosis of scrapie.

Figures 17-20 illustrate the type of result that the image analysis system produces. They also serve to illustrate that the system does not count non-scrapie associated spaces in the tissue such as blood vessels.

Having determined that the computerised image analysis system was able to differentiate the recognised degrees of vacuolar pathology, at least to the same degree as the three histological screeners who also scored the images, tissues from the experimental animals were examined.

Using the computerised system vacuolar pathology was assessed in the nine brain areas mentioned in Chapter 2.

3.1.3.1 Establishing a Baseline for Quantifying Vacuolation.

The first group of brains that were examined were from the control animals. These animals were injected i.c. with a preparation of non-infected brain and consequently do not develop scrapie. Quantifying the amount of 'vacuolation' in these brains provides a baseline with which to compare infected animals. In the case of these uninfected animals 'vacuolation' is used to describe the spaces in the tissue that can occur naturally, as a result of ageing, or as artefact, for example cracking of the tissue due to knife 'chatter'. It does not specifically denote disease associated degradation of the neuropil.

Groups of three animals were sacrificed at each of four timepoints. The timepoints were selected to cover the expected incubation periods of all the infected groups and are consequently relatively widely spaced.

Figure 21 shows the degree of tissue damage in each of the nine predetermined areas at each of the four selected timepoints.

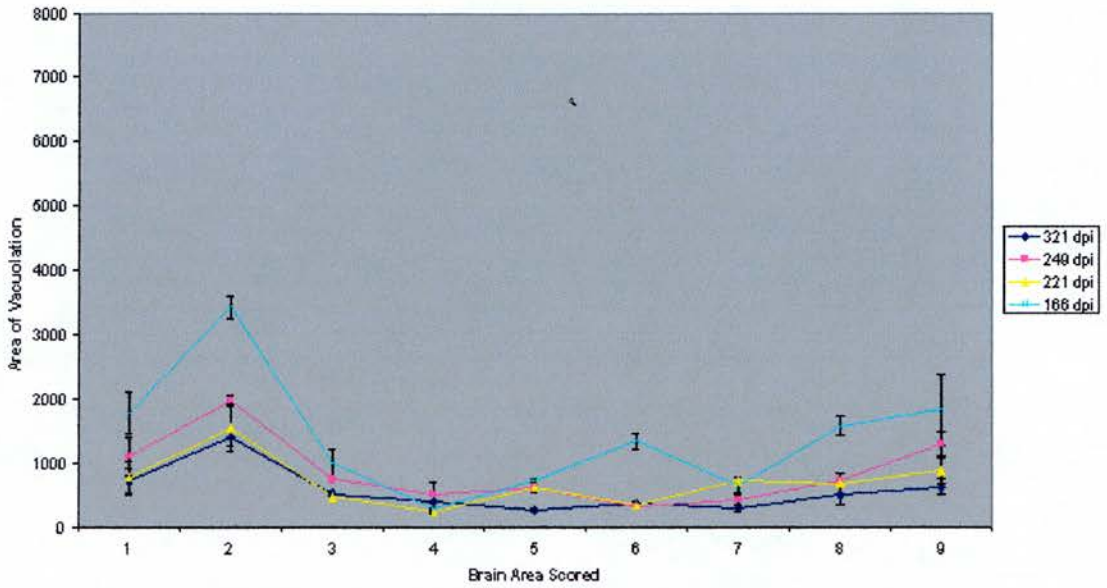

Figure 21: Shows the degree of non-specific 'vacuolation', or microcavitation, in the brain of uninfected animals. This does not change significantly during the course of these experiments.

As can be seen for the graph the amount of vacuolar-type microcavitation in an uninfected brain varies very little with time. The graphs are reasonably flat although there is some variation between brain regions. In particular region 2 and 9 show relatively high amounts of vacuolation This can be explained in terms of the amount of white matter in each of these regions. Region 2 corresponds to the caudate putamen and region 9 to the white matter of the cerebellum. Both of these regions as well as region 8, the brainstem, have a naturally vacuolar appearance on account of the high levels of white matter tracts and fibre bundles in these regions . This is not a disease associated feature and as such illustrates one of the limitations of the experimental design.

The graph shows that at 166 days post-injection there is significantly more vacuolation in certain regions than at any of the other timepoints. This is probably a reflection of the small numbers of animals involved it does not represent a real phenomenon. Occasionally one animal in a serial kill group will exhibit abnormally high level of pathology compared to its group mates and this will greatly influence the mean value obtained for that serial kill group. A table containing the actual

measurements of tissue damage in the brains of the control animals can be found in Appendix IV.

3.1.3.2 Vacuolation in Brains of Orally Infected Mice .

Groups of four orally infected animals were sacrificed at each of seven timepoints and the brains were taken for examination. Each brain was fixed and processed as described in Chapter 2. Figure 22 shows the mean area of vacuolation in each of the nine brain areas at each of the seven timepoints. The seven timepoints cover a period of time that encompasses pre-clinical infection and the terminal stages of the disease

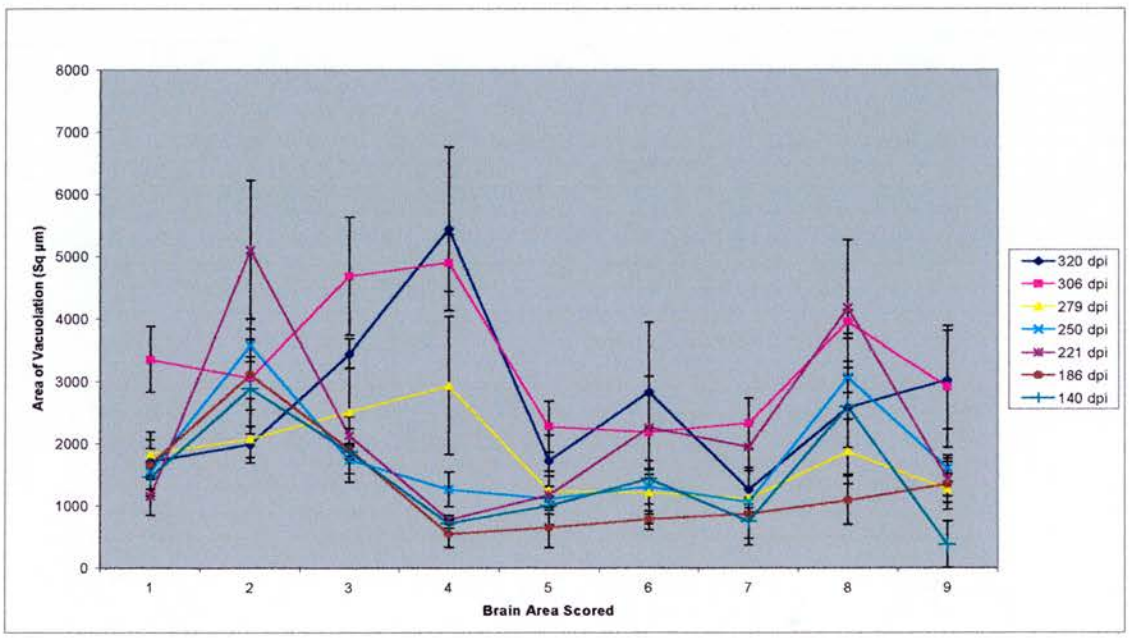

Figure 22: Shows the levels of vacuolation observed in the brain of orally infected animals throughout the incubation period.

As can be seen from the graph at each of the first four timepoints (140 days post injection - 250 days post injection) there is a considerable degree of similarity in the shape and height of the traces. This is especially apparent in areas 1, 3, 4 and 7 (frontal cortex, hippocampus, thalamus and parietal cortex respectively). This could be interpreted as a form of lag phase in the development of the disease. This will be discussed in Chapter 4.

Other findings are the overlapping standard errors and the fact that for the most part the most severe vacuolation is detected at 306 days post injection. Indeed with the exception of the thalamus and the superior colliculus every other region of the brain that was examined returned a more severe assessment of vacuolar pathology at 306 dpi. than at 320 dpi, there is however the caveat that the differences were not significant except in the case of area 3 (the hippocampus). Indeed at 306 dpi the degree of vacuolation is markedly higher than at 279 dpi in all the brain areas examined with the exception of the superior colliculus (area 6). Whether or not this is an actual result or a consequence of the small sample size, and therefore the experimental design., is unclear.

A further feature is the very high degree of vacuolation that was detected in area 2 (the Caudate Putamen) at 221 dpi. There is a similar, though not as pronounced, result at 250 dpi. The caudate is rich in white matter and it is conceivable that this can produce falsely elevated results. Another explanation might be the small sample size which has the effect of magnifying the importance of one unusually high result.

3.1.3.3 Vacuolation in the Brains of Mice Infected by the Intramuscular Route

Figure 23 shows the degree of vacuolation in each of the nine pre-selected brain areas during the course of infection. As can be seen from the traces on the graph, following intramuscular infection there is what could be considered a broadly linear increase in vacuolation levels at each of the brain areas examined. There is very little difference in the levels of detectable vacuolation between 140 dpi and 166 dpi with both traces being very close together.

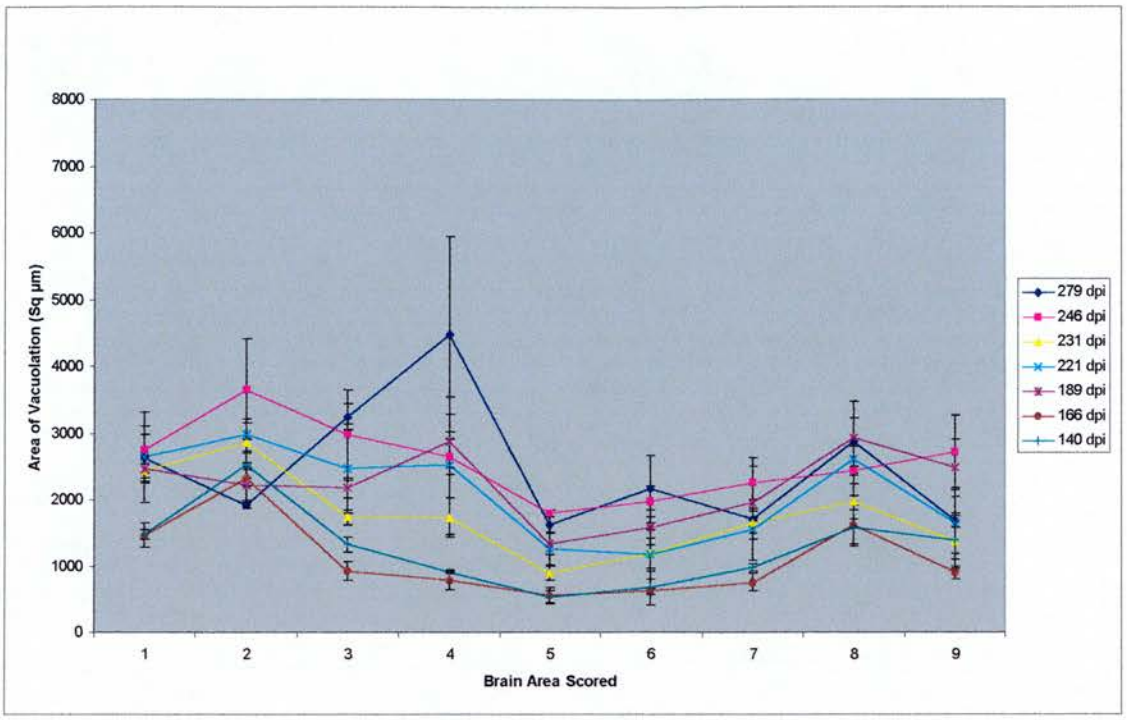

Figure 23: Illustrates the level of vacuolation throughout the brains of animals infected by the i.m. route.

In comparison with the result from the orally infected animals the severity of vacuolation (as evidenced by the height of the trace) does not appear to be as great in the mice infected intramuscularly. Furthermore, with the exception of the result relating to the thalamus at 279 dpi, the results from the intramuscular study indicate an *almost* uniform development of vacuolation. The evidence for this is in the broadly similar shapes of each trace and the way in which they more or less fit on top of each other. This is borne out by the results for PrP and GFAP accumulation following intramuscular challenge which are presented below. This tendency towards regularity between traces is not apparent, at least certainly not to the same degree, in either the orally or intraperitoneally infected mice. This poses questions about differences in peripheral processing of infectivity following route specific challenge with the scrapie agent, this is a point which will be addressed in Chapter 4.

One result which cannot be readily explained is that the degree of pathology (vacuolation, PrP accumulation and GFAP accumulation) at 231 dpi is less (with one exception, the GFAP levels in the superior colliculus) throughout the brain than at the previous timepoint, 221 dpi (189 dpi in the case of GFAP) This is apparently the case for all three markers of disease that have been examined in the course of this work. Again this observation will be discussed further in Chapter 4.

3.1.3.4 Vacuolation in the Brains of Mice Infected by the Intraperitoneal Route.

Figure 24 shows the progressive development of vacuolation in mouse brains following intraperitoneal infection with the ME7 strain of scrapie.
As can be seen from the traces early in relating to the earlier part of the incubation period there is generally little real difference in the height and shape of the graph (and by consequence the severity and distribution of vacuolar pathology) and certainly there is no evidence of any statistically significant differences. This is similar to what is seen in the vacuolar profile of the mice infected orally and could also represent a lag-phase of infection.

As can be seen from the graph the traces relating to the two latest time points are very similar. This is not unexpected as the two traces in question represent a period of only four days. However, the fact that there are differences is interesting, and probably the result of variables in sampling and incubation period range. The especially interesting feature of this result is the way than the trace relating to 231 dpi is very much higher than the trace relating to the terminal stage of the infection in certain areas of the brain. This is not a phenomenon observed in either PrP or GFAP accumulation (See figures 27 and 31 below). This will be discussed in Chapter 4. Also, on the whole, the level of vacuolation in the brain following intraperitoneal infection is less than is observed following oral infection. This is a similar trend to that which is seen following intramuscular infection.

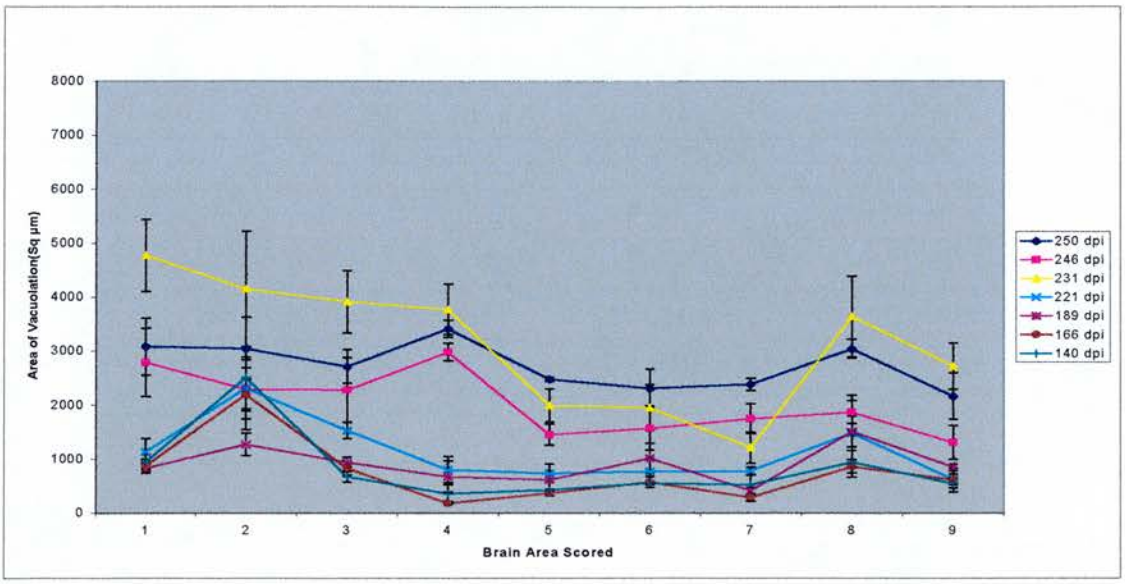

Figure 24: Illustrates the level of vacuolation following i.p. infection.

3.1.4 Comparison of PrP Accumulation Identification of Route Specific Differences.

Measurement of the amount of PrP in each of the brain sections studied was performed using a similar approach as that employed for assessment of vacuolation. There was however one significant difference in the protocols employed. Whereas the parameters defining a vacuole (in terms of its' size and shape) were constant , and consequently amenable to automation, the definition of positive immunostaining is not as straightforward. For each section that was assessed, individual thresholds had to be set. These thresholds varied between areas within a section as well as between sections and as such are recognised as a source of potential experimental errors. However, it was considered that this method enabled more information to be extracted from each section than if a constant, but subsequently low, threshold had been set. There was no detectable level of PrP in the brains of mice that had been injected with non-infective material.

3.1.4.1 PrP in the Brains of Orally Infected Mice

Figure 25 illustrates the temporal and spatial accumulation of PrP in the brains of mice infected orally with ME7 scrapie at each of five timepoints spanning approximately the final 100 days of the incubation period. At timepoints prior to 221 dpi there was no detectable PrP.

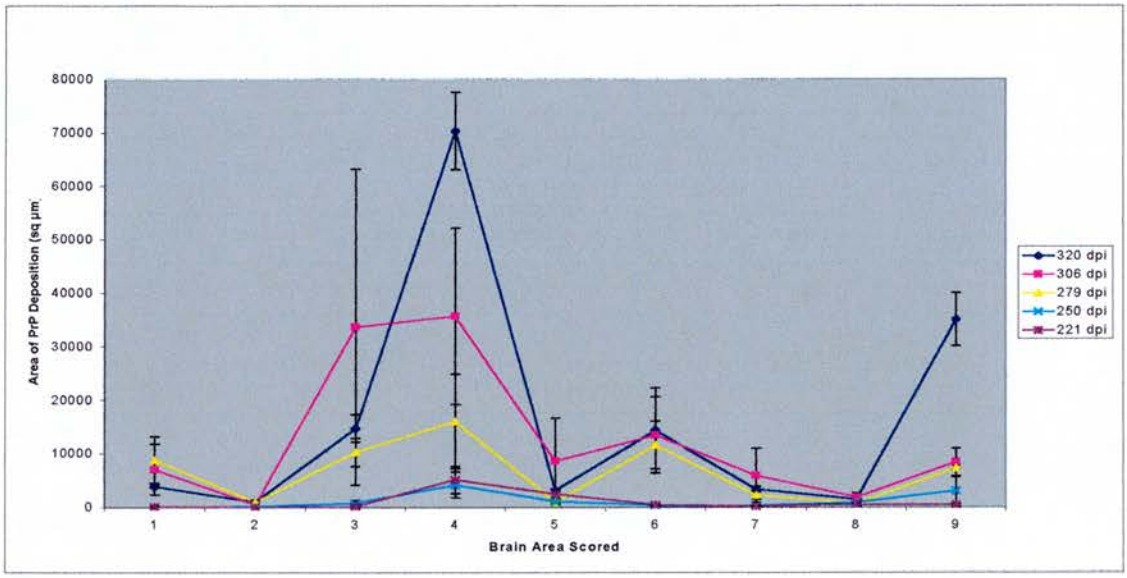

Figure 25: Progressive PrP accumulation throughout the brain following oral infection.

From this figure it can be seen that there is a progressive increase in the amount of PrP that accumulates in the brain and that certain areas of the brain are more susceptible to PrP accumulation than others. In particular the thalamus, area 4, displays not only a very high level of PrP at the terminal stage of the disease (when compared to the other routes of infection that were investigated) but also demonstrates a much quicker accumulation of the protein - when compared to the other brain regions studied - as indicated by the steepness of the trace.

The level of PrP seen in the hippocampus (area 3) at 306 dpi is elevated over the level seen at the terminal stage, 320 dpi. This is not in keeping with the general trends that can be extracted from the result. As mentioned above there was no detectable PrP prior to 221 dpi. However between 221 dpi and 250 dpi there is very little difference in the measurable amounts of the protein that are present in any of the

brain areas. At 279 dpi there is a marked increase and this represents the start of a significant build up of PrP in the brain. The pattern of deposition of the protein (as shown by the overall shape of each trace) is similar over the final three timepoints. This is suggestive of a steady increase in protein deposition over these brain areas.

3.1.4.2 PrP in the Brains of Mice Infected by the Intramuscular Route.

Figure 26 shows the result of the measurement of PrP levels in the brains of mice that had been experimentally infected by the intramuscular route.

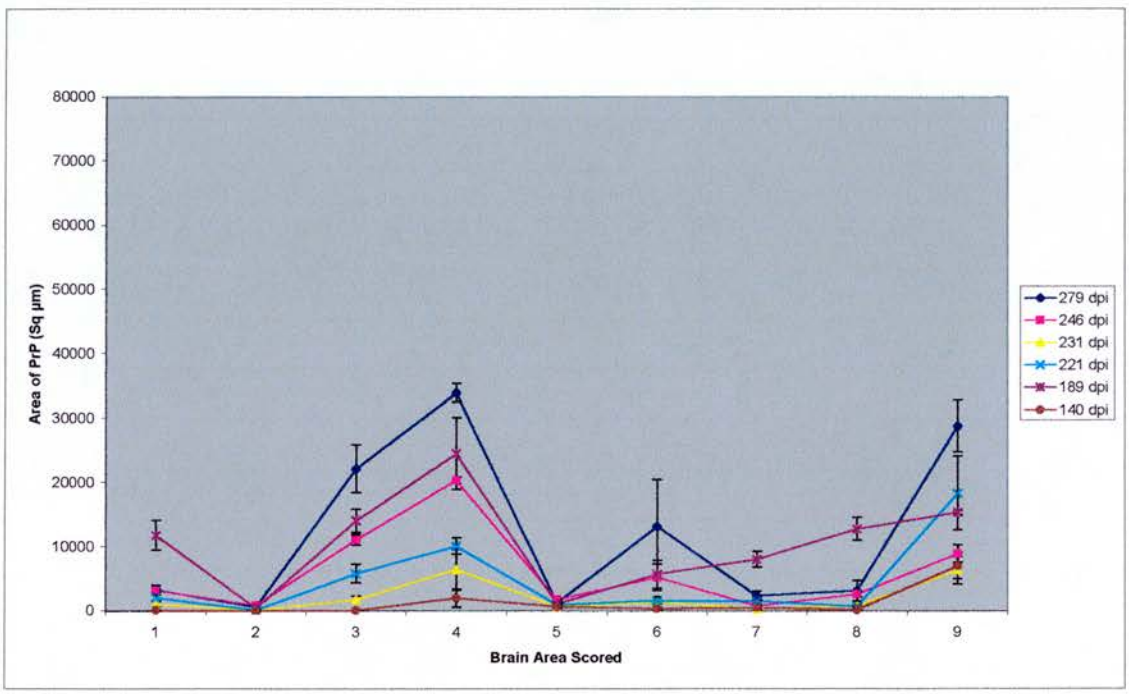

Figure 26: Progressive PrP accumulation in the brains of animals infected by the i.m. route.

This clearly illustrates that the maximum amount of PrP detectable in these brains is in the thalamus (area 4). This is the same as was seen in the brains of the orally infected animals. However, the actual amount of PrP that could be measured in these animals was approximately half the amount that was detected in the orally challenged mice.

For the most part the PrP detected in these brains follows a pattern where the levels in a given area relative to any other area follow a similar trend. The exceptions

to this are **i)** areas 7, 8 and 9 where at 189 dpi the level of detectable protein does not follow this trend and **ii)** The level of PrP that can be detected at 189 dpi throughout the brain is higher than at any other point during the incubation period. This result is illustrated below and appears to be real. Possible reasons for this will be discussed in Chapter 4.

3.1.4.3 PrP in the Brains of Mice infected by the Intraperitoneal Route.

The intraperitoneal route of infection has been widely used to establish disease in experimental animals, especially when questions regarding peripheral processing of infectivity have been asked. Figure 27 shows the progressive deposition of PrP in the CNS following intraperitoneal challenge.

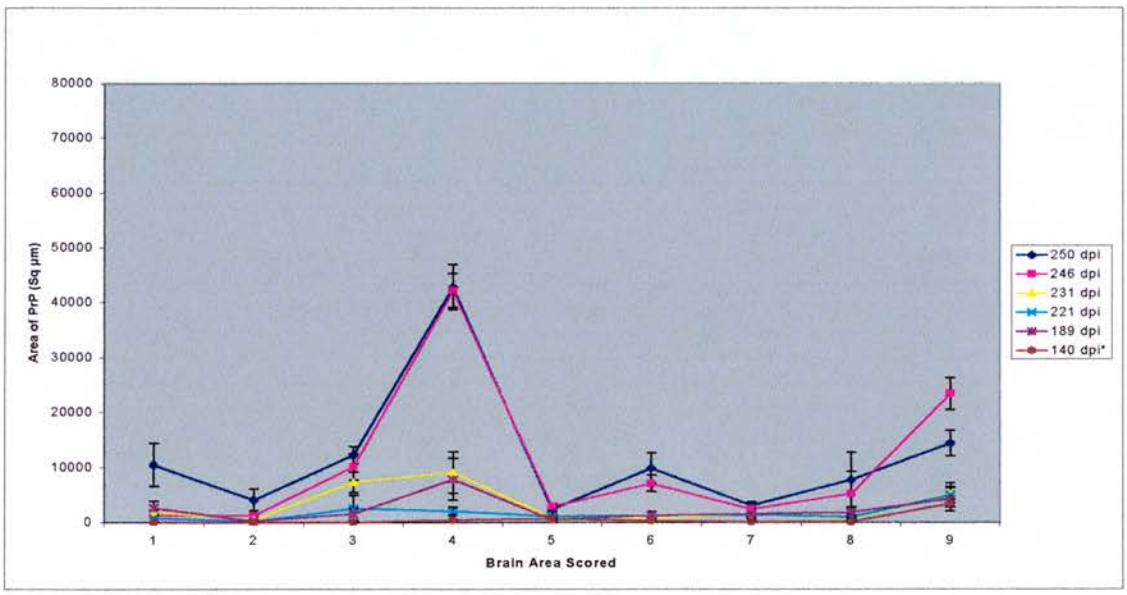

Figure 27: Illustrates the progressive accumulation of PrP in the brain following i.p. infection.

The figure clearly shows that the progressive deposition of the pathognomonic protein is not as irregular as is the case following oral challenge. This figure also highlights the differences that are seen in the actual detectable amounts of protein between the three routes examined. Following intramuscular or intraperitoneal infection the peak amount of detectable PrP occupies an area of approximately 40,000µm^2. Following oral challenge the peak amount of PrP that can be measured

occupies an area of nearly 80,000μm^2. In all three cases these peak measurements relate to the amounts of PrP found in the thalamus (area 4).

As with the previous results there appears to be a lag phase in the deposition of the protein. This is indicated by the low levels of PrP detected throughout the brain during the early stages of the investigation and by the roughly similar pattern of deposition that is seen. For the most part, the detectable levels of PrP in the brain are virtually the same until 231 dpi. At this time there is a noticeable increase in the hippocampus and in the thalamus (areas 3 and 4 respectively). There is also an observed increase at 189 dpi in the thalamus. The reason for this is not clear although the small numbers of experimental subjects are likely to produce some unusual results.

By far the most significant increase that is seen in these cases is in the thalamus between 231 dpi and the terminal stages of the disease at 246/250 dpi. Over this period a large increase is observed in the thalamus. There are also less striking increases in the hippocampus, superior colliculus (area 6), brainstem (area 8) and the cerebellum (area 9). The differences seen in the frontal cortex (area 1) between 246 dpi and 250 dpi are thought to be a function of the small sample size. These unusual results that have been attributed to the small sample size illustrate one of the shortcomings of the experimental design and the difficulty of carrying out a large study of this type.

3.1.5 Comparison of GFAP Accumulation: Identification of Route Specific Differences.

The degree of astrocytosis in the CNS of animals infected with scrapie, or any of the related TSEs, is indicated by the amount of GFAP produced by the astrocyte population. However, not all astrocytes that produce GFAP are activated as a result of scrapie infection.

3.1.5.1 GFAP in the Brains of Non-Infected Mice.

There is a detectable , though comparatively low, level of GFAP throughout the brain. This is not associated with reactive astrocytes such as those seen in TSE infections. Consequently this protein is not an index of pathology. However because the methods used to detect and measure GFAP in the brains of diseased animals will also detect GFAP produced by non-reactive astrocytes it was necessary to establish a 'baseline' level of GFAP against which measurements from infected animals could be compared.

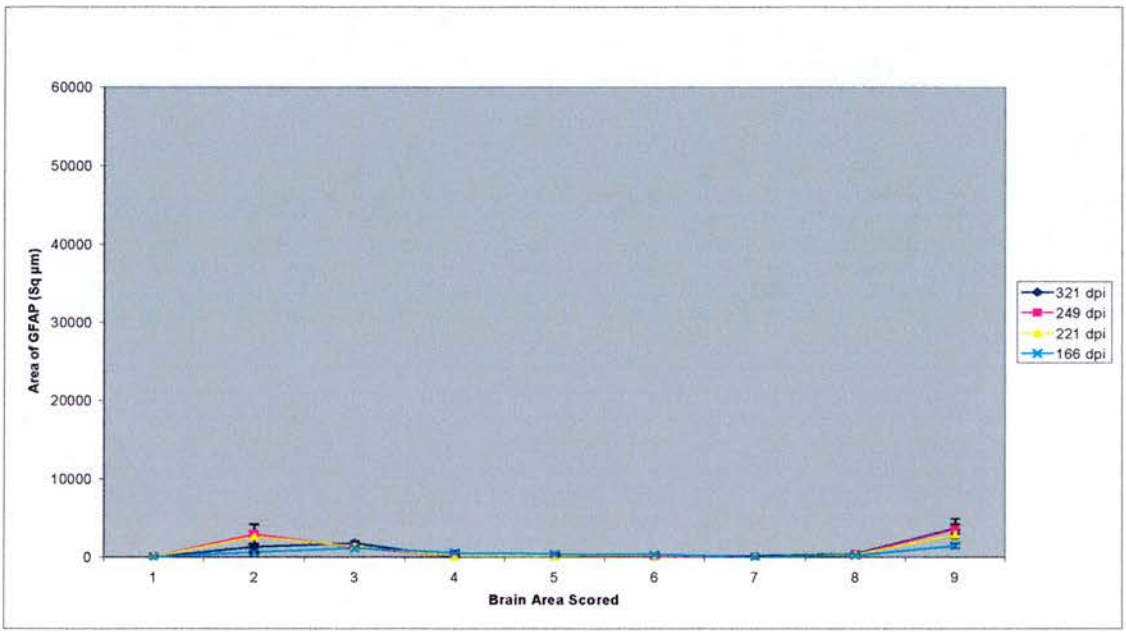

Figure 28: Shows the levels of GFAP that can be observed in the uninfected brain. This signifies the resting state for astrocytes.

Figure 28 shows the levels of GFAP that can be detected in non-infected, *normal*, mouse brains. As can be seen from the figure the levels are virtually constant within a given area of the brain over a period of 166 days. There are two small peaks , one in the caudate (area 2) and the other in the cerebellum (area 9), but these do not represent any statistically significant differences in the levels of GFAP at any particular timepoint in any particular region of the brain. This clearly illustrates that the level of GFAP normally found in the brain is very low when compared to the levels found in a scrapie infected brain (See Below).

3.1.5.2 GFAP in the Brains of Orally Infected Mice.

Figure 29 illustrates the accumulation, over a period of time, of GFAP in the brains of animals infected orally with the scrapie agent. Clearly there is a much greater amount of GFAP in these animals than was seen previously in the brains of uninfected control animals. There is an apparently rapid increase in GFAP levels between 250 dpi and 279 dpi. This is especially apparent in areas 1, 3, 4 and 7; and is indicated by the distances between the two traces relating to those timepoints in those brain areas and the consequent increase in gradient of the traces.

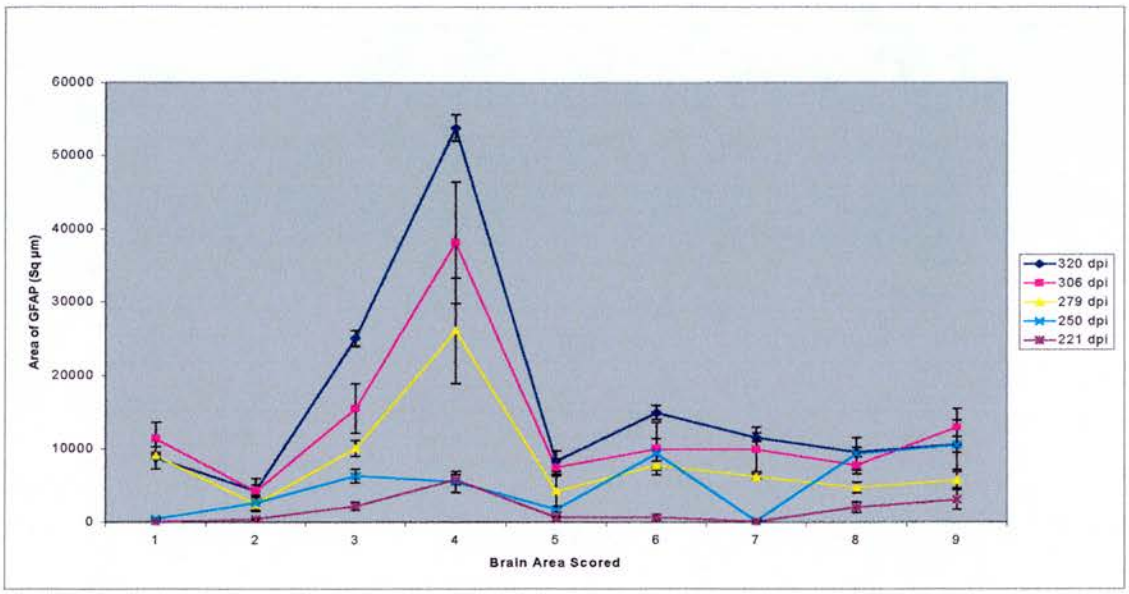

Figure 29: Levels of disease specific GFAP seen in the brain of orally infected mice during the incubation period.

From this figure it can be seen that, as in the case of PrP accumulation (and vacuolation although that result is more confused), the thalamus is the most seriously affected region of the brain (at least within the parameters of this experimental design). Thalamic levels of GFAP in the brains of orally challenged mice is higher than is seen in the brains of mice infected by the other routes under investigation. This observation also holds for PrP accumulation and development of vacuolation. In general animals infected by the oral route have developed more severe pathology than those infected intramuscularly or intraperitoneally.

3.1.5.3 GFAP in the Brains of Animals Infected Intramuscularly.

Figure 30 shows the levels of detectable GFAP at each of six timepoints ranging from very early in the disease incubation period (102 dpi) up to the terminal stages (279 dpi). From this figure it can be seen that the peak levels of GFAP that accumulates following intramuscular infection are much lower, <50% of the peak amount seen following oral infection, yet considerably higher than the peak amount found following intraperitoneal challenge (see below).

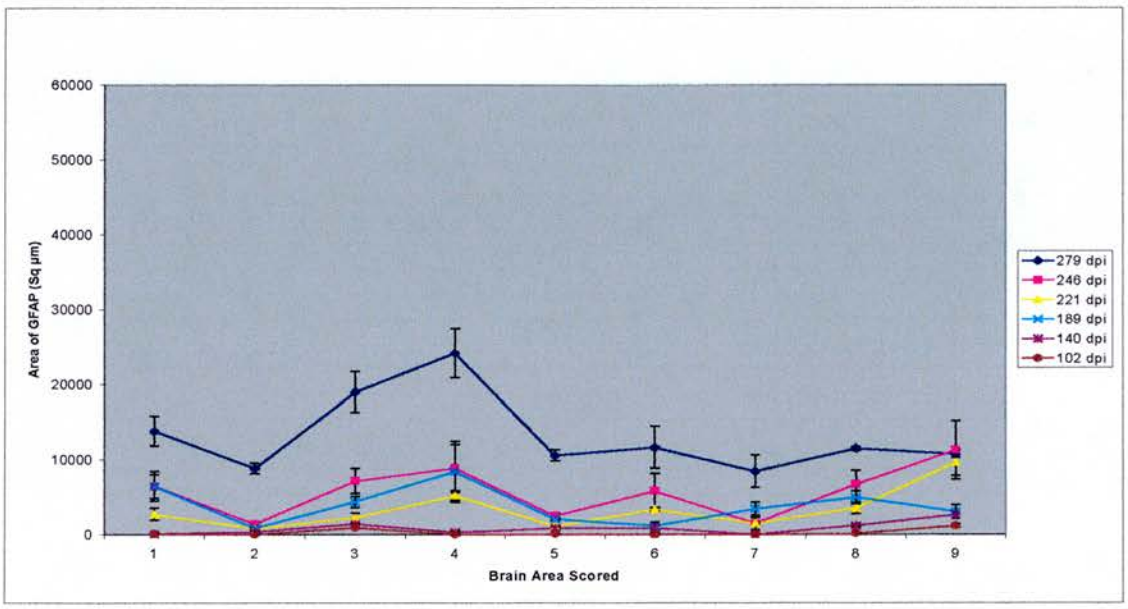

Figure 30: Progressive accumulation of GFAP in mouse brain following i.m. infection with ME7 scrapie.

What is also apparent from this figure is the marked increase seen throughout the brain, with the exception of region 9, between the penultimate and final timepoints. The levels of detectable GFAP at 102 and 140dpi are comparable with those observed in the non-infected control animals. Furthermore the levels of GFAP at the next three timepoints (relating to a period of 57 days) in all regions of the brain are very close together. This is similar 'lag-phase' that is seen in the accumulation of PrP following intramuscular and intraperitoneal challenge. The 'lag-phase' phenomenon will be discussed in Chapter 4.

Another feature of this result that is completely different from the result obtained following oral challenge is the gradient of the traces. Concentrating solely on the final trace in this figure and comparing it with the final trace in figure 29 above it is obvious that the gradients of the respective traces are very different. This suggests that the accumulation of GFAP in the brain following intramuscular infection is a much more widespread event than is the case in orally infected animals where the thalamus is by far the most affected region of the brain.

3.1.5.4 GFAP in the Brains of Intraperitoneally Infected Animals.

Following intraperitoneal challenge with the scrapie agent, the amount of GFAP that accumulates in the brain is less than is seen following either oral or intramuscular infection. Figure 31 illustrates this point. The highest peak in this figure relates to an amount of GFAP in the thalamus that occupies an area of less than 20,000μm^2. This compares to peaks of approximately 22,000μm^2 (intramuscular infection) and greater than 50,000μm^2 (oral infection). The overall shape of the traces are very similar to those relating to GFAP following intramuscular infection. However, from this trace it appears that only the thalamus and hippocampus are especially involved in the development of astrocytic pathology in the late stages of the disease. This is demonstrated by the relatively greater increases in amount of GFAP detected in these regions, between 231dpi and 250dpi. This level of increase is not observed in other regions of the brain. This contrasts with the intramuscular infection where at the late/end stage of the disease all of the regions examined, with the exception of the cerebellum (area 9) show a marked increase in the amount of GFAP over the levels detected at the penultimate timepoint.

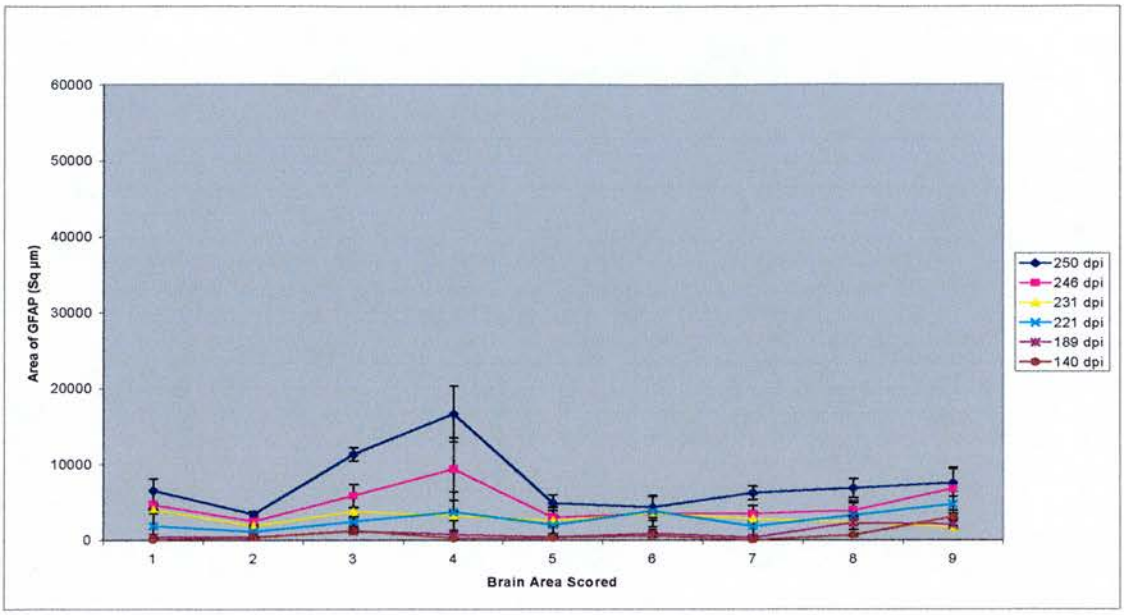

Figure 31: Progressive accumulation of GFAP in mouse brain following i.p. scrapie infection.

The reported increase in the amount of GFAP detected between 246dpi and 250dpi appears to be large, especially in the hippocampus and the thalamus. However given the very small time interval involved it seems unlikely that this represents a true pathological event. Small sample size has probably contributed to this, however this will be discussed further in Chapter 4.

3.2 Kinetics of Disease

The kinetics of the development of pathology were investigated so that it would be possible to directly compare any differences in pathogenesis that might occur as a function of the route of infection. In order to do this a way of standardising the non-uniform incubation periods had to be devised this is described in Chapter 2.

For each of the three routes of infection that were studied the amount of PrP and GFAP in each of three regions of the brain (frontal cortex, hippocampus and thalamus) were plotted against the percentage of the total incubation period that each serial kill date fell on. The hippocampus and thalamus especially were chosen because they appear to be the most significantly involved with regards to PrP accumulation and GFAP expression in each of the three routes examined; the frontal cortex was chosen as less variability was demonstrated in that region when comparing

intraperitoneal routes of infection. The expected similarity in the results of this region will validate this approach for comparing the other areas of interest.

In each of the figures below the rate of accumulation of PrP or GFAP is related to the gradient or steepness of the slope.

3.2.1 Kinetics of Disease in Orally Infected Mice.

Figures 32 (**a-f**) show the rate of change curves relating to the accumulation of PrP (**a-c**) and GFAP (**d-f**) in the thalamus, hippocampus and frontal cortex respectively.

In the orally infected animals the first PrP was detected at a time corresponding to approximately 70% of the total incubation period. Figure 32**a** maps the progressive deposition of PrP in the thalamus of an orally infected animals from this point through to the terminal stage of the disease. The development of pathology exhibits almost exponential behaviour as can be seen from the shape of the curve. The curve is based on the information gathered from five timepoints where pathology was evident. Figures 32**a**(**i-iv**) are graphic examples of the degree of PrP pathology seen in the thalamus at each of those timepoints and clearly illustrate the type of increases signified by the shape of the curve.

Figure 32**b** shows the way that PrP accumulated in the hippocampus of orally infected mice during the course of the incubation period. Clearly this figure shows that the amount of PrP accumulation is not as great as is seen in the thalamus although the rate of accumulation seems to be quicker. A particularly interesting feature and one that is also seen in the frontal cortex, though not in the thalamus, is the way that the graph peaks before the end point of the disease at which point the amount of PrP

(a)

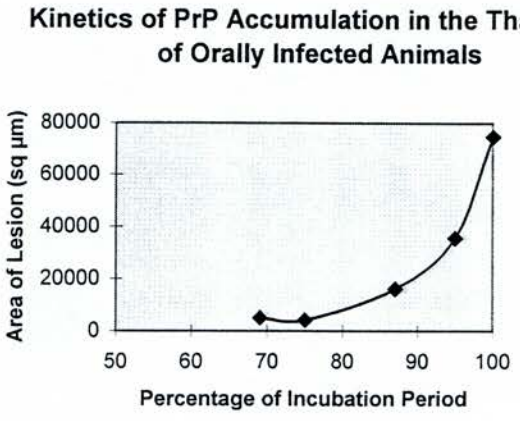

(b)

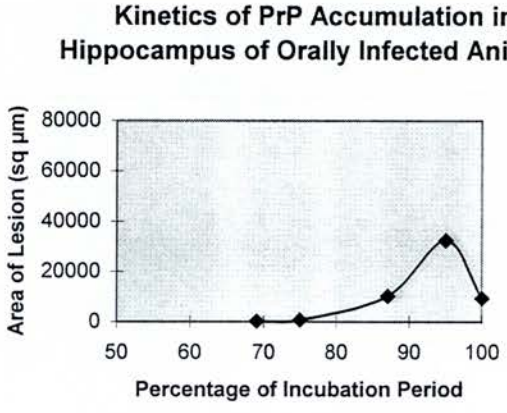

(c)

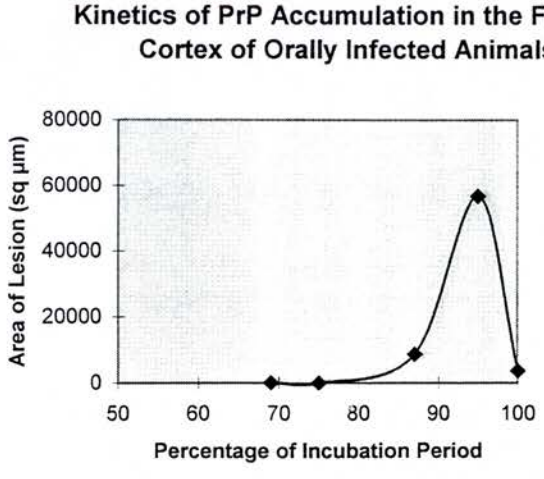

Figure 32 (a-c): Curves illustrate how the amount of detectable PrP changes with time during incubation in the thalamus (a), hippocampus (b) and frontal cortex (c) of C57Bl mice following oral infection with ME7 scrapie.

Figure32a(i).

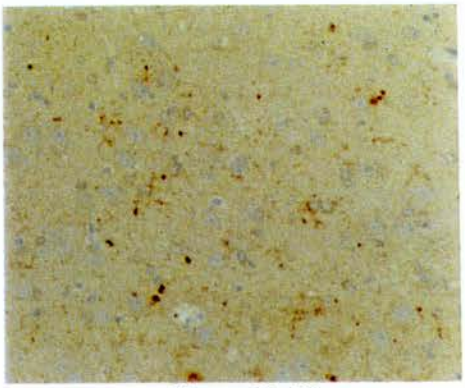

Figure 32a(ii).

Figure 32a(iii).

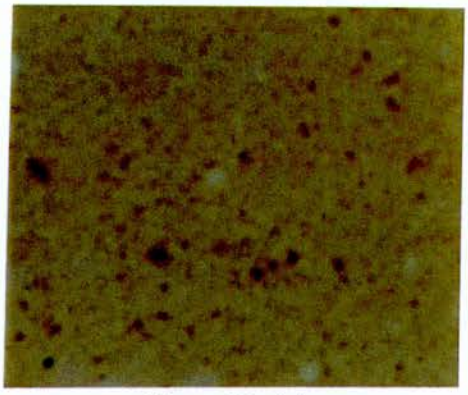

Figure 32a(iv).

Figures 32a (i-iv). Illustration of the changes in PrP pathology seen in the thalamus of orally infected mice during the incubation period. **32a(i)** Thalamus at 75% of total incubation period. **32a(ii)** Thalamus at 87% of total incubation period. **32a(iii)** Thalamus at 95% of total incubation period. **32a(iv)** Thalamus at terminal stage of disease (100% of incubation period). **All figures at x200 magnification.**

Figure32b(i).

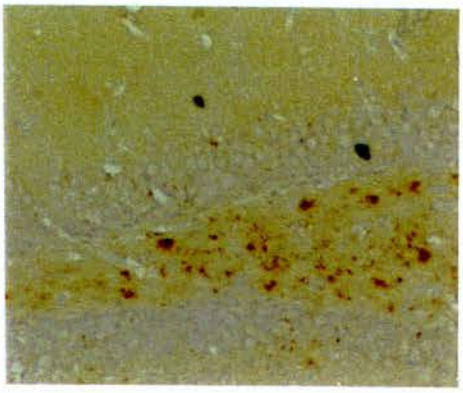

Figure 32b(ii).

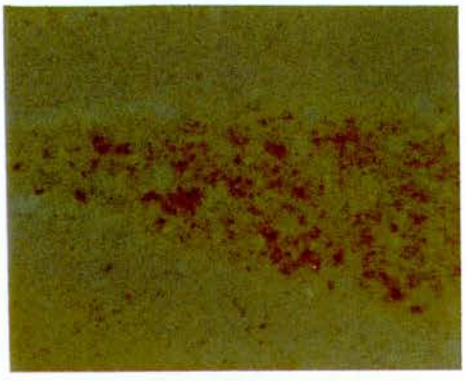

Figure 32b(iii).

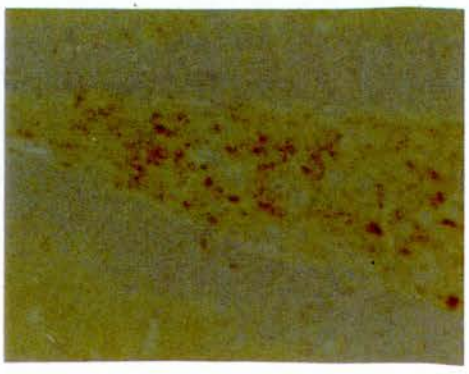

Figure 32b(iv).

Figures 32b (i-iv). Illustration of the changes in PrP pathology seen in the hippocampus of orally infected mice during the incubation period. **32b(i)** Hippocampus at 75% of total incubation period. **32b(ii)** Hippocampus at 87% of total incubation period. **32b(iii)** Hippocampus at 95% of total incubation period. **32b(iv)** Hippocampus at terminal stage of disease (100% of incubation period). **All figures at x200 magnification.**

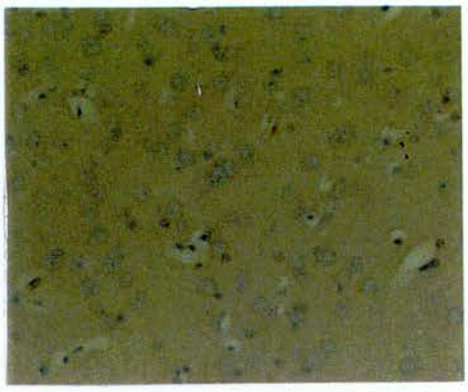

Figure32c(i).

Figure 32c(ii).

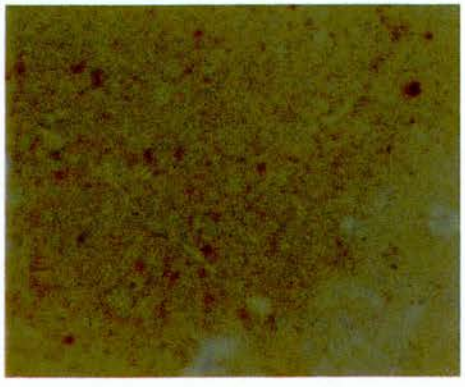

Figure 32c(iii).

Figure 32c(iv).

Figures 32c (i-iv). Illustration of the changes in PRP pathology seen in the Frontal cortex of orally infected mice during the incubation period. **32c(i)** Frontal cortex at 75% of total incubation period. **32c(ii)** Frontal cortex at 87% of total incubation period. **32c(iii)** Frontal cortex at 95% of total incubation period. **32c(iv)** Frontal cortex at terminal stage of disease (100% of incubation period). **All figures at x200 magnification.**

(d)

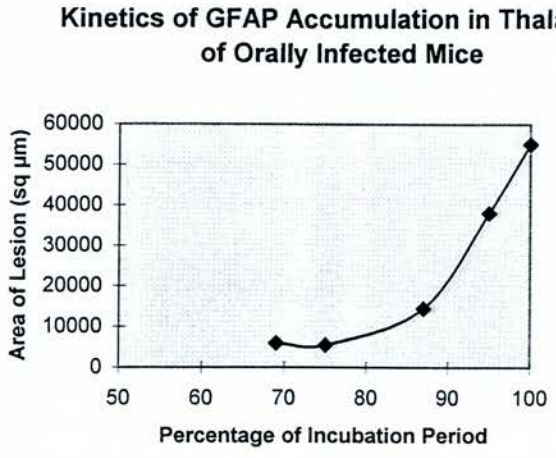

(e)

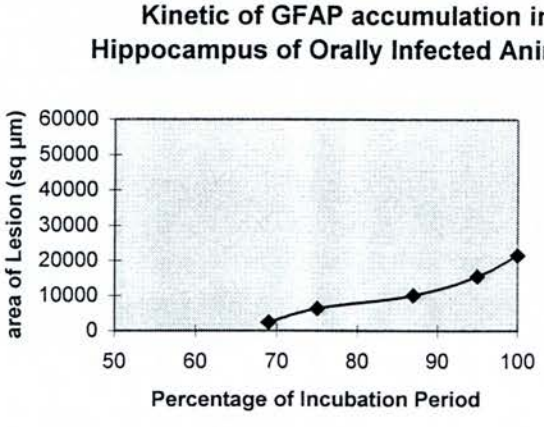

(f)

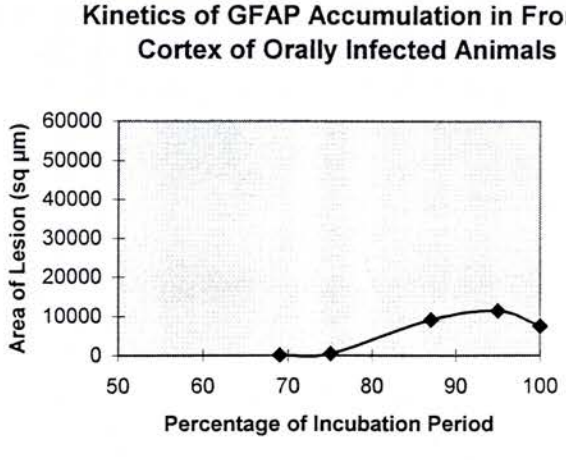

Figure 32 (d-f): Curves illustrate how the amount of detectable GFAP changes with time during incubation in the thalamus (a), hippocampus (b) and frontal cortex (c) of C57Bl mice following oral infection with ME7 scrapie.

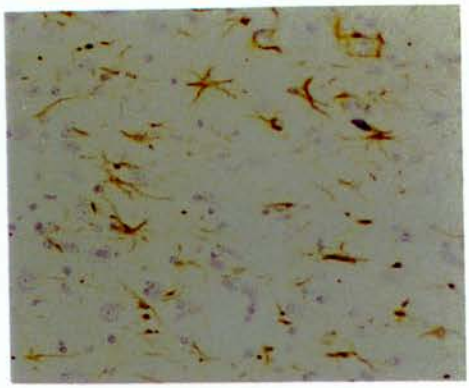

Figure32d(i).

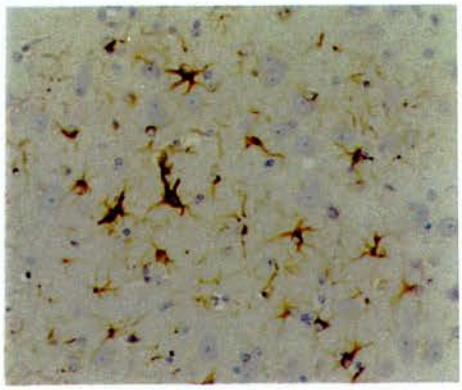

Figure 32d(ii).

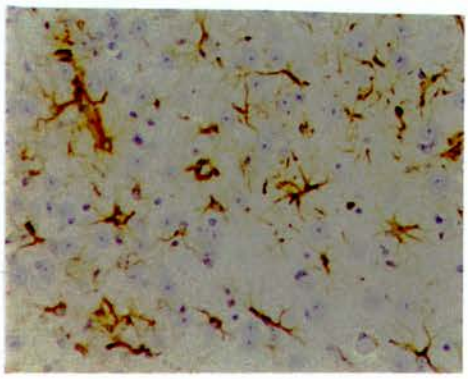

Figure 32d(iii).

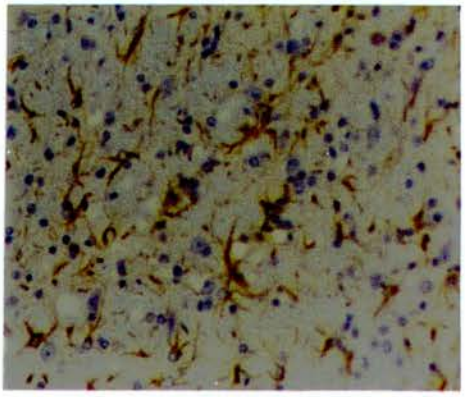

Figure 32d(iv).

Figures 32d (i-iv). Illustration of the changes in GFAP pathology seen in the thalamus of orally infected mice during the incubation period. **32d(i)** Thalamus at 75% of total incubation period. **32d(ii)** Thalamus at 87% of total incubation period. **32d(iii)** Thalamus at 95% of total incubation period. **32d(iv)** Thalamus at terminal stage of disease (100% of incubation period). **All figures at x200 magnification.**

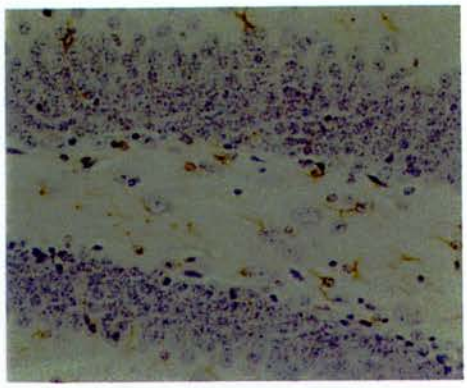

Figure32e(i).

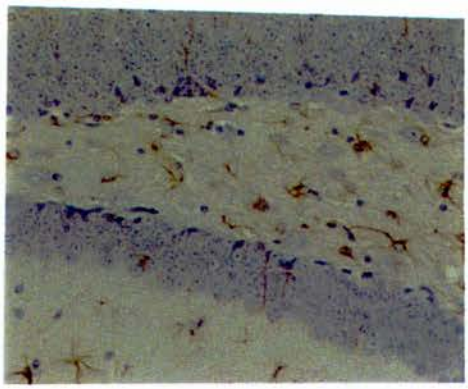

Figure 32e(ii).

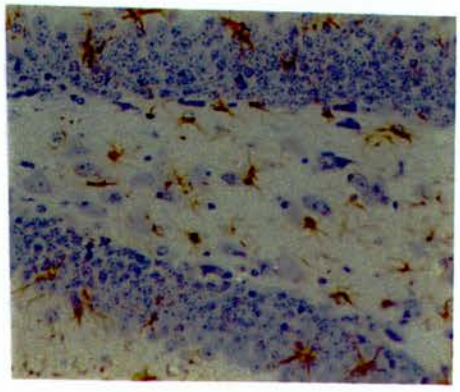

Figure 32e(iii).

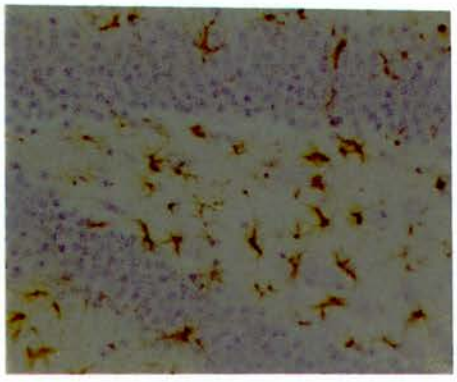

Figure 32e(iv).

Figures 32e (i-iv). Illustration of the changes in GFAP pathology seen in the hippocampus of orally infected mice during the incubation period. **32e(i)** Hippocampus at 75% of total incubation period. **32e(ii)** Hippocampus at 87% of total incubation period. **32e(iii)** Hippocampus at 95% of total incubation period. **32e(iv)** Hippocampus at terminal stage of disease (100% of incubation period). **All figures at x200 magnification.**

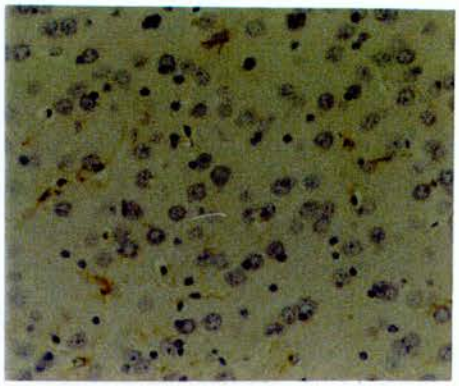

Figure32f(i).

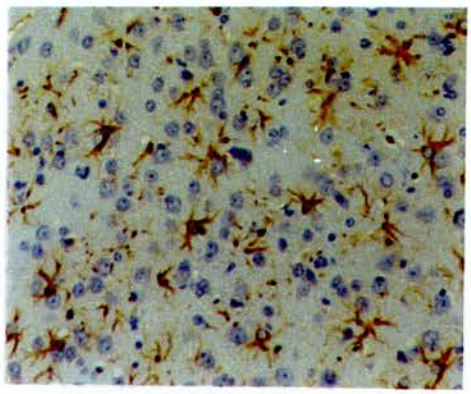

Figure 32f(ii).

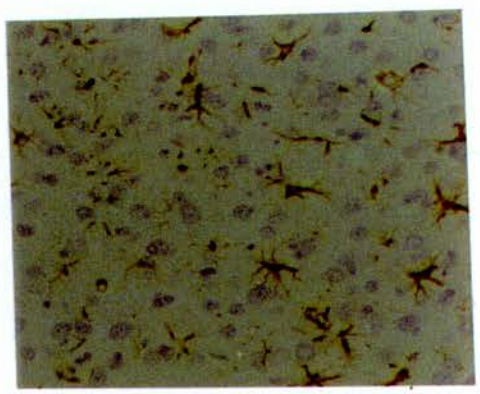

Figure 32f(iii).

Figures 32f (i-iii). Illustration of the changes in GFAP pathology seen in the frontal cortex of orally infected mice during the incubation period. **32f(i)** Frontal cortex at 75% of total incubation period. **32f(ii)** Frontal cortex at 95% of total incubation period. **32f(iii)** Frontal cortex at 100% of total incubation period. **All figures at x200 magnification.**

that can be detected in this region seems to decrease. Figures 32**b**(**i-iv**) illustrate this observation.

The rate at which PrP accumulates in the frontal cortex of the orally infected animals is represented by figure 32**c**. This figure shares a broadly similar shape with figure 32**b** above although the maximum value reached is much higher and the rate at which this maximum is reached is also much higher. This is shown by the gradient of the curve between 85% and 100% of the incubation period. This figure also illustrates a drop-off in the amount of detectable PrP prior to the last timepoint. Figures 32**c**(**i-iv**) show this decrease. Possible reasons for this will be discussed in Chapter 4.

Figure 32**d** shows the progressive accumulation of GFAP in the thalamus of the orally infected animals. The shape of the trace is broadly the same as was obtained for the kinetics of PrP accumulation although the gradient of the curve is not as steep. This result is not unexpected as colocalisation of PrP with reactive astrocytes has been seen in cases of ME7 scrapie. Figures 32**d**(**i-iv**) show the progressive accumulation of GFAP in this region.

Figure 32**e** illustrates the changes through time in the levels of GFAP that can be detected in the hippocampus. Compared to the accumulation of PrP there is an increased initial rate of GFAP accumulation although the peak level achieved is far below peak level of PrP detected. Also, in further contrast with the PrP result is the much more linear appearance of the graph. This suggests that the rate of accumulation of GFAP in the hippocampus occurs at a steady rate after a certain point in the incubation period. It seems unlikely that the difference observed between with GFAP result and that of PrP is a result of the small sample size upon which the results are based; instead this probably reflects a true phenomenon that occurs as a result of oral infection. This pattern is not seen in i.m. or i.p. infection. Figures 32**e**(**i-iv**) illustrate the information extracted from this graph.

Figure 32**f** shows the way in which GFAP accumulates in the frontal cortex following oral infection. Compared to the hippocampus and the thalamus GFAP accumulation in the frontal cortex occurs later and more slowly. However, when the

protein starts to accumulate, it does so fairly steadily (as seen by the almost linear progression between 75-95% of incubation) until the very late stages (>95%) where there is a slight decrease. This is not as marked a decrease as is seen the cases of PrP accumulation in orally infected mice and it is likely to be a function of the small number of observations that the result is based on. This will be discussed further in Chapter 4. Figures 32**f** (**i-iii**) are representative of the levels of GFAP seen in the frontal cortex at each of the five timepoints examined.

3.2.2 Kinetics of Disease in Intramuscularly Infected Mice.

Figures 33(**a-f**) are the rate of change curves relating to PrP and GFAP accumulation following intramuscular infection. As above figures (**a-c**) relate to PrP accumulation and figures (**d-f**) are concerned with GFAP build up.

Figure 33**a** illustrate the amount of PrP detectable, and the rate at which it accumulates in the thalamus during the incubation period. Figures 33**b** and 33**c** show similar information for the hippocampus and the frontal cortex respectively.

What is immediately apparent from these three figures is their remarkable similarity with respect to overall shape and behaviour. This contrasts with the results obtained from the orally infected animals, above, where the pattern and rate of accumulation varies greatly from one area to another. The overall picture of PrP accumulation following intramuscular is shown as one that begins earlier in the incubation period (50% of total incubation) than in the case of orally infected animals (~70%). In all three areas examined the level of PrP increases at a steady rate until about 70% of the incubation period is reached. There is then an apparent drop off in the amount of detectable PrP before a second stage of increased PrP deposition which continues until the end point of the incubation period.

Figures 33**a**(**i-iv**), 33**b**(**i-iv**) and 33**c**(**i-iii**) show the levels of detectable PrP in the thalamus, hippocampus and frontal cortex, respectively, during the incubation

(a)

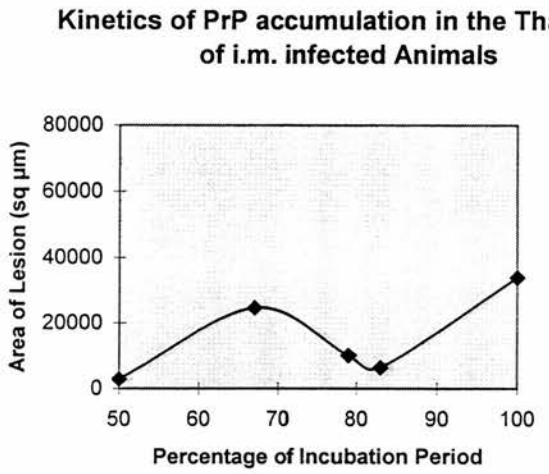

(b)

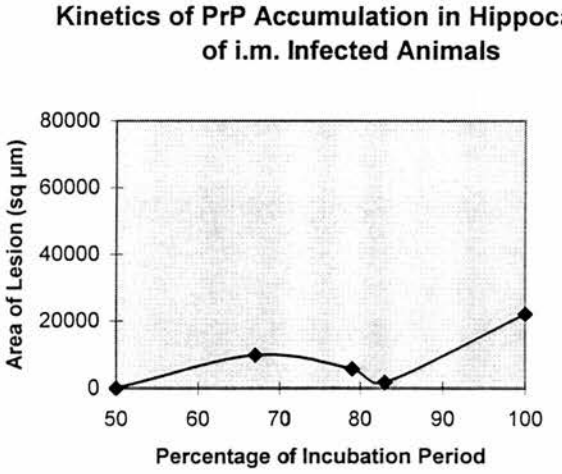

(c)

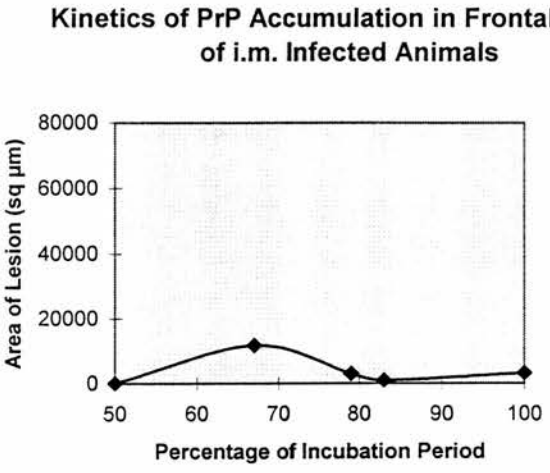

Figure 33 (a-c): Show changes in PrP levels with time during incubation in the thalamus (a), hippocampus (b) and frontal cortex (c) following i.m. infection with ME7 scrapie.

Figure33a(i).

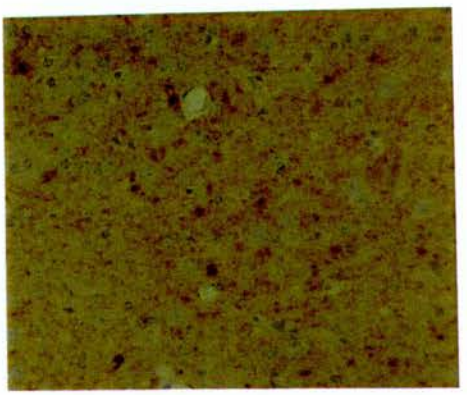

Figure 33a(ii).

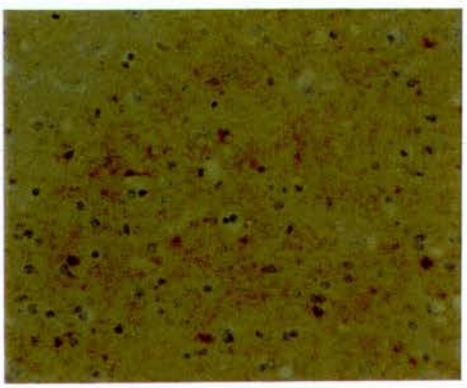

Figure 33a(iii).

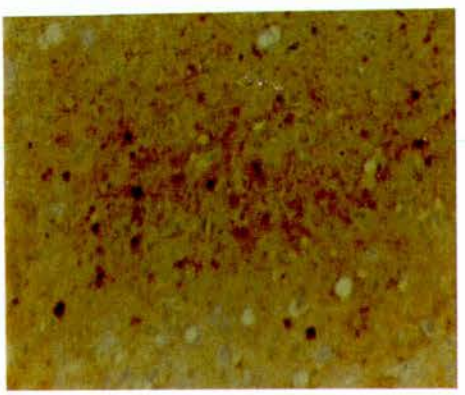

Figure 33a(iv).

Figures 33a (i-iv). Illustration of the changes in PrP pathology seen in the thalamus of i.m. infected mice during the incubation period. **33a(i)** Thalamus at 50% of total incubation period. **33a(ii)** Thalamus at 67% of total incubation period. **33a(iii)** Thalamus at 79% of total incubation period. **33a(iv)** Thalamus at terminal stage of disease (100% of incubation period). **All figures at x200 magnification.**

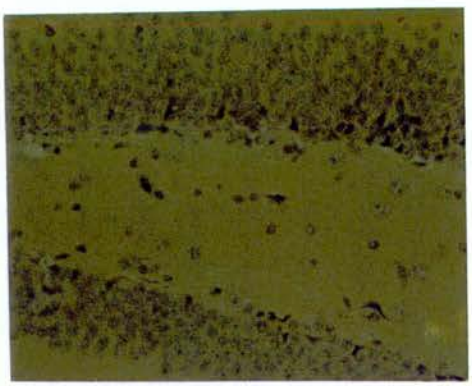

Figure33b(i).

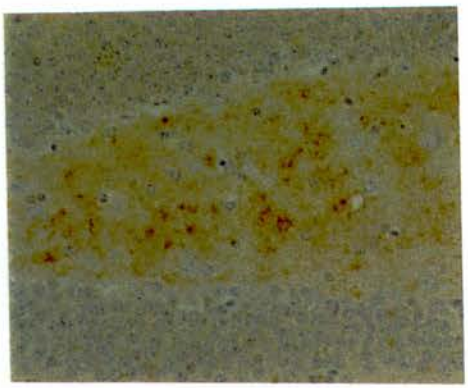

Figure 33b(ii).

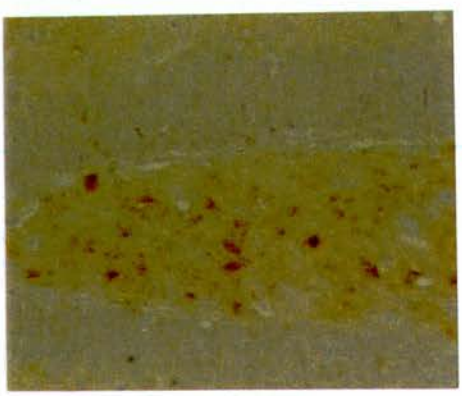

Figure 33b(iii).

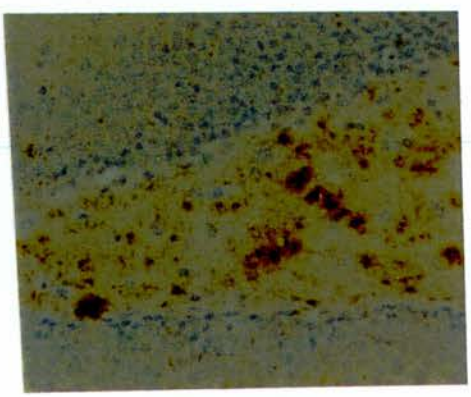

Figure 33b(iv).

Figures 33b (i-iv). Illustration of the changes in PrP pathology seen in the hippocampus of i.m. infected mice during the incubation period. **33b(i)** Hippocampus at 50% of total incubation period. **33b(ii)** Hippocampus at 67% of total incubation period. **33b(iii)** Hippocampus at 79% of total incubation period. **33b(iv)** Hippocampus at terminal stage of disease (100% of incubation period). **All figures at x200 magnification.**

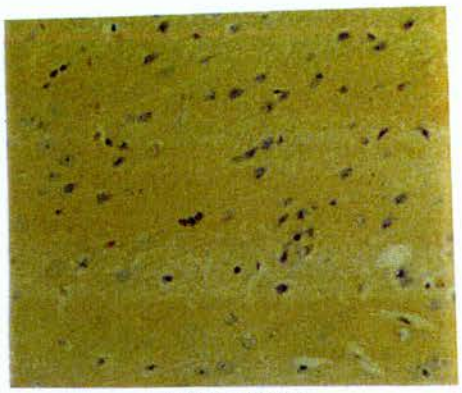

Figure33c(i).

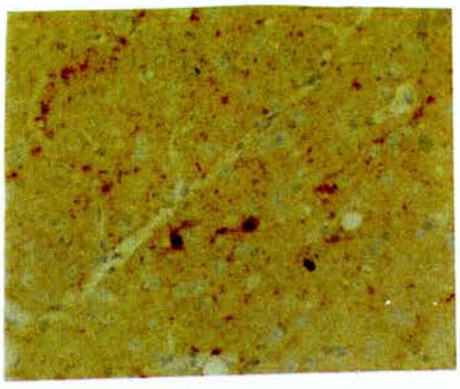

Figure 33c(ii).

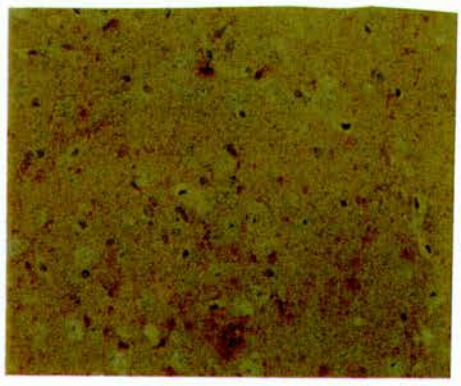

Figure 33c(iii).

Figures 33c (i-iii). Illustration of the changes in PrP pathology seen in the frontal cortex of i.m. infected mice during the incubation period. **33c(i)** Frontal cortex at 50% of total incubation period. **33c(ii)** Frontal cortex at 67% of total incubation period. **33c(iii)** Frontal cortex at 100% of total incubation period. **All figures at x200 magnification.**

(d)

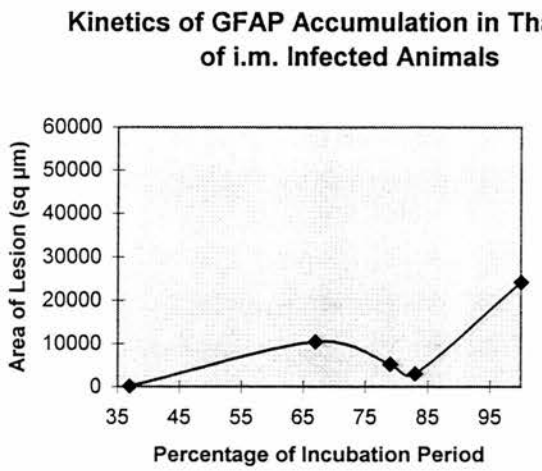

(e)

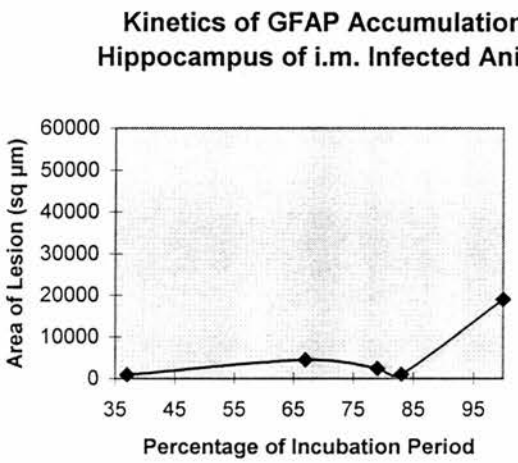

(f)

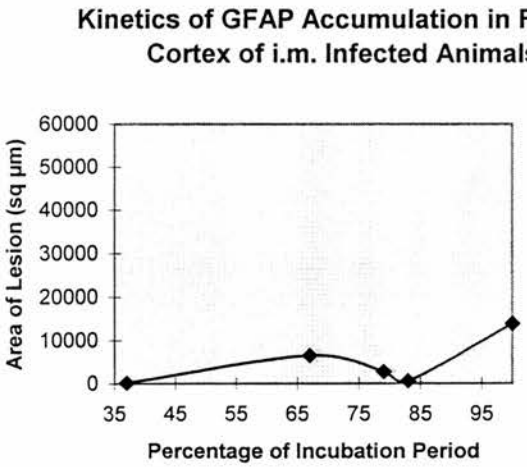

Figure 33 (d-f): Show changes in GFAP levels during the incubation period in the thalamus (a), hippocampus (b) and frontal cortex (c) of C57Bl mice following i.m. infection with ME7 scrapie.

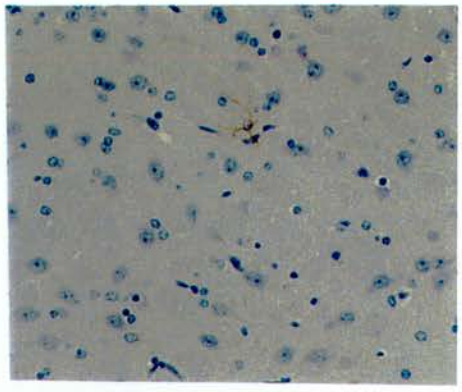

Figure33d(i).

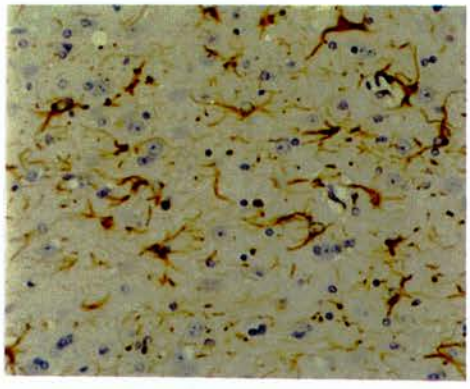

Figure 33d(ii).

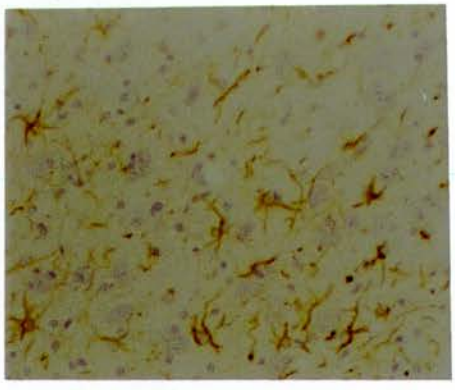

Figure 33d(iii).

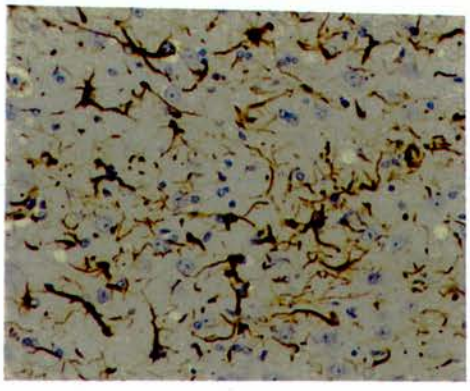

Figure 33d(iv).

Figures 33d (i-iv). Illustration of the changes in GFAP pathology seen in the Thalamus of i.m. infected mice during the incubation period. **33d(i)** Thalamus at 67% of total incubation period. **33d(ii)** Thalamus at 79% of total incubation period. **33d(iii)** Thalamus at 83% of total incubation period. **33d(iv)** Thalamus at terminal stage of disease (100% of incubation period). **All figures at x200 magnification.**

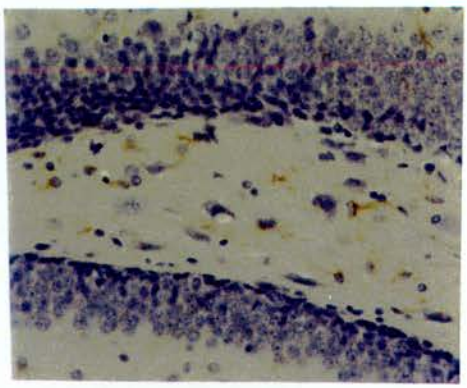

Figure33e(i).

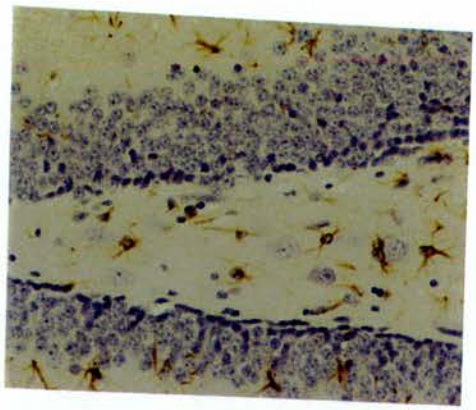

Figure 33e(ii).

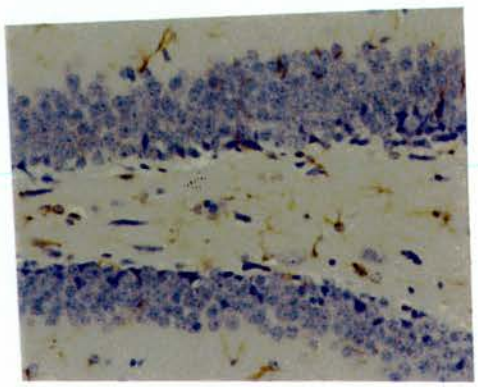

Figure 33e(iii).

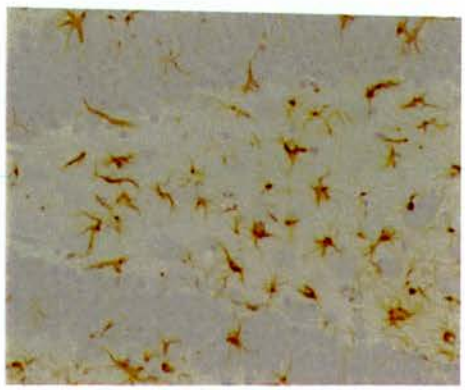

Figure 33e(iv).

Figures 33e (i-iv). Illustration of the changes in GFAP pathology seen in the hippocampus of i.m. infected mice during the incubation period. **33e(i)** Hippocampus at 67% of total incubation period. **33e(ii)** Hippocampus at 79% of total incubation period. **33e(iii)** Hippocampus at 83% of total incubation period. **33e(iv)** Hippocampus at terminal stage of disease (100% of incubation period). **All figures at x200 magnification.**

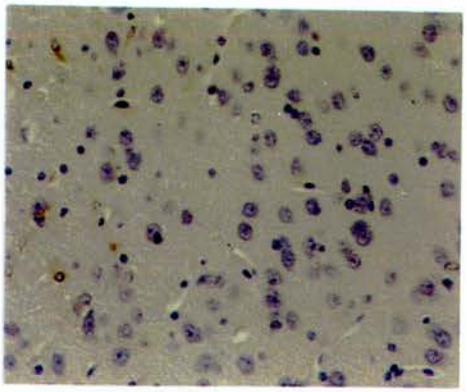

Figure33f(i).

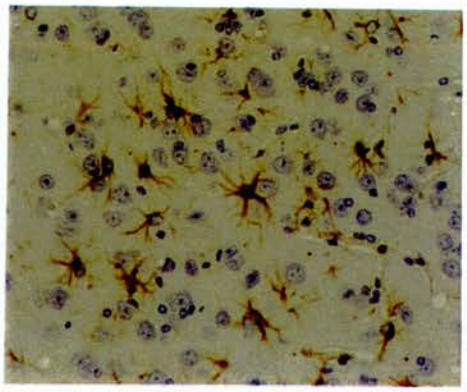

Figure 33f(ii).

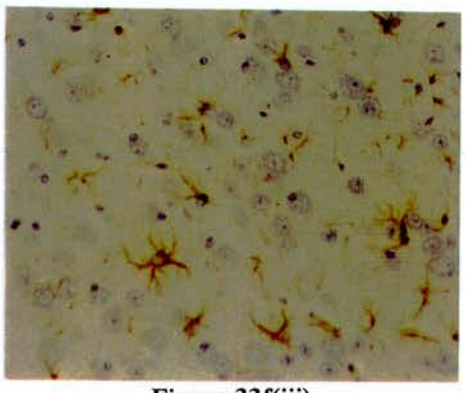

Figure 33f(iii).

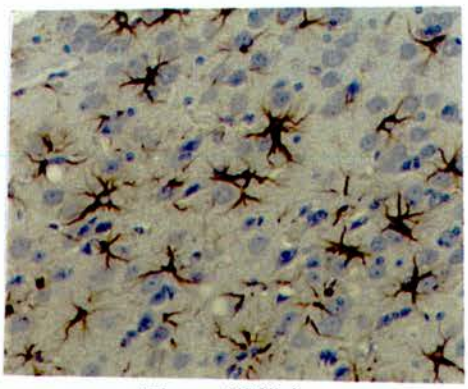

Figure 33f(iv).

Figures 33f (i-iv). Illustration of the changes in GFAP pathology seen in the frontal cortex of i.m. infected mice during the incubation period. **33f(i)** Frontal cortex at 67% of total incubation period. **33f(ii)** Frontal cortex at 79% of total incubation period. **33f(iii)** Frontal cortex at 83% of total incubation period. **33f(iv)** Frontal cortex at terminal stage of disease (100% of incubation period). **All figures at x200 magnification.**

period of the disease. From these images the peaks and troughs of the kinetics curves can be seen.

Figures 33**d** - 33**f** represent the kinetics of the disease with respect to the sequential accumulation of GFAP following intramuscular infection. These figures exhibit very similar characteristics as the figures for PrP kinetics, above.
The overall shape of these three figures is very similar, more so than the previous examples (PrP).

Again these figures show that the level of GFAP reaches a peak, troughs between 80 and 85% of the way through the incubation period before surging to even higher levels during the latest stages of the incubation period. Accounting for the differences in actual levels of protein detected in each of the three brain areas, the rate of accumulation (indicated by the steepness of the curve at a given point) appears to be very similar. This is certainly not the case in the orally infected animals. Figures 33**d**(**i-iv**), 33**e**(**i-iv**) and 33**f**(**i-iv**) illustrate the presence and the levels of GFAP in the thalamus, hippocampus and frontal cortex, respectively, of animals that were experimentally infected with scrapie by the intramuscular route.

3.2.3 Kinetics of Disease in Intraperitoneally Infected Mice.

Figures 34(**a-f**) represent the kinetics of PrP and GFAP accumulation in mice experimentally infected with scrapie by the intraperitoneal route. As in the cases of oral and intramuscular infection, above, the brain regions under investigation are the thalamus, hippocampus and the frontal cortex of the cerebrum.

Unlike the intramuscularly infected mice the patterns and rates of PrP accumulation in the three areas under investigation, Figures 34**a** - 34**c**, are quite different. They are also very different to the result seen in the orally infected animals.

In the thalamus the levels of PrP, which is detectable at a time corresponding to around 56% of the total incubation period, are reasonably constant as seen by the flatness of the early portion of the graph. There is a slight increase towards 70% of

(a)

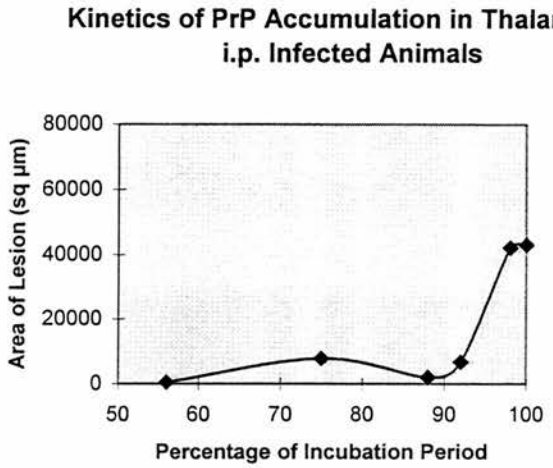

(b)

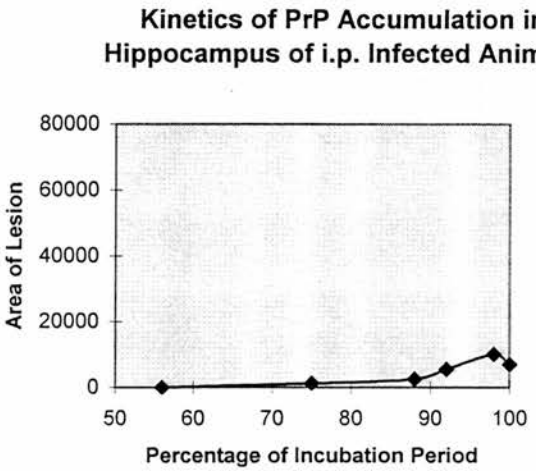

(c)

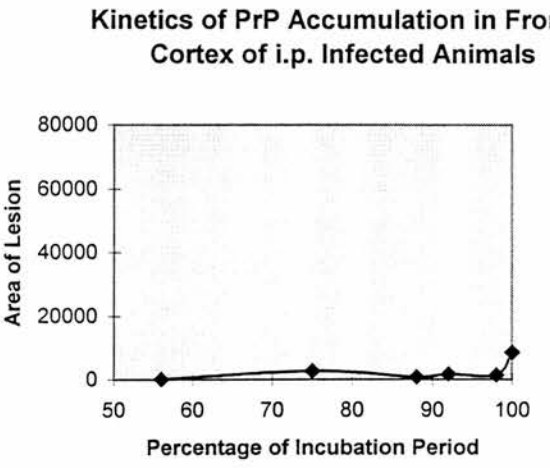

Figure 34 (a-c): Show changes in the detectable levels of PrP during the incubation period in the thalamus (a), hippocampus (b) and frontal cortex (c) of C57Bl mice following i.p. infection with ME7 scrapie.

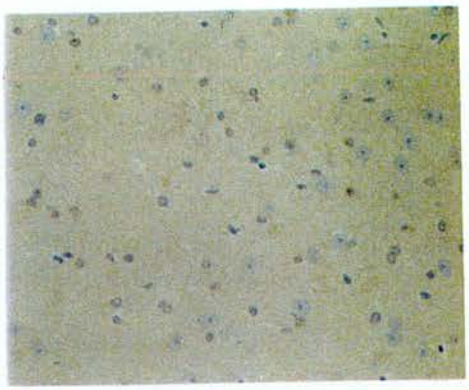

Figure34a(i).

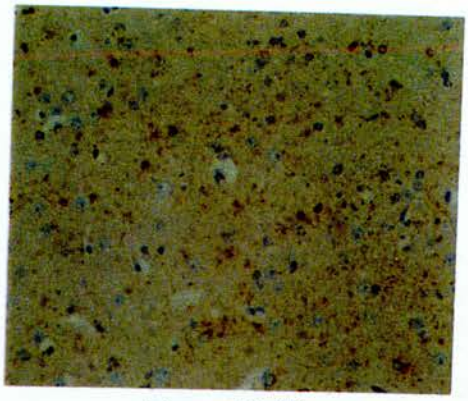

Figure 34a(ii).

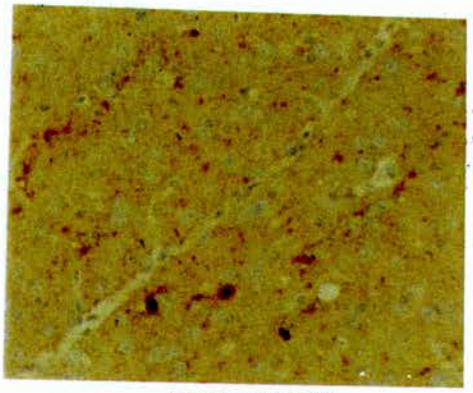

Figure 34a(iii).

Figures 34a (i-iii). Illustration of the changes in PRP pathology seen in the thalamus of i.p. infected mice during the incubation period. **34a(i)** Thalamus at 56% of total incubation period. **34a(ii)** Thalamus at 75% of total incubation period. **34a(iii)** Thalamus at 100% of total incubation period. **All figures at x200 magnification.**

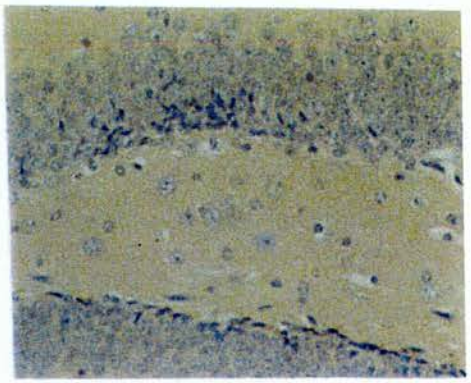

Figure34b(i).

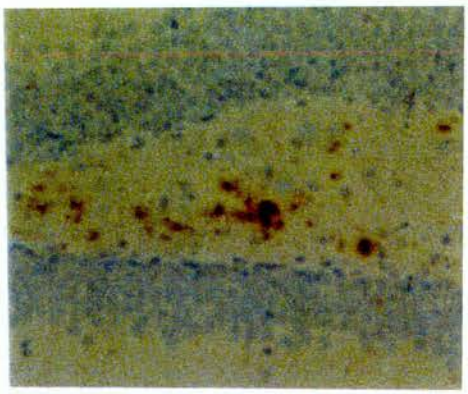

Figure 34b(ii).

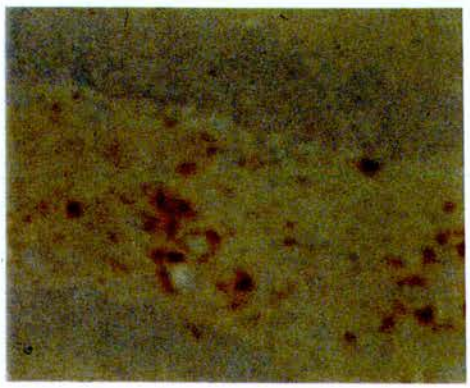

Figure 34b(iii).

Figures 34b (i-iii). Illustration of the changes in PRP pathology seen in the hippocampus of i.p. infected mice during the incubation period. **34b(i)** Hippocampus at 75% of total incubation period. **34b(ii)** Hippocampus at 92% of total incubation period. **34b(iii)** Hippocampus at 100% of total incubation period. **All figures at x200 magnification.**

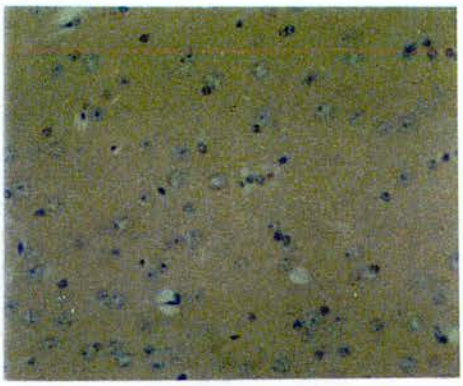

Figure34c(i).

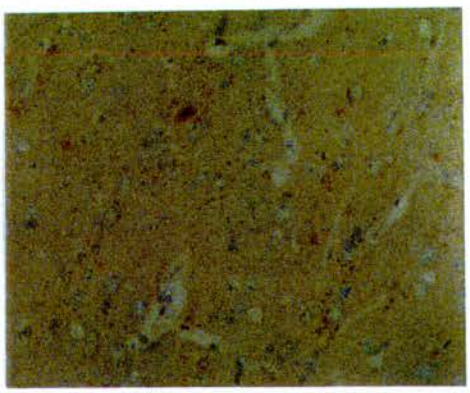

Figure 34c(ii).

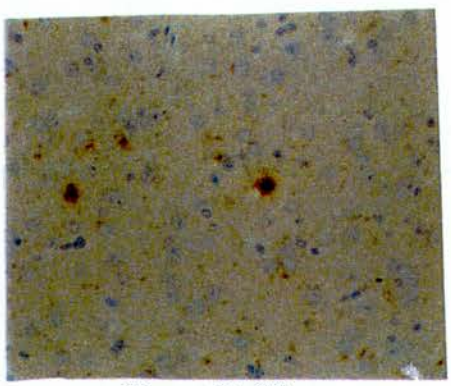

Figure 34c(iii).

Figures 34c (i-iii). Illustration of the changes in PRP pathology seen in the frontal cortex of i.p. infected mice during the incubation period. **34c(i)** Frontal cortex at 88% of total incubation period. **34c(ii)** Frontal cortex at 92% of total incubation period. **34c(iii)** Frontal cortex at 100% of total incubation period. **All figures at x200 magnification.**

the incubation period. However, this could be as a result of the small sample size. The major increase in the amount of PrP is seen between 90 and 98% of the incubation period where there is a rapid increase in the amount of PrP that can be detected. The speed of this increase is indicated by the steepness of the curve. Just prior to the end of the incubation period there appears to be a plateau, where there is no more PrP being deposited.

This is similar to the hippocampus where the level of PrP increases very slowly, almost imperceptibly until just before 90% of the incubation period has passes. At this time there is an increase in the rate of deposition towards the end point. Between 98 and 100% of the incubation period there is a small decrease in the level of PrP that can be detected, this is due to experimental variation and doesn't constitute an actual phenomenon. In the frontal cortex, the level of PrP is virtually constant from the time when it can be first detected until almost the end of the incubation period. At the end of the incubation period there is an increase in the rate at which PrP is deposited. This results in an increase in the amount of detectable protein. This trend of very late, very sudden increase in the area occupied by the accumulated PrP is only in the i.p. infected animals. A similar [late] observation can be made in the case of i.m. infected mice, However, the increase in rate does not occur as late and the resulting shift leads to a relatively greater deposition of PrP than is seen in the i.p cases.

Figures 34**a(i-iii)**, 34**b(i-iii)** and 34**c(i-iii)** show the consistency between timepoints of the amount of PrP that can be detected.

Figures 34**d** - 34**f** show the results of assessing the kinetics of GFAP deposition in i.p. infected mice. In the thalamus (Fig. 34**d**) the gradient of the curve is shallow indicating a low rate of deposition. There is a sharp upturn in the curve between 98 and 100% of the incubation period but this is most likely a result of variation between animals and the small sample size.

Similar graphs are produced from the results gathered in the hippocampus and frontal cortex (Figures 34**e** and 34**f** respectively). Figures 34**d(i-iii)**, 34**e(i-iii)** and

(d)

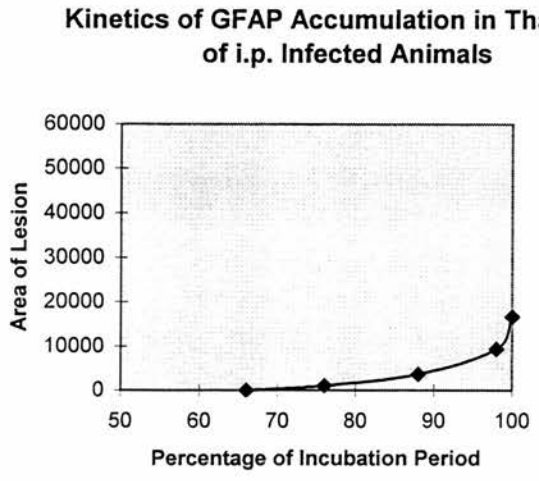

(e)

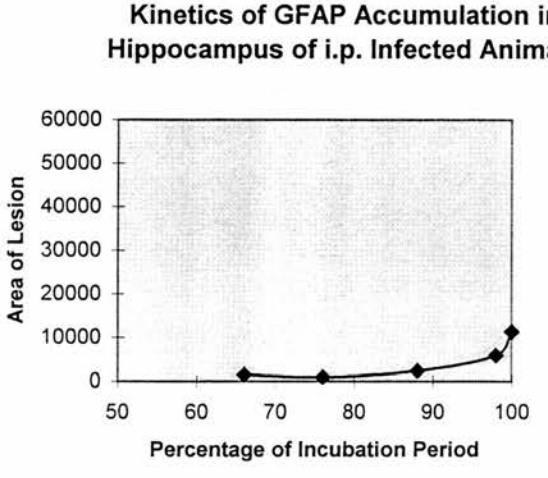

(f)

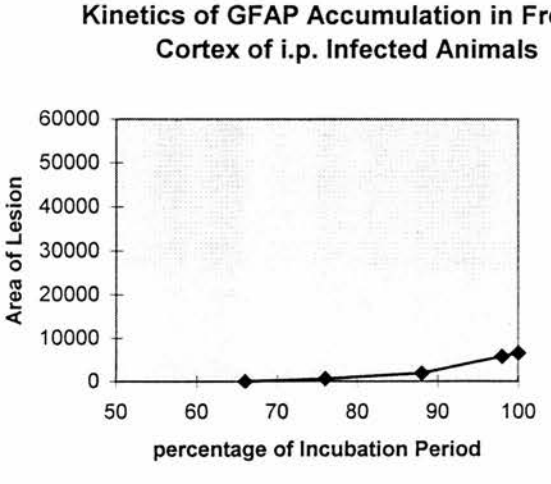

Figure 34 (d-f): Shows progressive Changes in GFAP levels in thalamus (a), hippocampus (b), and frontal cortex (c) of C57Bl mice infected with ME7 scrapie.

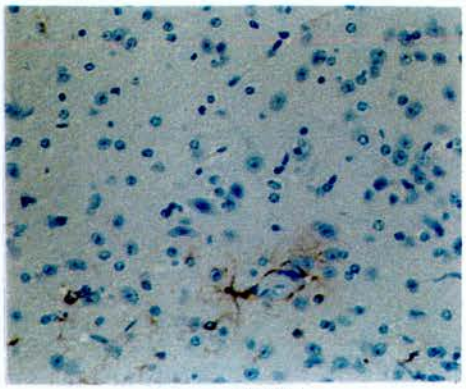

Figure34d(i).

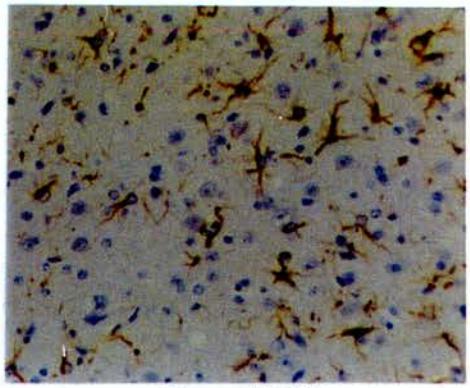

Figure 34d(ii).

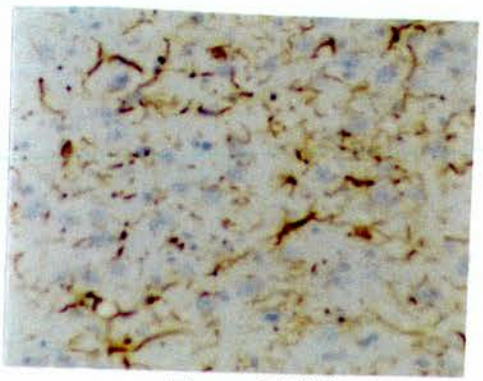

Figure 34d(iii).

Figures 34d (i-iii). Illustration of the changes in GFAP pathology seen in the thalamus of i.p. infected mice during the incubation period. **34d(i)** Thalamus at 67% of total incubation period. **34d(ii)** Thalamus at 79% of total incubation period. **34d(iii)** Thalamus at 100% of total incubation period. **All figures at x200 magnification.**

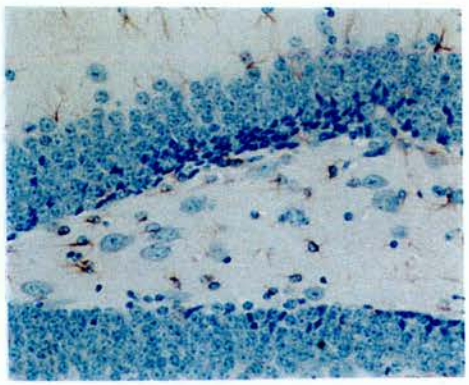

Figure34e(i).

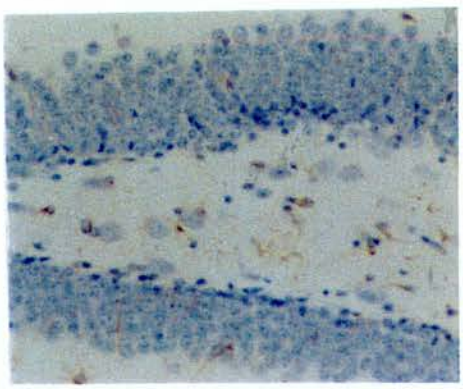

Figure 34e(ii).

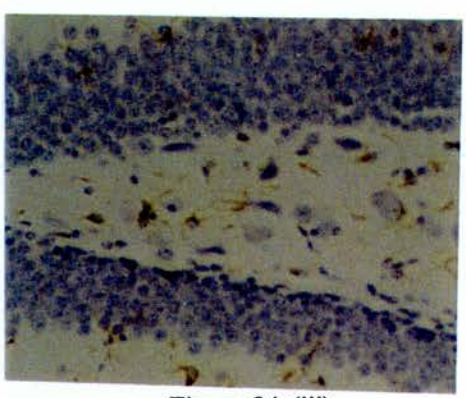

Figure 34e(iii).

Figures 34e (i-iii). Illustration of the changes in GFAP pathology seen in the hippocampus of i.p. infected mice during the incubation period. **34e(i)** Hippocampus at 79% of total incubation period. **34e(ii)** Hippocampus at 83% of total incubation period. **34e(iii)** Hippocampus at 100% of total incubation period. **All figures at x200 magnification.**

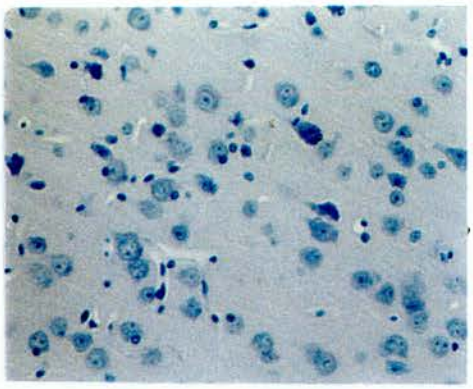

Figure34f(i).

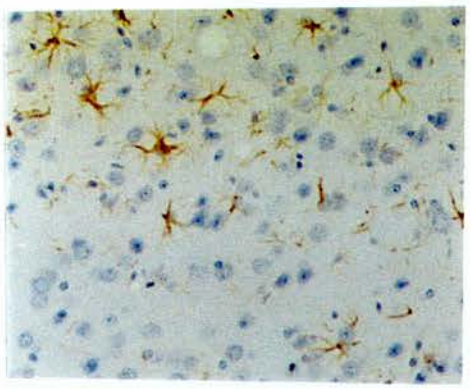

Figure 34f(ii).

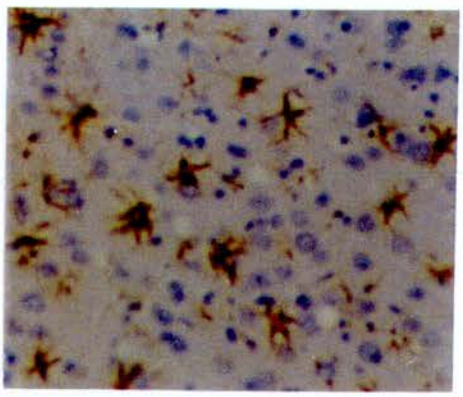

Figure 34f(iii).

Figures 34f (i-iii). Illustration of the changes in GFAP pathology seen in the frontal cortex of i.p. infected mice during the incubation period. **34f(i)** Frontal cortex at 67% of total incubation period. **34f(ii)** Frontal cortex at 79% of total incubation period. **34f(iii)** Frontal cortex at 100% of total incubation period. **All figures at x200 magnification.**

34**f(i-iii)** show the detectable levels of GFAP seen in these areas of the brain throughout the course of the incubation period.

These results indicate potential differences in the pathogenesis of experimental scrapie which may be attributable to differences in the route of infection. This will be discussed in further detail in Chapter 4.

3.3 Identification of PrP in Lymphoreticular System Following Experimental Challenge.

Figures 35 -37 show clearly that PrP is detectable in the spleen following challenge by the three routes under investigation here. PrP is identified by the red immunohistochemical product. The brown pigment that is visible in some of the images is haemosiderin, an iron-containing pigment that occurs in ageing animals as a result of red blood cell breakdown. It has no relevance to scrapie infection.

In all cases where PrP can be detected the distribution of the protein in the spleen is restricted to the germinal centres of the splenic follicles. However, PrP is not necessarily detected in every follicle.

These figures are all taken from the spleens of animals at the late stages of the disease. Figures 35(**a-c**) show the spleens of animals infected orally and sacrificed at 250, 279 and 320dpi respectively. From this result there appears to be a diminution in the amount of PrP located in the spleen as the disease progresses towards the terminal stages. There is also a noticeably higher amount of haemosiderin present in Figure 35**c** than in Figures 35(**a** or **b**). Whether or not this represents a genuine decrease with time, of the amount of PrP, is not clear. It may represent a period of replication prior to transport of the protein to the CNS.

Figures 36(**a** and **b**) show PrP in the spleens of animals that had been infected by the intramuscular route. As for the orally infected animals these spleens were harvested at the late stages of the disease, 246 and 279dpi respectively. In these figures there is clearly more PrP detectable in the spleen at the later timepoint than the

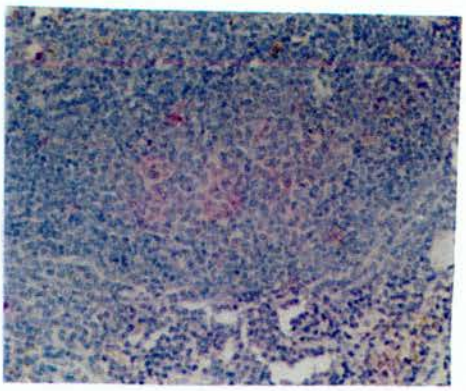

Figure35a.

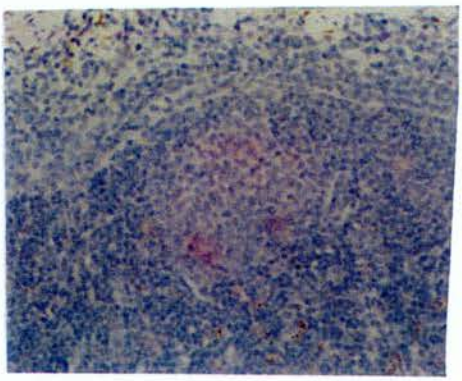

Figure 35b.

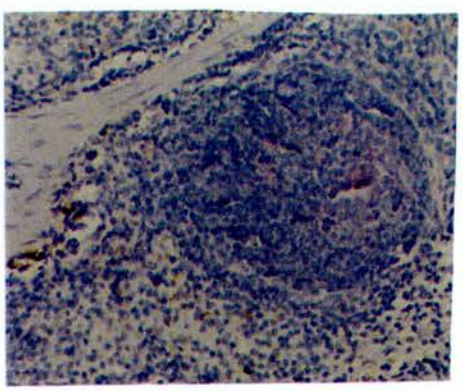

Figure 35c.

Figures 35a-c. Demonstrate the presence of PrP (shown here as red precipitate) in the spleens of animals infected with ME7 scrapie by the oral route. **Fig. 35a** spleen from animal sacrificed at 250dpi. **Fig. 35b** spleen from animal sacrificed at 279dpi. **Fig. 35c** spleen from orally infected animal sacrificed at terminal stage of infection, 320dpi. **All figures at x200 magnification.**

Unfortunately there are no available photographs of the uninfected controls. However the spleens of uninfected animals demonstrated no detectable PrP.

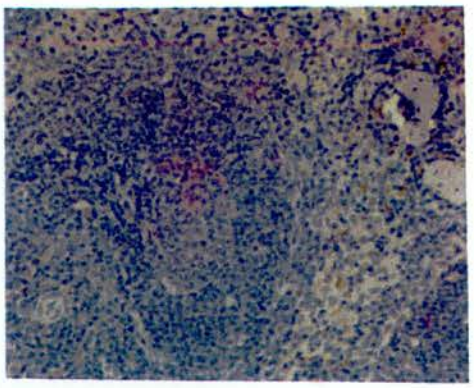

Figure36a.

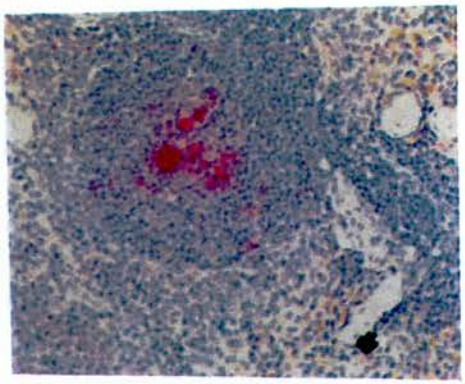

Figure 36b.

Figure 36 a-b. Illustrate the presence of PrP (red precipitate) in the spleens of animals infected with ME7 scrapie by the i.m. route. **Fig. 36a** animal sacrificed at 246dpi. **Fig. 36b** animal sacrificed at end stage of disease, 279dpi. **X200 magnification.**

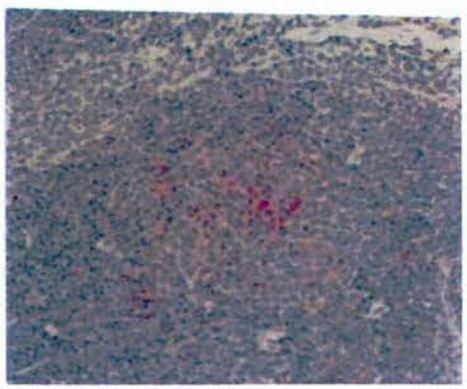

Figure 37a.

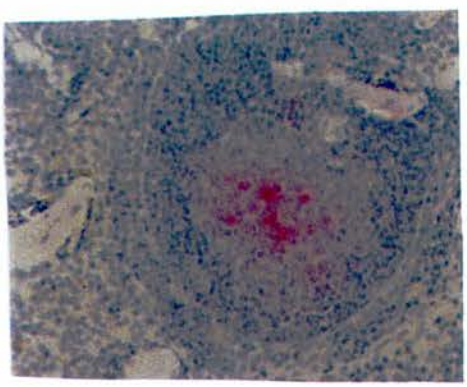

Figure 37b.

Figures 37a-b. Demonstrates the presence of PrP in the spleens of animals infected with ME7 scrapie by the i.p. route. **Fig. 37a** animal sacrificed at 231dpi. **Fig. 37b** animal sacrificed at terminal stage of infection, 250dpi. **x200 magnification.**

earlier. This could be suggestive of an accumulation of PrP in the spleen that continues until the terminal stage of the disease. The PrP in the spleen at 246 dpi is not especially concentrated and appears as a pale pink product when detected immunohistochemically. In contrast, at the end stage of the disease, the PrP is clearly identified as an intense red product in the germinal centre of the follicle.

Figures 37(**a** and **b**) illustrate PrP in the spleens of animals infected by the intraperitoneal route. As with the previous examples, these figures represent the late stages of the infection, 231 and 250dpi respectively. This result differs from the previous two examples with respect to the relative amounts of PrP detected. In these intraperitoneal cases there are no readily apparent differences with respect to the amount of protein detected. In both of these figures the PrP appears as a diffuse pink coloured product in the germinal centre. Non-infected spleens, from non-infected mice were also stained as a means of control but did not exhibit visible PrP. These tissues are not shown here, however all results were confirmed in conference with Dr Martin Jeffrey.

These results appear to suggest that the involvement of the spleen and, by extrapolation, other components of the lymphoreticular system is variable depending on the initial route of infection. The obvious caveat to this observation is that it is based on a very small sample size. Further experiments would be required before any true conclusions can be reached. This will be discussed in Chapter 4.

3.4 Comparison with Human Acquired TSE.

The rationale behind much of the work presented in this thesis was an attempt to elucidate the events of infection in humans, especially with the agents of Creutzfeldt-Jakob disease and the recently identified new variant. It was intended that by choosing the oral and intramuscular routes of infection it would be possible to model new variant CJD and iatrogenic CJD infection. These diseases share common pathological characteristics, both with sporadic CJD and each other, although in the case of variant CJD the clinical presentation is markedly different. However, there are

also differences in terms of the appearance and distribution of the established pathological markers of vacuolation and PrP. These differences enable an experienced pathologist to make an accurate diagnosis. It is acknowledged by the author that this may have been an over ambitious course of action given the limitations of the experimental model and the complexity of naturally acquired human TSEs. However in light of the MRC funding for this work, and the otherwise overtly veterinary nature of the studies presented in this thesis, it was felt by the author that some attempt to integrate aspects of human TSE infection into this study was required. Unfortunately the results of this particular study serve only to illustrate the difficulty of translating results from animal systems to human diseases. The limitations of this study are described in greater detail in Chapter 4.

Tissues from cases of sporadic, iatrogenic and new variant CJD were obtained from the National CJD Surveillance Unit in Edinburgh. The tissues were taken from the CJD unit archive and had been immunostained to detect PrP. Parallel sections were stained with haematoxylin and eosin for the purpose of detecting vacuolar change. Most of the comparisons are based on the pathology in the cerebellum as this particular region is known to produce striking differences between the different human CJD types.

An important consideration when making these comparisons is the size of the human brain versus that of the mouse brain. Due to the extreme differences in size the relative areas that can be examined for comparative purposes are much greater in the mouse brain. This is a potential source of error in this type of study. However as the most easily identifiable differences relate to the morphology of the PrP deposits, and not necessarily the overall pattern of distribution of the lesion, it is not thought that this difference will not adversely influence the observations.

3.4.1 Comparison of vCJD with Orally Acquired Experimental Scrapie.

Figure 38 **(a-b)** show PrP deposition in the brain of a patient diagnosed at post-mortem with new variant CJD. Figure 39 **(a-b)** show PrP deposition in the cerebellum of the brain taken from a mouse experimentally infected with scrapie by the oral route. Examples of the typical pathology observed in the mouse brain, in regions other than the cerebellum, for example the hippocampus and thalamus can be seen above.

These figures clearly show the presence of large plaques in the cerebellum of the vCJD case. These plaques are perhaps the most striking difference between the human disease and the experimentally established murine model although the perineuronal staining seen in the cerebellar cortex of the vCJD case is not seen in the animal model. One other difference that can be seen in the cerebellum is the level of staining seen in the central white matter region, the *arbor vitem*. In the experimental model there is widespread, diffuse PrP deposition. This is in contrast to the vCJD section where, relative to the rest of the cerebellum, there is very little PrP. Furthermore what PrP is detectable in the cerebellar white matter is much more distinct and discreet than is seen in the animal disease. In the frontal cortex there are widespread plaques visible in the vCJD case. There is also a 'feathery' appearance to some of the PrP deposits. This is visible at the boundary of cells and is associated with neurones. However, the most striking feature in this section is the widespread deposition of plaques. In the equivalent area of the brain from the experimentally infected mouse the PrP appears to be much more diffuse and although there are some structures which could be plaques they are in no way as widespread or intense as those seen in the human disease. Routine H&E sections from these cases also show considerable differences. Figures 40 and 41 show some of these differences between vCJD and orally induced scrapie. In the molecular layer of the cerebellum, and in the cerebellar cortex (in the case of vCJD) there are readily identifiable vacuoles. This region is relatively spared in the animal model. The most notable feature of vCJD, which is absent from orally induced ME7 scrapie, is the presence of 'florid' plaques. These are deposits of amyloid surrounded by a halo of spongiform change. Figure

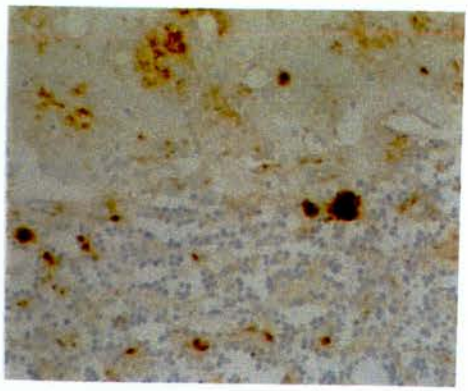

Figure38a.

Figure 38b.

Figure 38 a-b. Demonstrates the presence of PrP in the brain of a patient who died as a result of nvCJD infection. **Fig. 38a** Shows PrP in the granular and molecular layer of the cerebellum and illustrates the presence of PrP in the form of plaques as well as more diffuse deposits.. **Fig. 38b** shows limited deposition of PrP in the white matter of the cerebellum. **X200 magnification.**

Figure 39a.

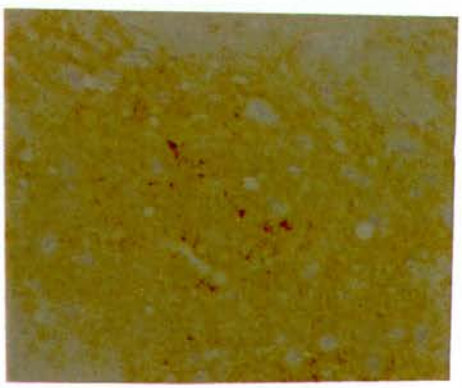

Figure 39b.

Figures 39a-b. Demonstrates the presence of PrP in the cerebellum of mice infected with ME7 scrapie by the oral route. **Fig. 39a** PrP in the granular and molecular layer of the cerebellum. Note the absence of PrP amyloid plaques and the presence of a much more diffuse deposit than is seen in vCJD. **Fig .39b** PrP present in the cerebellar white matter, this is much more involved than is the case seen in human oral TSE infection. **X200 magnification.**.

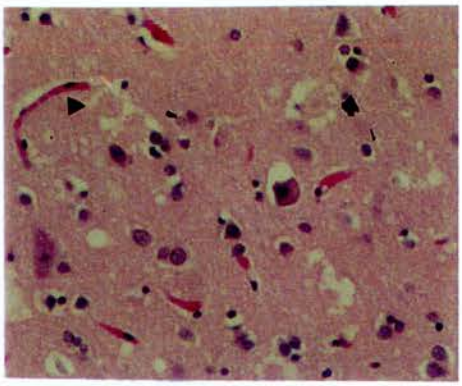

Figure40a.

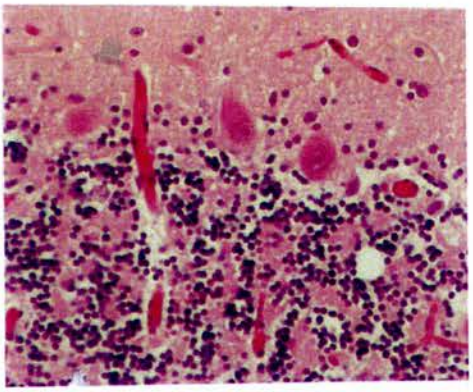

Figure 40b.

Figure 40 a-b. Illustrate some of the features seen in H&E stained sections from a patient who died as a result of vCJD infection. **Fig. 40a** Shows 'florid plaques' (arrowheads) in the frontal cortex these are a feature of vCJD not seen in any of the other human acquired TSEs. **Fig. 40b** shows vacuolar degeneration of the tissue in the cerebellum around the granular and molecular layers. **X100 magnification.**

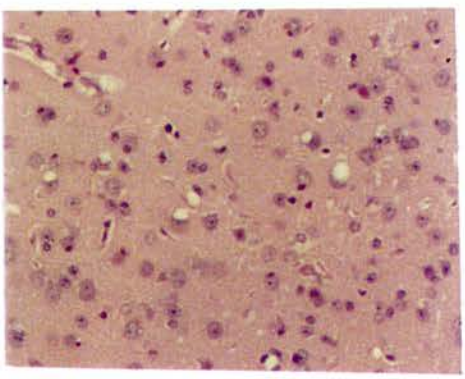

Figure 41a.

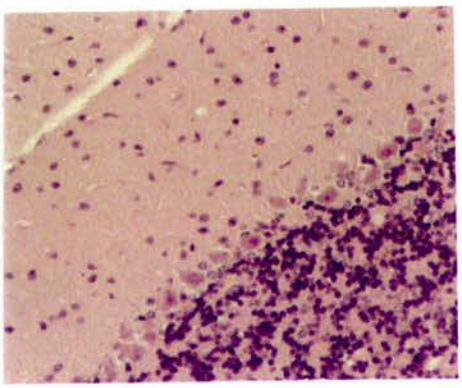

Figure 41b.

Figures 41a-b. Illustrate the degree of vacuolar change in orally infected animals. **Fig. 41a** vacuolation in the frontal cortex of an orally infected animal. Note the absence of any 'florid' plaques.. **Fig. 41b** Vacuolation in the cerebellum. There appears to be only limited involvement. **X100 magnification.**

40**a** shows florid plaques in the frontal cortex of a vCJD patient. In contrast the frontal cortex of the mouse shows the presence of vacuolation but there are no eosinophillic plaques.

3.4.2 Comparison of Iatrogenic CJD with Intramuscularly Acquired Experimental Disease.

Iatrogenic CJD was caused by the administration of pituitary derived growth hormone which was inadvertently contaminated with a human TSE agent. These hormone injections were given intramuscularly over a period of months or years with onset of disease occurring 7-35 years later (Brown et. al., 1992).

Figure 42 demonstrates the presence of PrP in the brain of a patient who died as a result of iatrogenic transmission of CJD. Broadly parallel sections of cerebellum taken from a mouse that had been infected with scrapie via the *biceps femoralis* are shown for comparison (Figure 43). Sections of murine brain for comparison with human frontal cortex are presented above.

Figure 42**a** shows the white matter of the cerebellum of a patient who, having received growth hormone therapy, eventually died of CJD. Clearly there is very little evidence of PrP deposition, especially when compared to the corresponding region of the brain in a vCJD patient. The PrP that is present in this section appears to have formed small aggregates which have formed a chain, possibly along the length of a neuronal process.

When this is compared to the cerebellar white matter from a mouse infected with scrapie by the intramuscular route, there are obvious and striking differences. Figure 43**a** demonstrates how much more significant the PrP deposition is in this region of the murine model. In the centre of the white matter there is a widespread diffuse covering of PrP which has the appearance of being almost laminar. There are also some larger aggregates of protein which have the appearance of plaques. These plaques are larger than the deposits seen in the cerebellum of the iatrogenic cases.

In the molecular layer and cerebellar cortex of the iatrogenic case there is more widespread, intense PrP deposition. Figure 42**b** illustrates clearly the borders of the PrP deposition and the sparing of the cerebellar white matter (bottom left of the figure). This figure also shows the presence of PrP in the cerebellar cortex. The cortical PrP is much more diffuse than in the molecular layer. Figure 42**c** is a higher magnification example of PrP in the molecular layer. Figure 43**b** shows a large section of the murine cerebellum and includes regions of white matter, cortex and the molecular layer. There is a diffuse spread of PrP visible in this section. Although there is no obvious sign of plaques there are some small discrete deposits in both the molecular layer and in the cerebellar cortex. These do not present with the same intensity as is seen in the human iatrogenic disease.

Figure 42**d** shows that the levels of PrP in the frontal cortex of an iatrogenic CJD case are low. The PrP seen in this figure is closely associated with neuronal cell bodies and processes By comparison there is a proportionally greater concentration of PrP in the frontal cortex of an intramuscularly infected mouse with a more widespread, diffuse deposition of the protein being apparent, this can be seen in the figures in Section 3.2.2, above. However the PrP in the mouse model doesn't demonstrate the same type of perineuronal pattern in its distribution. There are some small plaque like aggregates present in the mouse model that are not observed in the iatrogenic case.

Figure 42**e** shows the presence of vacuolar change in the frontal cortex of the iatrogenically infected CJD case; figure 43**c** shows the corresponding region in the mouse brain. It is difficult to identify any differences in the quality and distribution of vacuolation from these examples however, it can be seen that neither the iatrogenic case nor the mouse model (or for that matter the mouse model of oral infection) have any florid plaques in them. In the mouse model of intramuscular infection there are no obvious plaques, this is also the case for this example of iatrogenic infection in the human. This is in keeping with the pattern of PrP deposition that has been observed.

Figure42a.

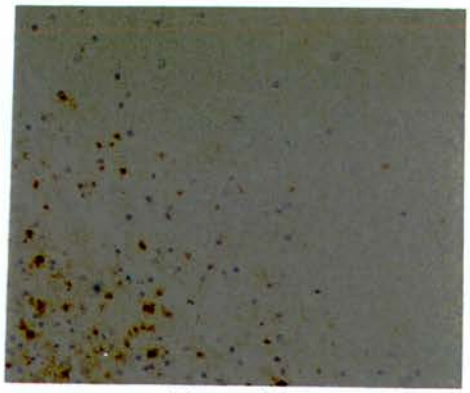

Figure 42b.

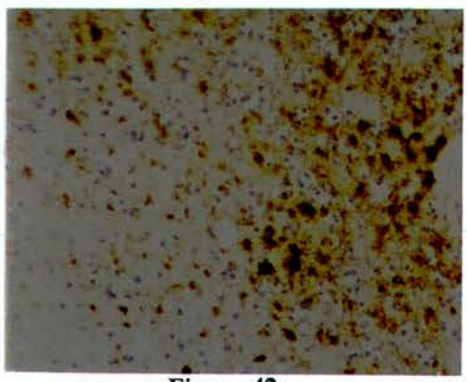

Figure 42c.

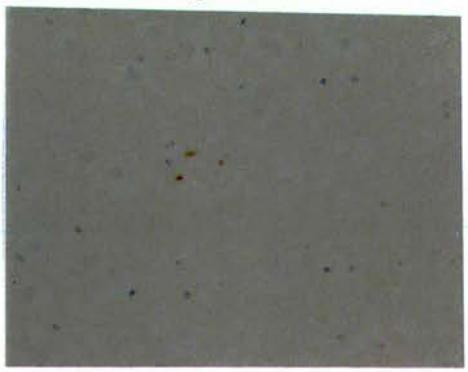

Figure 42d.

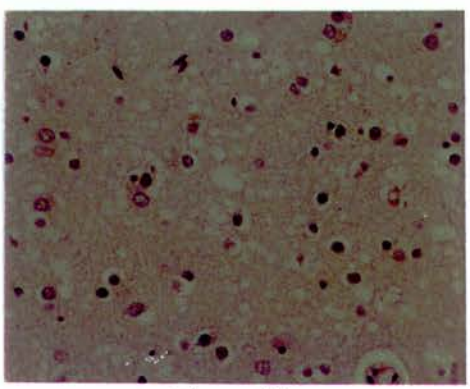

Figure 42e.

Figures 42a-e. Illustrate the pathology seen in the brain of a patient who died as a result of iatrogenic CJD. **Fig. 42a** Cerebellar white matter stained for PrP. There appears to be limited involvement. **Fig. 42b**. Cerebellar cortex stained for the presence of PrP. **Fig. 42c** Molecular layer of cerebellum stained for PrP. **Fig. 42d** PrP detected in the frontal cortex of patient with iatrogenically acquired CJD. **Fig. 42e** Vacuolar change in frontal cortex of growth hormone associated iatrogenic CJD case. Note there are no 'florid' plaques. **x100 magnification.**

Figure 43a.

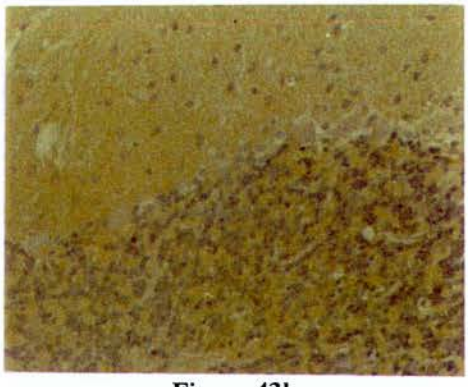

Figure 43b.

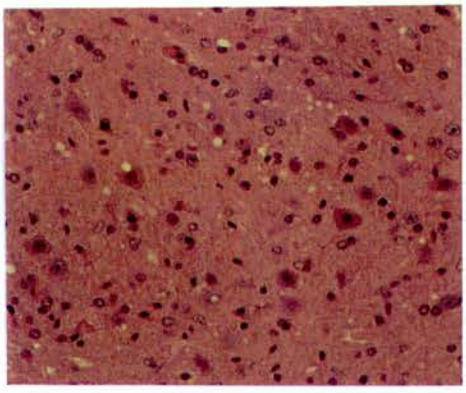

Figure 43c.

Figures 43a-c. Illustrate the pathology seen in the brain of an animal that was infected with ME7 scrapie by the i.m. route. **Fig. 43a** Cerebellar white matter stained for PrP. There appears to be more involvement than is seen in the human case. **Fig. 43b**. Large field of cerebellum including molecular layer and cerebellar cortex labelled for PrP. **Fig. 43c** H & E stained section of murine frontal cortex shows vacuolar degeneration. It is difficult to discern any differences in the quality and distribution of vacuolation in i.m. infected animals and iatrogenically infected human cases. **x100 magnification.**

3.4.3 Comparison of Human Sporadic CJD with Intraperitoneally Acquired Experimental Disease.

The aetiology of sporadic CJD is not clearly understood. Whether the disease is purely one of host genetics or if there is an element of acquisition of an infective agent by an unknown route is not categorically known. It is not the intention to draw any comparisons between the pathology of sporadic CJD and intraperitoneally established experimental infection nor is it the intention to suggest that sporadic CJD is the result of some form of intraperitoneally acquired infection although a recent epidemiological study has suggested that general surgery may be a risk factor for sporadic CJD (Collins et al., 1999). The main reasons for examining the differences in pathology between sporadic CJD and acquired scrapie is that doing so illustrates further the differences between the types of pathology, especially PrP pathology, seen in the human diseases at the same time as highlighting the pathological similarities seen in the murine model where the strain of the infective agent has been controlled.

The ability to draw comparisons, especially between sporadic CJD and vCJD, is enhanced by the fact that the PrP genotype of the patient who succumbed to sporadic CJD is known. This patient was homozygous for methionine (M/M) at codon 129 of the PrP gene. The same genotype has been found in all the cases of vCJD so far identified and may be a relative risk factor for infection. Figure 44**a** shows PrP deposition in the cerebellum of a sporadic CJD patient. From this figure it is evident that the white matter of the cerebellum is almost completely spared and that there are certainly no plaques as have been observed in the corresponding brain region in vCJD. What little PrP there is in this section appears to be associated with cell membranes and does not seem to involve the surrounding neuropil. This is also different to the pattern of PrP deposition seen in the cerebellum of iatrogenic cases.

Figure 45 demonstrates the presence of PrP in the cerebellar white matter of an i.p. infected mouse. Compared to the human diseases none of the animal models demonstrate the same degree of sparing of the cerebellar white matter. Of the three animal models examined the i.p. infected animals have visibly less PrP in the cerebellum than either the i.m or the orally infected animals (which have the most).

However, apart from the differences in the actual amounts of PrP detected in this area; the pattern and morphology of the protein deposition are similar. This is unlike the three human diseases examined. As mentioned above, in the case of sporadic CJD the cerebellar white matter is almost completely spared. This contrasts with iatrogenic CJD, where several small plaque-like structures are observed, and vCJD where there is evidence of plaques as well as more diffuse PrP deposits. Some of these deposits appear to be associated with neuronal processes giving them a 'chain-like' appearance.

Figure 44**b** shows the border of the molecular layer and the cortex in the cerebellum of a sporadic CJD case. In contrast to the cerebellar white matter these regions are heavily affected by PrP. The cortex has a broad, diffuse covering of PrP with some small punctate deposits. The molecular layer by contrast is affected by larger, darkly staining, aggregates. This type of aggregate is not seen in the molecular layer of the i.p. infected animal model to the same degree. The mouse presents with a more uniform, diffuse pattern of protein deposition. This is the same pattern of PrP deposition that is seen in the i.m. and orally infected animals although the intensity of staining varies.

Figure 44**c** shows the deposition of PrP in the frontal cortex of a sporadic CJD case. The widespread diffuse deposition of PrP is in stark contrast to the pattern seen in vCJD, where there is an incredible amount of very concentrated protein, or iatrogenic CJD where the PrP appears in a perineuronal pattern. Vacuolation in the cortex of the sporadic case is shown in figure 44**d** This is similar to the iatrogenic case as it lacks the presence of florid plaques (found in vCJD).

This exercise has demonstrated that the differences in type and distribution of pathology (especially PrP pathology) seen in human CJD-type diseases are not necessarily seen in animal models of those disease.

In the animal models the distribution and type of PrP pathology seen in the brain was broadly similar irrespective of method of infection. What was different was the intensity/severity of the pathology. This is not an entirely unexpected result as the

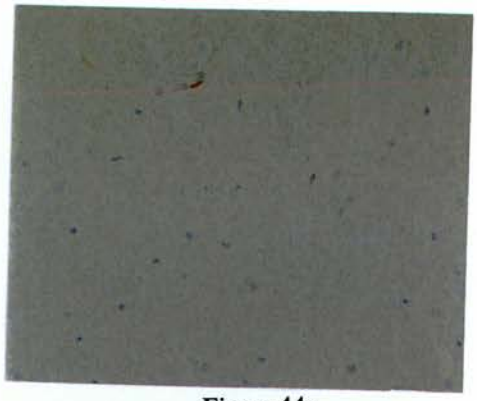

Figure44a.

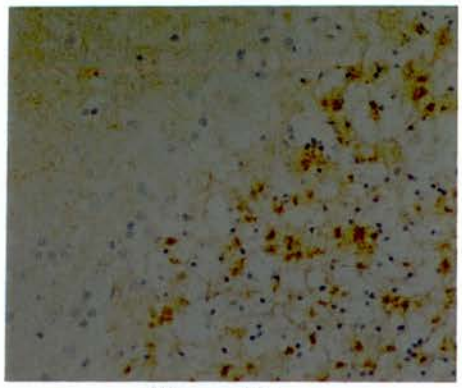

Figure 44b.

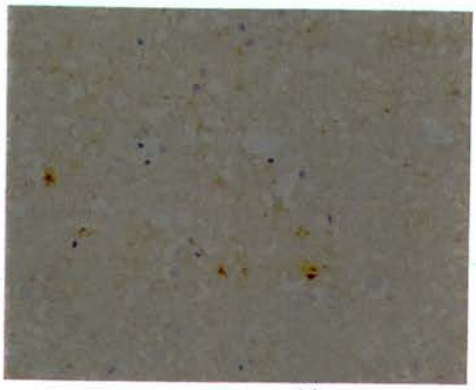

Figure 44c.

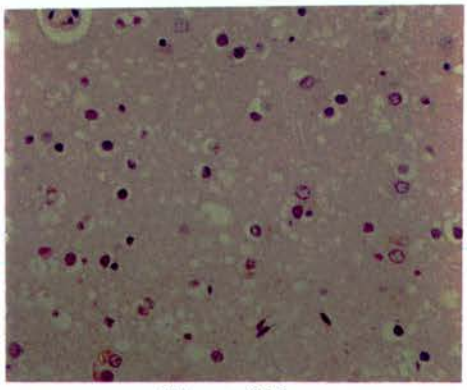

Figure 44d.

Figures 44a-d. Illustrate the pathology observed in the CNS of a patient who died of sporadic CJD. **Fig. 44a** PrP in the cerebellum of a sporadic CJD case. Note there is a total absence of PrP amyloid plaques and there is a general sparing of this region unlike in the case of vCJD. **Fig. 44b** PrP present in the cerebellar cortex and molecular layer in a sporadic CJD case. **Fig. 44c** Widespread deposition of PrP in the frontal cortex. **Fig 44d** H&E stained section of frontal cortex, similar in appearance to iatrogenic CJD but different from vCJD due to the lack of 'florid' plaques. **X200 magnification.**

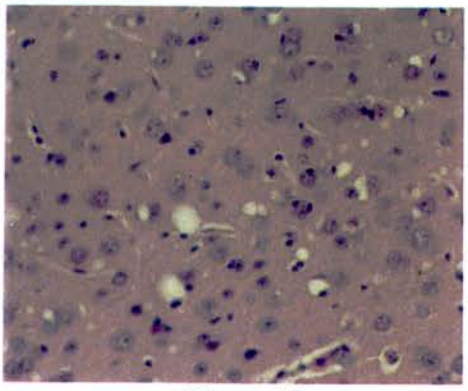

Figure 45.

Figure 45 Illustrates the presence of PrP in the cerebellar white matter of an i.p. infected animal. This is in keeping with the other animal models which do not exhibit the same degree of cerebellar white matter sparing that is generally seen in the human disease. In general there are very few differences between the animal models at the terminal stage of infection. **X200 magnification.**

mice used in the study were inbred and the strain of scrapie used was kept constant throughout. This is unlikely to be the same situation in the human cases that were examined. This serves to illustrate that the agent strain, recipient species and other variables are what determine pathology. Unfortunately it does not allow for the extent of influence of each of these factors to be individually determined.

3.5 Transport of infectivity in $PrP^{0/0}$ mice.

Part of the work described in this thesis was concerned with the transport, or lack thereof, of scrapie infectivity in the CNS of mice lacking a functional PrP gene (*prn-p*). Consequently these animals are unable to produce the native PrP protein which has been reported as being essential for propagation of disease. The details of the experimental design are given in Chapter 2, but briefly, two groups of animals (one group PrP-nulls the other the 129 strain wild type) were injected intraocularly with the ME7 strain scrapie agent. At a series of time points specific regions of the brain (regions which are known to be projections of the retina) were harvested. These harvested tissues were used to prepare inoculum to inject into a series of C57BL, assay mice. The C57BL mice were then maintained in the animal unit and observed for signs of neurological disease. Animals exhibiting neurological signs were culled and the brains taken for pathological assessment; the final diagnosis of scrapie was confirmed solely on this assessment. The results of this experiment are given in Tables 9 and 10.

These tables illustrate the number of animals from each group to have succumbed to scrapie following experimental intracerebral infection with visual system material from PrP null and PrP wild-type animals. Of special interest it should be noted that there are three animals, in the first group of mice (24 hours post injection) that received tissues from PrP null animals, that succumbed to the disease. The brains from these animals were examined histopathologically by an experienced technician and by Dr Jan Fraser and a diagnosis of scrapie infection, with the ME7 strain of the agent, was made (Aileen Chree personal commuication). The severity and distribution of pathology seen in these mice was however much lower than would be expected from an end point infected mouse. This case is indicative of infection

with a relatively low titre of the infective agent. Sections of the brains from these animals were then immunostained for the PrP protein, the result of this was positive. This result would appear to demonstrate that scrapie infectivity can in fact be transported through the central nervous system of animals lacking a functional PrP gene, although admittedly the numbers involved are very low. The incubation periods for these three animals (2 from the optic nerve group and one from the superior colliculus) were all around 305 days. This compares very closely with the three positive control animals from the corresponding timepoint that developed the disease. Table 11 displays the mean incubation period data for the animals in this experiment.

Time Point	24 hours post injection		41 days post injection		54 days post injection		71 days post injection		83 days post injection		117 days post injection	
Tissue used as inoculum	Path +ve	n	Path +ve	n	Path +ve	n	Path +ve	n	Path +ve	n	Path +ve	n
O.N.	Yes	3/8	Yes	2/7	No	-	Yes	2/7	Yes	7/7	Yes	2/8
S.C.	No	-	Yes	7/7	No	-	No	-	Yes	6/9	Yes	8/8
dLGN	No	-	Yes	9/9	No	-	No	-	Yes	5/7	Yes	6/6

Table 9: Results of infectivity assay in C57Bl mice using tissues harvested from PrP wild-type animals.

O.N. = Optic Nerve

S.C. = Superior Colliculus

dLGN = Dorsal Lateral Geniculate Nucleus

n = number of animals exhibiting positive pathological lesions (vacuolation). Expressed as a proportion of the animals in that group.

Group sizes vary due to intercurrent deaths and undetected deaths that rendered the brain too autolytic to examine effectively.

All figures correct at the time of writing. (-) = no deaths in this group at this time.

Time Point	24 hours post injection		41 days post injection		54 days post injection		71 days post injection		83 days post injection		117 days post injection	
Tissue used as inoculum	Path +ve	n	Path +ve	n	Path +ve	n	Path +ve	n	Path +ve	n	Path +ve	n
O.N.	Yes	2/8	No	-	No	-	No	-	No	-	No	-
S.C.	Yes	1/9	No	-	No	-	No	-	No	-	No	-
dLGN	NO	-	No	-	No	-	No	-	No	-	No	-

Table 10: Results of infectivity assay in C57Bl mice using tissues harvested from PrP-null animals.

O.N. = Optic Nerve

S.C. = Superior Colliculus

dLGN = Dorsal Lateral Geniculate Nucleus

n = number of animals exhibiting positive pathological lesions (vacuolation). Expressed as a proportion of the animals in that group. Group sizes vary due to intercurrent deaths and undetected deaths that rendered the brain too autolytic to examine effectively. All figures correct at the time of writing. (-) = no deaths in this group at this time.

Serial kill timepoint.	24 hours p.i.		41 d.p.i.		54 d.p.i.		71 d.p.i.		83 d.p.i.		117 d.p.i.	
Tissue	**w.t.**	**null**	**w.t.**	**null**	**w.t.**	**null**	**w.t.**	**null**	**w.t.**	**null**	**w.t.**	**null**
O.N.	265	304	256	-	-	-	244	-	232	-	245	-
S.C.	-	316	233	-	-	-	-	-	234	-	215	-
dLGN	-	-	244	-	-	-	-	-	254	-	241	-

Table11: Shows the mean incubation periods of C57BL mice infected with tissues harvested from PrP-null and PrP wild-type mice. Where no number is entered the animals were still alive at the time of writing or they had died undetected and the brains were too autolytic for pathological determinations to be made.

O.N. = Optic nerve, S.C. = Superior colliculus, dLGN = Dorsal lateral geniculate nucleus.

-. Denotes no cases of clinical/pathological disease at that timepoint.

The fact that the incubation periods in the three animals that were infected with PrP-null derived tissue are longer than those infected with PrP-wild type tissue is to be expected. The recent literature surrounding the role of the PrP protein in processing and trafficking of infectivity states that animals devoid of endogenous PrP are unable to process exogenous infectivity and cultivate the disease. This result appears to indicate that this may not be the case and that limited transport of infectivity is possible even although replication cannot occur. Although there is little doubt that host-encoded PrP is important for disease development, it is reasonable to expect that animals lacking endogenous PrP will be less efficient at processing infectivity than their wild-type counterparts; this is suggested by the extended incubation periods in those mice although the very small infecting dose administered in these cases is doubtless also a factor. The amount of infectivity present in the inoculum source, the titre, can be calculated by referring to a standard dose-response curve. The dose response curve for C57BL mice infected intracerebrally with ME7 scrapie can be seen in Appendix II. The infectivity titres for these cases, as determined by interpolation with the curve are shown in Table 12. This demonstrates the very low level of infectivity present in the null-mouse tissues.

Infecting Tissue	Number of Animals Affected	Mean Incubation Period (days)	Estimated Infecting Dose (From Curve).
Optic Nerve	2	304	Beyond Range of Standard Curve
Superior Colliculus	1	265‡	Log_{10} -1.3 infectious units

Table 12: Estimation of the initial infecting dose that caused disease in three C57BL mice. Tissues harvested from the visual system of previously inoculated PrP-null mice were used as the source of the inoculum. ‡Only one animal exposed to this inoculum source succumbed to disease therefore this incubation period is an absolute value and not a mean value.

One other point of interest to arise from this work, and one that may be worth closer examination, is the apparent 'troughing' that is seen in the recipients of PrP wild-type (129 mouse strain) tissues between 41 days post injection and 83 days post injection. In the case of the animals that were infected with tissues harvested from PrP wild-type animals there were groups which demonstrate no, or very few, cases of disease. In particular the group of animals infected with the tissues harvested from the PrP wild-type donor animals at 54 days post injection have not produced a single case of experimental scrapie. Furthermore in the group of animals infected with the tissues from the 71 days post injection wild-type donors there have been only two cases of transmission identified, both of which were in recipients of the optic nerve preparation. These two groups of animals are in contrast to those groups either side of them where 18/23 and 18/23 animals succumbed to disease. These results will be discussed in Chapter 4.

Discussion and Conclusions.

4. Discussion of Results.

4.1 Objectives.

The work presented in this thesis was designed to test the hypothesis that different routes of infection result in different patterns of development of neuropathological lesions and hence influence the phenotype of infection. In order to examine this hypothesis experiments were designed which had three main objectives: (i) to map and quantify the appearance and extent of three pathological markers of TSE infection - vacuolation , PrP accumulation and astrocytic reactivity - in mice experimentally infected with ME7 scrapie by a variety of different routes, (ii) to identify differences in the pathological profiles that could then be attributed solely to the route of infection, (iii) to assess the suitability of these infections in animals for use as models of acquisition of human spongiform encephalopathy. In concert with this work a secondary set of experiments were undertaken, these were designed to investigate the possibility that scrapie infectivity can be replicated and/or transported within the CNS of animals lacking endogenous PrP protein.

In order to carry out the work as planned it was necessary to adapt and develop protocols for the assessment of pathology; in particular the adoption of computerised image analysis software and hardware that had not previously been used at the Neuropathogenesis Unit.

4.2 Route of Infection Influences Pathology of Experimental Scrapie.

4.2.1 Differences in Incubation Periods.

As stated above, the main aim of the project was to test the hypothesis that different routes of TSE infection result in different patterns of development of neuropathological lesions and hence influence disease phenotype. It is important to recognise that in this section efficiency is often referred to when talking about different routes of infection. The results of the study clearly indicate that each of the

routes examined is an efficient means of causing disease. Each of these routes produced 100% mortality in their experimental groups, it may therefore be correct to say that no route is more, or less, efficient than another. However for the sake of comparison between routes of infection efficiency is used to describe not only the ability to produce experimental disease in an animal model but also the characteristics of the disease with respect to the mean incubation period, especially the standard errors associated with those means, and the actual range of individual incubation periods for a given route of infection.

As expected, the routes that were examined: intraperitoneal, intramuscular and oral gave different incubation periods with intramuscular being the shortest (mean incubation 238 days ± 10) and oral being the longest (307 days ± 2). The length of the oral incubation period was not unexpected; but the apparent efficiency (defined in this case in terms of the ability to infect a population in such a way that the incubation period from animal to animal is very similar) of this route of infection as indicated by the exceptionally small standard error attached to the incubation period was somewhat surprising as the oral route of dosing has been previously reported as being one of the least efficient at establishing infection in mice (Kimberlin and Walker, 1988). Recent reports concerning the oral infection of hamsters with scrapie (Diringer et. al., 1998) suggest that repeated dosing is a more effective method of establishing infection. While this is true of the hamster system, the single-dose approach described in this project has resulted in a highly efficient incidence of infection. Indeed, with the exception of the intracerebral route of infection (mice infected by this route were used as positive controls to insure the quality of the inoculum source) the oral route of infection has been demonstrated to be more efficient (defined as outlined above) at causing infection than either the i.p. or the i.m. routes although, as mentioned, oral dosing does result in a protracted incubation period and the amount of infectivity required to establish infection is greater. Exactly how much greater is unclear; in this study the orally infected mice were dosed with 100µl of inoculum as opposed to 20µl for i.c., i.p. and i.m.. This was an arbitrarily assigned amount, which was clearly adequate and actually only

represents the difference between a dose of 10^{-2} and $5x10^{-2}$ infectious units. This small difference, equivalent to half of one log would be lost in a full titration, and is therefore not considered a significant source of error. An experiment of this nature would be able to identify if there is a critical dose required to establish infection and how that dose compares to critical doses in the cases of i.m. and i.p. infections. This would help to categorically establish the efficiency of the oral route as a means of causing infection, certainly in a disease model and it may have ramifications for human disease especially with regards to predicting the size of any potential vCJD epidemic.

The extended nature of the oral incubation period is not surprising and is certainly, at least in part, a function of the speed of infectivity transport due to the physical distance between the mouth/digestive system and the central nervous system and the way in which the innervation of the gut interfaces with the CNS. The high efficiency of the oral route that has been demonstrated in this project is probably due to the uniformity of the system. The oral route of infection can almost be considered as a 'closed-system' where the establishment of disease is much more likely to follow a linear series of events, such as uptake of infectivity in the lymphoid tissues associated with the mouth such as tonsil as well as gingival tissue of the gum (Ingrosso et. al., 1999), than is the case following i.p. infection; there is also recent evidence that the digestive tract is involved in uptake of infectivity in the case of experimental murine scrapie (Maignien et. al., 1999). This degree of order is supported by the narrow range of incubation periods observed in animals infected orally. When a source of infectivity is introduced to the main body cavity, as in i.p. dosing, there is no way of knowing accurately how the infectivity is distributed. Following oral dosing, the infectivity will be subject to the same uptake by the same peripheral nerves in every case; this leads to infectivity transport to both the CNS and to the LRS, as evidenced by the presence of detectable PrP^{SC} in the spleens of orally infected mice at the late stages of the disease. Following i.p. infection the infectivity is likely to be taken up by a variety of routes governed by distribution of peripheral nerves in the peritoneal space. This differential uptake of infectivity may

be responsible for the extended incubation period range, which is reflected in the standard error of the means.

The route taken by infectivity from the periphery to the CNS is worth closer examination especially as the extended incubation period range seen in this study for the animals infected by the i.p. route is much more widespread than has been seen in comparable previous infections at the Neuropathogenesis Unit (Kimberlin and Walker, 1988). The incubation period of the mice infected by the i.p. route in this experiment was 251±9 days (based on a group of 13 observations) with an incubation period range of 92 days. This compares with the incubation period and range from the orally infected mice which was based on a group of 15 animals and calculated to be 307±2 days with a range of less than 30 days. The oral route also compares favourably to the i.m. route. The point suggested above, that the more organised nature of oral acquisition is responsible for the narrow range of incubation periods is supported further by the results gathered from the i.c. and i.m. infected animals. As would be expected following direct administration of the agent to the CNS (as in the case of i.c. infection) the incubation period range is only 14 days.

Following i.m. infection the observed incubation period range was approximately 75 days. This is less than was observed for the i.p. infected animals but obviously more than either the orally or i.c. infected animals. This suggests that the degree of order governing the transport of infectivity from the *biceps femoralis* is higher than in the case of i.p infection. The suggestion again is that this is due to the limited number of nerves in the muscle that would be capable of transporting infectivity from the periphery to the CNS. There is also a possibility that there is some degree of blood borne transport of infectivity to the LRS perhaps prior to invasion of the nervous system. The LRS involvement is demonstrated by the presence of PrP^{SC} in the spleens of i.m. infected animals. However, in order to fully address the questions surrounding the nature of this LRS involvement, more experimental work to investigate the events following i.m. infection would have to be undertaken.

The difference between the incubation period ranges of the orally infected and the i.m. infected animals may be a function of physical distance between site of infection and entry to CNS. One of the contributory factors may be the presence of lymphoid tissue associated with the digestive system which may be responsible for some processing of the infectivity. The results of this study have shown that there is PrP in the spleen of these infected animals and that it is detectable at the late stages of the incubation period regardless of the route of infection, this is in contrast to BSE in cattle where although the putative route of infection is oral there is no evidence of involvement of the LRS (Somerville et. al., 1997). There is a replication of infectivity phase in the course of the infection, this takes place in the spleen (Dickinson, 1975) and probably in other lymphoid tissues (Brown et. al., 1999). Recent reports of PrP in the tonsil of sheep with scrapie and human variant CJD cases, as well as in the appendix of CJD patients support this observation. The fact that there is almost immediate contact between lymphoid tissue and the infective agent following oral infection, in the buccal cavity, may be in part responsible for the efficiency of the oral route of infection. The relatively short incubation period range of the orally infected group is suggested to be a result of (at least) two factors: (i) the organisation of the digestive system such that the number of available relays to take up infectivity and transport it to the CNS is relatively small and the consequent suggestion that a given peripheral nerve will, in every case, be responsible for this event, and (ii) the presence of lymphoid tissue in the mouth may accelerate the processing of infectivity by supplementing the function of the spleen. The wider incubation period range seen in i.m. cases may not reflect the same sort of differential uptake that has been suggested for those animals infected by the i.p. route as the inervation of the muscles in the leg is very defined. More likely is the fact that there are fewer 'shortcuts' to lymphoid processing of the infectivity following infection at that site and the physical distance between the *biceps femoralis* and the spleen or the CNS is greater than in the case of oral infection.

There have been studies recently concerning the pathogenesis of orally induced scrapie in hamsters infected with the 263K strain of the agent. These studies report that following ingestion of the agent, spread of infectivity to the brain occurs via the vagus nerve rather than along the spinal cord (Baldauf et. al., 1997; Beekes et. al., 1997; Beekes et. al.,1998). This suggests an alternative or perhaps complementary direct route by which orally acquired infectivity can access the brain. This is an avenue that may be worthy of further study in the murine model to determine whether or not this is simply a species (hamster) specific event. Especially interesting would be an examination of the spinal cord pathology that was unfortunately not possible in this study for reasons explained in Chapter 3. To assess the pathogenesis of scrapie in mice following oral infection a number of animals would be required as to be infected and then serially killed at intervals leading up to the time where the first signs of pathology are evident in the brain. The spinal cord, vagus nerve and tissues of the lymphoreticular system could then be examined for the presence of disease specific PrP, by immunohistochemistry, and infectivity, by bioassay. This would provide answers to the questions concerning the course of events between ingestion of the agent and initial signs of the disease in the CNS. The results from the work described in this thesis provide clues as to when to start looking and what the total incubation period will be as well as details of the first areas of the brain that are affected. This, in conjunction with the proposed experiment should enable a map of events to be created.

4.2.2 Differences in Appearance of Pathological Markers.

As discussed above, each of the routes of infection that were examined for this study produced disease after different lengths of incubation. It is suggested that at least part of the reason for these differences is the way in which the infectivity is processed and transported from the periphery to the nerves of the spinal cord and ultimately to the brain. As a consequence of these assumed differences in routing it is likely that there would be differences in the emergence of pathological markers (in

this case special attention was focused on PrP and GFAP) both in terms of when in the incubation period they appear and where in the brain they are first evident.

To enable the results from the three models to be compared in a meaningful way the incubation periods had to be converted to a percentage scale. On this scale day zero (the day of injection/infection) was assigned to be zero percent of the incubation time, the mean incubation period for each route of infection was assigned as 100 percent of the incubation. It is acknowledged that as this is based on a mean, which in all three cases have a standard error greater than zero, that the 100 percent mark does not encompass every animal from every group. However this was considered the most suitable way of making direct comparisons between models and the animals that exhibited incubation periods greater than the mean would not overly influence the result as the most meaningful and significant, route-dependant, pathological differences would be present in the early stages of the incubation.

In the case of both the i.m. and the i.p. infected mice, the first PrP was detected at roughly the same point in the incubation period. This point was 56% of the total incubation period for the i.p. challenged animals and 58% for the i.m. infected group. This is considerably different from the orally challenged group where the first detectable PrP was found relatively later at 72% of the incubation period. Especially interesting about this observation is the fact that although each timepoint in the experiment was based on a group of four animals in the i.p. infected group, at this early timepoint (56% relating to 140 d.p.i) PrP could only be detected in the brain of one animal. Furthermore at the next timepoint (166 d.p.i) none of the four animals examined had any measurable amounts of PrP in their brains, only at timepoints beyond this did all of the i.p. infected animals present with detectable quantities of PrP. This compares to the i.m. group where all four of the animals examined at the early timepoint (58% of the total incubation period, which equates to 140 d.p.i.) displayed the presence of disease-associated PrP. PrP was also detectable in all the i.m. infected animals sacrificed at timepoints after 140 d.p.i..

The point in the incubation period that corresponds with the upregulation of astrocytic activity was also determined for each of the three routes of infection under investigation. It is reasonable to expect that the similarities and differences seen between routes of infection with respect to the deposition of PrP, (that is the relative points in the incubation period at which they occur), would also be seen in the case of GFAP accumulation. This is in fact not the case. The first signs of astrocytic hypertrophy or hyperplasia, indicated by an increase in the amount of astrocytic reactivity as evidenced by increased amounts of GFAP, in the brains of animals infected by the intraperitoneal route occur at the same time as the first PrP is detected, this is at 56% of the total incubation period length. However, the first GFAP detectable following intramuscular infection is not seen until relatively later, at around 70% of the total incubation period for that model. This is very close to the same relative point at which reactive astrocytes can be detected in the brains of mice infected orally with ME7 scrapie, the actual figure for these animals being 72% of the total incubation period. This result appears to support the hypothesis that the route of infection influences the progress of pathology, this may be a consequence of the number or available relays between the peripheral nervous system in the region of infection and the CNS. It has been shown at the Neuropathogenesis Unit that different agent-strain/mouse-strain combinations will exhibit differences in the sequence of appearance of pathological lesions with regards to which marker appears earliest in the incubation period (personal communication Jan Fraser and Debbie Brown). This is attributed to a combination of the different genetic characteristics of the recipient mouse and differences in agent strain. However in the case of this experiment, only a single strain of the scrapie agent was used (ME7) and all the mice infected were genetically identical, inbred, therefore this cannot be the case in this instance.

As well as the relative temporal differences that are observed with respect to the appearance of PrP and GFAP in animals infected by different routes there are also route of infection-dependant differences in the regions of the brain that are affected. This is true of the appearance of pathology early in the incubation periods. At the

terminal stage of the disease it more difficult to differentiate between animals infected by different routes on the basis of their pattern of PrP and GFAP deposition, that is to say that there is similarly widespread gross pathology throughout the central nervous system of animals infected by all three routes such that the best way of differentiating between routes of infection is to consider the differences in the severity of the pathology throughout the CNS.

In the case of the animals infected by the intraperitoneal and intramuscular routes the earliest signs of PrP are seen at 140 days post injection. However, the distribution of PrP at this timepoint in these animals displays many differences. Although there are affected areas common to both routes of infection such as the deep mesencephalic nucleus, the red nucleus, the anterior and posterior interposed cerebellar nuclei and the numerous nuclei of the posterior and ventral thalamic groups there are also regions of PrP deposition that are apparent in one model but not in the other. For example in the intraperitoneally infected animals there is evidence of PrP being deposited as a band in the fourth layer of the cerebral cortex. This band runs from the forebrain to the dorsal aspect of the cerebrum and is a feature of i.p. infection that is not seen in either i.m. or oral infection. Certainly in the case of i.m. infected animals, although there are signs of PrP deposition in the cerebral cortex these deposits are much more discrete and are not present throughout the length of the cerebrum.

In cases of oral infection there is no detectable PrP in the cerebral cortex until approximately 80% of the way through the incubation period. At this point small deposits of PrP are detectable in the frontal area of the cerebral cortex. This PrP does not extend dorsally through the cerebrum and is more like the deposits seen in the i.m. infected cases than in those animals infected by the i.p. route. Other route-dependant, early lesions have been identified in the hippocampal structure. In the orally infected animals there is obvious PrP in the CA3 region of the hippocampus after 221 days; this corresponds with the earliest timepoint that PrP is detectable anywhere in the brain. Also at this timepoint PrP can be detected among other

regions the thalamus; the venterolateral thalamic nucleus, lateral posterior nucleus and the anterodorsal thalamic nucleus; the cerebellum, posterior interposed cerebellar nucleus and in the pontine reticular nucleus. This represents a wide distribution of low levels of PrP throughout the brain at point in the incubation at which the presence of PrP is only just becoming apparent.

Although different specific areas of the brain are affected in the i.m. and i.p. infected mice the general observation that there is a fairly widespread distribution of PrP is the same as in the orally infected mice. The intensity of the protein deposition is much less than is seen at later stages of the incubation period; this is not unexpected. The observation that the spatial development of PrP pathology, with particular emphasis on very early pathological events, differs from group to group depending on which route of infection has been used reinforces the suggestion that the peripheral processing of the agent, prior to establishment in the CNS, is a factor in determining the pattern of early pathological lesions. This is supported by the fact that in the case of both i.m. and i.p. infections, which both have very similar incubation periods and ultimately similar pathological profiles, there are visible differences in the patterns of early PrP deposition which can be attributed to route of initial infection.

These route-associated pathological differences are similarly a feature of GFAP accumulation in the early stages of the disease. The first notable difference occurs in those animals infected by the intramuscular route. In these animals the first detectable signs of upregulation of astrocytic activity are seen at 166 days post injection. This is 26 days after the first signs of detectable PrP in the same animals. It is accepted that the 26 day interval is a function of experimental design with regards to sampling and that it is actually the case that the first reactive astrocytes appeared prior to 166 days post injection; somewhere between 140 and 166 days post injection. However, this observation of GFAP appearing after the initial identification of disease-specific PrP is not repeated in the animals infected either orally or by the i.p. route. In those cases GFAP was first detected at the same time as

the first PrP. It is possible that this observed lag in GFAP hypertrophy, when compared to the other two routes of infection, may be a response to the amount of PrP present. If astrocytes upregulate as a response to damage in the central nervous system and PrP either causes damage directly by some neurotoxic mechanism (Forloni et. al., 1993; Selvaggini et. al., 1993) or is simply a marker of the disease then there may be a threshold level of PrP below which astrocytes are not stimulated. This threshold level may be below the level of sensitivity of the assay system described in this thesis. This again could be a consequence of the peripheral processing of the agent and the physical distance from the site of infection to the CNS. It is conceivable that because the *biceps femoralis* is apparently physically further from the CNS than either the major body cavity or the digestive system that any infectivity introduced at this site would take longer to process. Another possible explanation is that there may be a greater number of neuronal relays for infectivity to negotiate whilst travelling from the i.m. site to the CNS than is the case in either of the other routes under investigation. This question cannot be satisfactorily answered using the data produced in this experiment and would require a more stringently designed course of work to address this issue. Consequently although PrP can be detected in both i.m. and i.p. infected animals at 140 days post injection the amount present in the brain of i.m. infected animals may well be less than is in the brain of their i.p. infected counterparts. If this were the case then it might not be unexpected that the level of disease-associated PrP required to elicit an astrocytic response might not have been reached by 140 days post injection following i.m. infection. Suggestions for further experiments that may address this question are given below.

4.2.3 Route of Infection Influences Pathological Profile.

Disease in experimentally challenged animals has been shown to develop at different rates depending on the route of infection. Furthermore, the pattern of pathological changes - at least in the early stages of the incubation period - also exhibit route-of-infection dependant differences. What has also become evident, from the work presented in this thesis, is that the profile of terminal stage pathology

in these experimental cases are different, even though the agent-strain/mouse-strain combination used in this study is constant. These differences are attributed to a combination of route of infection and incubation period. By mapping the progressive accumulation of PrP, GFAP and vacuolation these differences have been quantified and have allowed comparisons to be drawn between routes. The fact that the intramuscularly infected animals had a similar incubation period to the intraperitoneally infected mice provides a crude way of assessing the extent of influence that the incubation period had over the eventual pathological profile.

The vacuolar profiles from all three groups are significantly different from one and other. Of particular concern is the oral profile which displays no real discernible pattern with respect to either linear or exponential development of vacuolar change. Indeed the oral profile displays regions where the degree of vacuolation detectable and measurable, within the parameters set, at relatively early stages of the disease is very much higher than is seen at the terminal stage of the disease the main example being at 221d.p.i. when the degree of vacuolation measured in the caudate and in the brainstem is much higher than is seen at the terminal stage of the disease, 320d.p.i.. One factor that may have influenced this result is shrinkage of the tissue as the disease develops such that lesions that may have been identified by the computer as vacuoles (by virtue of their size and shape) at an earlier timepoint are no longer recognised as true markers of pathology. Another factor which may influence this result is the location of vacuoles within neurones (Jeffrey et. al., 1992) and subsequent neuronal loss which is a feature of some scrapie models (Jeffrey and Halliday, 1994; Fraser et. al., 1997; Chretien et. al., 1999). Consequently loss of neurones may result in loss of vacuoles which may account for this observation. The fact that neither the PrP or GFAP profiles exhibit the same degree of discrepancy would appear to support this assumption, or at least suggest that this observation does not completely represent the true course of disease development in orally infected animals. In order to address this issue it may be possible, with highly defined neuroanatomical regions, to compare the volume/area of said regions at different disease timepoints and in this way determine the degree of

tissue shrinkage. This could then be taken into account when considering the size of a true vacuole at the later stages of the disease. This however presents other problems being that it does not make allowances for naturally occurring biological diversity, nor does it recognise that tissue shrinkage as a result of fixation and processing may occur non-uniformly depending on the reagents used. One other solution is for an experienced pathologist/pathological screener to redefine the values that dictate to the image analysis software what is and is not a disease specific vacuole. This detracts from the objectivity of the exercise. These suggestions also have their own intrinsic errors and it is arguable that until better and 'smarter' image processing software becomes available these errors will remain.

The PrP and GFAP profiles of the orally infected animals are the most consistent and possibly the most significant results to arise from this work. The magnitude of these profiles is far greater than their relative counterparts from the i.m. and i.p. infected groups. In the case of GFAP accumulation in the orally infected animals there is an almost linear pattern to the development of astrocytic pathology. This is especially true after the 250d.p.i. timepoint. Beyond this timepoint the traces are virtually the same shape, the only real differences being in the height of the points on each trace. The only real aberration to this pattern is the 250 d.p.i. trace which shows higher than expected level of GFAP in regions 6,8 and 9. This may be due to sampling and animal variation. The Oral PrP trace shows a peak value in brain region 4 of the terminal group of almost 80,000μm^2 which is almost double the peak amount seen in the same region of either of the other two groups at the same relative time point. The shape of the PrP profiles from the orally challenged mice are broadly similar to those seen for GFAP, which is not unexpected given the observed co-localisation that occurs between PrP and GFAP. However, there is one region (region3, the hippocampus) which demonstrates a much higher level of PrP at a preterminal timepoint that is observed at the terminal stage of the incubation period. This can be traced back to a single animal in that preterminal sample group which had levels of PrP far in excess of its sample partners. Indeed this particular animal had levels of PrP that were far higher than any of the animals in the subsequent

terminal group. This animal specific variability is an unfortunate consequence of the small number of mice sampled at each timepoint and is indicative of a shortcoming in the design of the study. However, the numbers of animals that can be made available for a given experiment is strictly regulated by an ethics committee at NPU. It is unlikely that a much larger experiment would have been approved.

As described above, the vacuolar profiles from each of the three groups under study vary quite substantially from each other in terms of severity and distribution. However, unlike the oral profile both the i.m. and i.p. infected mice produce vacuolation profiles that exhibit a reasonable degree of linearity. As a general observation there is less overlap between timepoints than has been observed in the case of orally infected mice. Of course this is not absolute and the best case to illustrate is in the i.m. infected group where there is consistently more vacuolation detected throughout the brain at189 d.p.i than there is at 221 d.p.i. and more at 221 d.p.i. than at 231 d.p.i.. This may also be a consequence of tissue shrinkage or neuronal loss as the brain becomes more affected by the disease although the difference between the 221 d.p.i. and 231 d.p.i groups is more likely to be a sampling result, again a consequence of the small numbers of animals selected at each timepoint although in this case the closeness of the timepoints may also be a factor.

The measurements of GFAP and PrP in the i.m. infected group produce traces that are very different from those obtained in the orally infected cases. In general the profiles are much flatter than in the oral cases and the progression of disease much more regular. This is suggested by the similarity in shape of the profiles for each timepoint. One particularly interesting point concerning the i.m. results is in the comparison between the GFAP and PrP traces. At the terminal stages the profiles for both GFAP and PrP have similar shapes and even where the shapes are less similar the trend is the same. However, on the whole, the GFAP results show a steady temporal increase in the amount of protein present. The traces fit on top of each other as the disease progresses towards endpoint. This is not always the case, but

where there is a break from this pattern there is only an inversion of one timepoint and the resulting differences do not appear to be significant.

It ought to be pointed out however that because of shortcomings in the experimental design, in particular the small number of animals examined at each timepoint, statistically meaningful results cannot be produced. An example of this is in the GFAP trace where the 189 d.p.i. trace lies above the 221 d.p.i. trace throughout much of the brain. A similar inversion is seen between 221 d.p.i. and 231 d.p.i. in the PrP result. More striking however, in the PrP result, is the 189 d.p.i. trace. This shows that at 189 days following infection the amount of PrP detectable in almost every region of the brain that was examined was greater than at any other time apart from the end stage of the disease. This is an apparently anomalous result. Scrapie and the associated TSEs are by their nature progressive diseases. If this result is considered solely on the information obtained from the computerised image analysis system then the suggestion is that relatively early in the disease incubation following i.m. infection (this is not seen in either orally or i.p. infected mice) there is a large deposition of PrP in the brain which is subsequently cleared, or trafficked to a region or regions of the brain out with the scope of this study, only to be redistributed back in the same areas as it was previously detected, at the terminal stages of the incubation period.

A different interpretation (and one which seems more plausible given the limitations of the image analysis system that was used to produce the results) might be that this observation is a result of protein aggregation. Consider an hypothesis that accepts the result observed at 189 d.p.i. and the subsequent timepoints to be genuine with regards to the area of the brain occupied by detectable PrP. The important consideration here is that the image analysis system employed in this study does not have the capacity to measure the actual amount of protein in the brain, instead it measured the area that the protein of interest occupied. It is known that PrP forms aggregates of protein, for example amyloid plaques (Bruce, 1981; Hope et. al., 1988). One interpretation of the results might be that the PrP detected at 189 d.p.i. is

in a non-aggregated or less-aggregated form than is present at the end-stage of the disease. If it can be assumed that aggregation of PrP results in concentration of the protein then it is feasible that the area occupied by a given amount of PrP would be less if the protein was in an aggregated state. The actual amount of protein would be identical but without a means of measuring the concentration of the protein in a section the result as obtained by the image analysis system would show an apparent decrease in the level of PrP in the brain.

With this suggested mechanism of protein concentration the results can be explained in terms of an early stage of PrP release into the neuropil prior to any aggregation (Jeffrey et. al., 1994). This would then be followed by a combined sequence of deposition and concentration - this would explain how the level of PrP increases to its endpoint peak - until the terminal stage of the disease. The observations made by the image analysis system in this case would be much as has been seen. Of course in order to test this hypothesis it would be necessary to develop an assay capable of measuring the actual amount of PrP in an aggregate. The simplest approach would be to perform a total protein extraction from the brain and perform a quantitative Western analysis using specific anti-PrP antibodies (ideally anti-PrP^{SC} antibodies such as those developed by Prionics in Switzerland, Korth et. al., 1997) and subsequent densitometric analysis. However, as this destroys the tissue that is under investigation it is obviously not suitable in cases where pathology and histology are paramount considerations. Another possible method of determining the amount of protein depends on the development of an effective tool for measuring both area occupied by the protein and the optical density of the region of interest. This is theoretically possible, although technically it is beyond the capability of the system used in this study. If a system of this sort could be developed then it would become possible to measure absolute amounts of immunostained product, this in turn would overcome the potential problem of comparing different types of PrP deposit that exists when they are considered only in terms of the area that they occupy within a section or a microscope field.

The results of this thesis with respect to orally challenged mice have been very interesting especially in comparison to what has been reported in the literature regarding the relative inefficiency of the system and requirement for significantly higher infecting doses to produce disease (Kimberlin and Walker, 1988; Kimberlin, 1994). The work presented in this thesis shows that this is not in fact the case. This is in keeping with recent reports regarding oral pathogenesis in hamsters infected with the 263K strain of scrapie (Diringer et. al., 1997; Beekes et. al., 1998) which report the oral route of infection as being an efficient means of establishing disease in Syrian golden hamsters. This efficiency is increased if repeated or multiple dosing regimes are adopted (Diringer et. al., 1998) however it is not wise to assume that the hamster model acts in exactly the same way as the murine model described in this thesis. The fact that 100% infection was achieved in mice following a single dose of infectivity may simply indicate that oral dosing is perhaps more efficient in mice than in hamsters at establishing infection. These differences in efficiency may that oral pathogenesis is perhaps best studied in mice although the shorter incubation period seen in the hamster/263K combination is an attractive feature for researchers in the field.

4.3 How do the Kinetics of Infection Vary With Route?

The kinetics of experimental infection were investigated to determine what effect any route-dependant differences in the processing of infectivity might have on the pattern of pathology, especially the speed and rate at which pathological markers accumulate. The results in Chapter 3 demonstrate the rate at which pathology develops in three specific brain areas (the thalamus, the hippocampus and the frontal cortex) following infection by each of the three routes under investigation. These regions of the brain were chosen as they are the regions that appear to be most involved in terms of detectable pathology (in the case of hippocampus and thalamus) for all the routes of infection studied. The frontal cortex was chosen as it appeared to be less involved and could be thought of as a test of the ability of the image analysis system to detect subtle changes in the pathological status of a given region. These are

not true kinetics as defined in terms of information regarding rate of agent replication, but the information that they do provide can be assumed to be a parallel of this. The most attractive feature of the information as it is presented is that it demonstrates the development of pathology from that earliest point in the incubation at which PrP and GFAP can be detected. In order to draw meaningful comparisons between routes of infection it was necessary to 'normalise' the incubation period for each model. It was decided that the simplest way to do this was to convert the incubation period into a scale of 100 equally spaced points. In this way events occurring at a particular point in the incubation period of an i.m. infected mouse can be directly compared with the same relative point in an orally infected mouse. This is not a perfect solution as the standard errors associated with the incubation periods mean that some of the animals considered as representing 100% of the incubation period actually succumbed to disease at some time after that point. This is acknowledged as a source of error and represents a shortcoming in the experimental design but as this study is especially concerned with early pathological events and because each of the experimental groups is subject to this source of error it is considered acceptable and not likely to significantly bias the results.

4.3.1 PrP Kinetics in Experimental Infection.

In the orally infected group of mice the first PrP that is detectable by the image analysis system is seen relatively later than is the case in either the i.m. or the i.p. groups (approximately 70% of the total incubation period compared to 50% in the i.m. cases and 56% in the i.p. cases). This could be interpreted as an indication of the reported inefficiency of the oral route of infection (Kimberlin and Walker, 1988) and evidence of an extended replication phase of the agent outside of the CNS.

From the time of first detection in the thalamus until the end of the incubation period there is a rapid almost exponential increase in the amount of PrP that can be measured. The steep gradient of this curve is indicative of a high rate of PrP

deposition. The maximum value is reached at the very end of the incubation period. This is not unexpected and would be an intuitive assumption given the progressive nature of the disease. However, although the same exponential type of increase is seen in the hippocampus and the frontal cortex, the maximum level of PrP is achieved at a time period prior to the terminal stage of the disease. These maxima occur in both cases at approximately 95% of the total incubation period, after which time there is a noticeable, and especially in the case of the cortex highly substantial diminution in the amount of PrP that can be measured. In the case of the frontal cortex the gradient of the slope leading towards the maximum value is steeper than in the thalamus or in the hippocampus this suggests that the rate of PrP deposition in the cortex of orally infected mice is greater than in the thalamus of similarly infected animals although the amount of protein deposited there is not as great.

The apparent drop in the amount of protein in the cortex and hippocampus prior to the terminal stage of the incubation period is a particularly puzzling feature as it is not seen in either of the other two models under investigation nor is it seen in the measurements of GFAP made in parallel regions of serial sections of orally infected mouse brain. Indeed it seems to be a feature that is particular to the orally infected group of animals. The reasons for this are unclear but it is possible to theorise that given the extended nature of the oral incubation period compared to the i.m. and i.p. models that the rapid decrease is perhaps related to this longer incubation. This theory makes no assumption about what triggers the fatal event in scrapie infection that leads to the death of the animal. It is particularly difficult to address that question with the information presented here: for example if death from scrapie infection were solely the result of excessive amounts of PrP in the brain then it may be expected, from this data, that the incubation periods of the i.m. and i.p. infected animals (in which there was measurably less PrP at the terminal stages of the infection than was seen in the oral cases) would be extended. This is clearly not what has been observed in this study. It is conceivable that given the longer incubation period which is associated with the oral infection that there is a greater degree of processing of the disease associated PrP. PrP is known to form aggregates and the

longer incubation period may allow the PrP to aggregate into tighter and more defined structures, for example amyloid plaques, this is however only a theory at this time as there is no evidence that plaque formation is a direct function of incubation period. These would have the appearance of being darker - as the protein becomes more concentrated - than in cases where there was a lesser degree of organisation but it may also have the effect of reducing the total area of the brain that is occupied by the protein whilst at the same time representing an increase in the actual amount of PrP present. Using the image analysis system described in Chapter 2 it would be impossible to differentiate between a protein concentration event of this type or a genuine decrease in the amount of PrP present. However, given that scrapie is a progressive disease and there is no evidence of any instances where the amount of PrP in an infected animals brain has decreased, perhaps as the result of scavenging by phagocytic cells in the CNS, prior to death this seems unlikely. What is very clear from this study is that the maximum level of PrP, as measured by the area that the protein occupies, in the brains of these orally infected mice is far in excess of the levels detected in their i.m. or i.p. infected counterparts and the rate at which the protein accumulates following its initial detection is also far greater in the orally dosed group.

In the i.p. infected group the most heavily affected region was the thalamus. This is also the case in the i.m. infected mice as well as in the oral group described above. However, the maximum levels of PrP that can be detected in either the i.m. or the i.p. group is approximately half that which is seen in the oral group (the i.p. infected animals present with more thalamic PrP than the i.m. group, but this is still far below the level seen following oral challenge). This is in keeping with the idea that an extended incubation period means that there is more opportunity for greater amounts of PrP accumulate in the brain, and that high levels of PrP alone are not sufficient to cause death. However, neither the i.p. nor the i.m. infected mice display the same sort of rate of accumulation. For the most part both of these groups display a fairly steady level of PrP until very late in the incubation period. There is a notable hump in the early part of the curves for both groups, which is not seen in the orally

infected mice. In the i.p. group this occurs at around 75% of the way through the incubation and in the i.m. group at around 67% of the total incubation period. This hump is seen in all three of the brain areas examined with the exception of the hippocampus in the i.p. infected group. This may be the result of an intermediate stage in the processing of the PrP in the brain, as has been postulated above. If this type of proposed packaging of the PrP protein is actually occurring then this part of the incubation period may coincide with the key event in the formation of amyloid plaques. This would result in a temporary reduction in the amount of diffuse non-aggregated PrP in the brain. This level would then start to rise again as more PrP^{SC} was deposited in the brain. As in the case of the oral kinetics this is purely speculation and further work, including the development of a more powerful analysis system, capable of measuring the concentration of protein contained within a given aggregate, is required before observation can be examined more closely. Two things are very clear from the kinetics study; first is that the amount of PrP found in the brain of orally infected animals is much more than is found in the brains of animals infected by the other routes under study. This is almost certainly a function of the extended incubation period that is seen in the case of oral infection. Second, although the appearance of PrP in the CNS occurs later in the course of the disease, relative to the length of the whole incubation period, of orally infected animals than in either of the i.m. or i.p. groups, after it is detected the rate at which it accumulates is very much higher than in the other groups.

4.3.2 GFAP Kinetics in Experimental Scrapie Infection.

As with the results of the PrP kinetics study one of the first observations that was made regarding the deposition of GFAP was that the levels that could be measured in the thalamus were far higher at the end stages of oral infection than after infection by either the i.m. or i.p. routes. This is not unexpected as there is a strong relationship between PrP deposition and GFAP accumulation and the rate of this GFAP accumulation appears to be similar to the rate of PrP deposition, as seen by the almost identical gradient of the trace. However, unlike the PrP results which showed

markedly higher levels of the protein in the orally infected animals in all three regions studied, this is not the case for GFAP.

In the orally infected group one of the more interesting observations regards the levels of GFAP seen in the hippocampus compared with the frontal cortex. The level of hippocampal GFAP is approximately double the amount that is seen in the frontal cortex, this is an inversion of what is seen with respect to the levels of PrP in these areas. It is possible that this is due simply to the number of astrocytes that are found in each of these respective areas but this is unclear and information regarding the normal distribution of astrocytes in the murine CNS is not readily available.

The deposition of GFAP in the hippocampus of orally infected mice is a much more linear affair than is seen with the PrP accumulation. Following first detection of reactive astrocytes, which occurs at the same time as the first PrP is seen, there is a steady progression in the hippocampus. In the frontal cortex of the orally infected mice the pattern of accumulation depicts a rather extended lag phase where there is very little GFAP to be seen. This then proceeds slowly, as defined by the low slope of the trace, to a peak that is not only far lower than in either of the other two regions examined in the orally infected mice but it is also much lower than is seen in the corresponding area of the other two groups of mice, i.m. and i.p. infected. This is unusual given that the peak amount of PrP detectable in the frontal cortex of the orally challenged mice is many times higher (approximately five times) than the peak amount registered in the i.m. group.

Examination of the kinetics of PrP and GFAP accumulation in each of the three brain areas in i.m. and i.p. infected animals show that the deposition of PrP is closely mirrored by the accumulation of GFAP, and by inference the activation of astrocytes. This is indicated by the similarity in shape and gradient of the PrP and GFAP traces. It is also the case that the kinetics results from each of the three areas in each of the i.m. and i.p. groups are very similar. This close similarity, both within a group and between the i.m. and i.p. groups, suggests that the processing of

infectivity and the progression of the disease in these cases are similar. The fact that those two groups are so similar whereas the orally infected group is markedly different - (not only from the other groups but even within it's own group, where the GFAP and PrP traces for a given area are very different except for the thalamus), suggest that these differences are the result of an alternate route of infection.

This suggests that infection of a given strain of mouse with a given strain of scrapie, via the oral route will result in an infection that develops a more severe degree of pathology than if the infection were established by another route. Furthermore the observed parallel between PrP and GFAP that has been seen in the i.m. and i.p. groups is not observed. This phenomenon may not solely be a function of route of infection but these differences coupled with the extended incubation period (when compared to other peripheral infections) encourage questions about the role of both PrP and GFAP in disease development and these observations again raise questions about what the fatal event in scrapie infection actually is. If for example death from ME7 scrapie is the result of neuronal loss brought about by a PrP^{SC} mediated acute inflammatory response (Betmouni and Perry, 1999) then it seems intuitive that the model producing the most PrP^{SC} would have the shortest incubation period, or, that the model with the shortest incubation period would indicate what the 'lethal' amount of PrP^{SC} required to produce a fatal degree of neuronal loss ought to be. The results of this study would suggest that PrP^{SC} mediated neuronal loss is not the only factor in causing death by ME7 scrapie.

4.4 The Role of the Lymphoreticular System in Experimental Scrapie Infection.

Replication of the scrapie agent in the tissues of the lymphoreticular system (LRS), following extra-neural infection, is recognised as an important stage in the development of disease prior to the observation of pathology within the CNS. This peripheral processing occurs without obvious tissue damage to the LRS or any signs of physiological deficit. Of particular importance in this process is the spleen

(Eklund et. al., 1967) which constitutes the major organ of the LRS, although other components of the LRS are involved such as the lymph nodes. In the case of human TSE infection there is evidence for involvement of the tonsil and appendix (Hilton et. al., 1998). There is also demonstrable involvement of the spleen following intracerebral infection with some strains of the scrapie which appear to undergo a replication stage in the spleen despite the fact that they have been introduced directly to the target organ, the brain and CNS. The target cell for this replication stage is thought to be the follicular dendritic cell, or FDC (Brown et. al., 1999; O'Rourke et. al., 1994).

In the later stages of the studies described in this thesis it was decided to examine the spleens of animals infected by alternate, extra-neural, routes at the late stages of the incubation period in order to determine whether or not there was an accumulation of disease associated PrP^{SC} in the organ. As mentioned above the tissues that were examined were harvested from animals in the late stages of the disease incubation period. This unfortunately means that data concerning the early accumulation of infectivity - as indicated by PrP accumulation- is lost. This is an obvious shortcoming in the study. However, the decision to investigate the spleens for markers of infection was not taken until after the early incubation period animals had been sacrificed and examination of the lymphoreticular system was not one of the original objectives of the study. From the tissues that were available it was possible to show that there is detectable PrP in the spleen of animals infected orally, i.m. or i.p. at the late stages of the disease. The PrP is restricted to the germinal centres of the follicles, the site of residence of FDCs. This is in keeping with previously published observations (McBride et. al., 1992).

Spleens were recovered from animals sacrificed at the three latest timepoints in the orally infected mice. This represented a period from approximately 80% of the total incubation until the terminal stages of the disease. PrP is detectable in the spleen at this timepoint (80% of the total incubation) as it is in spleens of animals sacrificed at the two subsequent time points (corresponding to 87% and 100% of the

incubation period respectively). However, there appears to be a decrease in the amount of PrP that can be detected in these spleens as the end stage of the disease is reached. In the case of the i.p. and i.m. infected animals spleens were taken from the penultimate group of animals to be sacrificed and the terminal group. This was due to the reduced total incubation period, compared to that of the orally infected mice. In the spleens taken from the i.m. infected mice PrP was detectable and was localised to the follicles as expected. However contrary to the observations made in the orally infected mouse spleens, of an apparent decrease in PrP levels, in these animals there appeared to be more protein in the spleens of animals sacrificed at the terminal stage (100% of total incubation period) of the disease than at the penultimate timepoint (89% of the total incubation period). To further confuse the issue, in the spleens removed from the i.p. infected animals there was no apparent difference between the amounts of PrP detected at the penultimate stage of the incubation period (91% of the total) and the terminal stage. Given the small number of observations and the fact that only spleens from animals at the late stages of the incubation were examined, a further, more in-depth study is required to investigate the possibility that these results are a function of sampling errors.

These observation demonstrate that the spleen is involved in the disease process and remains involved up to the end of the incubation period. There is also a suggestion that the route of infection may have an influence on the involvement of the spleen, and by extrapolation other elements of the LRS in the processing of scrapie infectivity as indicated by the presence of PrP. For example, in the case of the orally infected mice where there is apparently a reduction in the amount of PrP in the spleen as the disease reaches endpoint perhaps there is a mechanism at work to transport the protein out of the LRS and into the CNS via the spinal nerves. This could be part of the reason that the amount of PrP found in the brain of orally infected animals is so much higher than in animals infected by the other routes under study, although the extended incubation period is the most likely reason.

These are however, subjective observations and hypotheses made on the basis of few observations. As such there is no way to substantiate the suggestion that route of infection influences the role of the LRS in experimental scrapie infection. In order to decide whether or not these observations are genuine it would be necessary to perform more experiments. Proposals for this and other further work are discussed below.

4.5 Does the Pathology Observed in Animal TSE Models Compare with Acquired Human Disease?

The main aim of the work described in this thesis was to test a hypothesis that suggested that the route of infection had a significant influence on the pathological outcome in cases of experimental scrapie. By choosing the i.p. and especially the oral and i.m. routes of infection it was possible to examine scrapie under the guise of an acquired TSE infection, such as has been seen in man with vCJD and iatrogenic CJD infections.

The proximity of the Neuropathogenesis Unit, where this study was carried out, to the National CJD Surveillance Unit in Edinburgh and the close professional relationship that exists between both centres made it possible to examine any similarities and differences in the pathological profiles of acquired human CJD with an animal analogue. The basis for comparison between animal models and human cases of acquired CJD centred on the distribution of vacuolar change and the distribution and appearance of PrP depositions within certain brain regions.

One of the implicit drawbacks with this sort of comparative exercise is that although there is the opportunity to study the development of pathology in the animal models at various timepoints throughout the disease incubation, it is only possible to examine terminally affected tissue in the human cases. On this basis the tissues selected for comparison with the human cases were taken from the endpoint animals infected by each of the routes under study. Immediately this poses a challenge with respect to extracting useful information from the exercise. Although there are early

differences in the distribution of lesions; by the time the disease reaches the terminal stages the severity of the pathology that can be seen, in terms of vacuolation GFAP accumulation and PrP deposition, as well as the broad regional distribution of these markers is the same in the different animal models. The same is obviously not true of human disease where there are obvious regional differences in the pathology that can be seen depending on the type of infection involved (iatrogenic, vCJD or sporadic). Indeed it is these differences in distribution along with the appearance of other indicators (for example, 'florid plaques' in vCJD and analysis of PrP genotype) that allow a diagnosis to be reached. It is difficult in these circumstances to draw any conclusions regarding the influence that route of infection has in TSE infections acquired by humans. In the animal models the observations made in this study indicate that early pathological events are more likely to be influenced by the route of infection than the eventual pathological profile. The animals used in this study were all of the same inbred strain and they were all infected with the same strain of scrapie. This is obviously not the case in human acquired disease, where not only are the host genetics subject to variability between cases but the infecting agent cannot be assumed to be of the same strain in each case. Proof exists that the strain of agent responsible for vCJD in man is also the strain responsible for BSE in cattle (Bruce et. al., 1997), this however is different from the agent responsible for infection in iatrogenic cases or sporadic cases, although there is a possible argument that the agent responsible for iatrogenic infection resulting from pituitary derived growth hormone therapy may be the same as the agent responsible for sporadic CJD. Strain typing experiments such as the one that proved that BSE in cattle and vCJD in man were caused by the same strain of agent could be used to examine this. There is however, no current evidence to support this assertion.

Current epidemiological evidence from Australia suggests that people who have undergone more than three general surgical procedures double their risk of developing sporadic CJD (Collins et. al., 1999). The likely explanation for this increased risk is one of increased exposure with surgical exposure resulting in an unrecognised iatrogenic infection. Reuse of surgical instruments that may not have

been completely decontaminated following procedures, such as tonsillectomy, in patients who may have gone on to develop CJD. It has been shown that PrP and by association infectivity can be detected in these tissues in humans with variant CJD (Hill et. al., 1999). Tonsils are negative for PrP both by immunohistochemistry and Western blot in cases of sporadic CJD, this however does not discount the presence of infectivity in other tissues and the consequent risk of carry-over infection. In sheep (scrapie) and cattle (BSE) PrP can be detected far in advance of the onset of any neurological symptoms (Van Keulen et. al., 1996) so it is conceivable that residual infectivity could transmit the disease - in much the same way as contaminated neurosurgical electrodes have been linked to transmission of the disease. Of course transmission as a result of general surgery is likely to be far less efficient than transmission from neurosurgery. In terms of the experimental models described in this study sporadic CJD as a result of infection following surgery might be an iatrogenic event that represents a route of infection similar to the i.p. infection used in animals; unfortunately there is only very limited data on infectivity outside the CNS in sporadic CJD.

The differences in pathology, both distribution and type, observed in the human cases are not seen in the animal models at the terminal stages. This does not necessarily mean that the route of infection does not influence the pathological presentation of these diseases in humans, but, due to the number of variables that are not controlled in human disease it is not possible to assess to what extent this route dependant influence may extend.

It has not been possible, from this comparative study to draw any conclusions, regarding the role that route of infection plays in the development of human CJD and the appearance and distribution of lesions in the CNS at the terminal stages of the disease. The fact that the terminal pathology in each of the human cases is markedly different would suggest that the early pathological events are also different. This is similar to what is seen in the animal models where the early pathological changes are most likely to exhibit differences which, considering the constant agent strain/host genetics combination, can be attributed to the route of infection. So it is possible and

indeed likely that route of infection affects early pathology, by virtue of the way in which the infectivity is processed in the periphery prior to invasion of the CNS. The subsequent differences in pathology that are seen in the human disease, but which are largely absent from the animal models must then be a function of other factors including host genetics and agent strain. Table 13 summarises some of the differences that are seen in the various different types of human CJD infection in certain areas of the brain. Of particular interest are the pathological differences seen in the sporadic cases which appear to be a function of the host genotype, in particular at codon-129 of the PrP gene. Comparison of the methionine homozygotic, sporadic CJD, profile with the variant CJD profile, where all cases to date share the same PrP genotype (129MM) reveals differences in pathology that can be attributed to either strain of agent and/or route of infection. Unfortunately neither of these factors are known to be common to both disease subtypes. It is therefore difficult to determine how much influence the route of infection alone exerts on the pathological phenotype.

Subtype	Cerebrum	Basal Ganglia	Cerebellum
Sporadic CJD PRNP 129 MM	spongiform change ++ perivacuolar/synaptic PrP	spongiform change + synaptic PrP	spongiform change + synaptic PrP
Sporadic CJD PRNP 129 VV	spongiform change + synaptic/perineuronal PrP	spongiform change ++ synaptic PrP	spongiform change + synaptic PrP
Sporadic CJD PRNP 129 MV	spongiform change + perivacuolar/synaptic PrP	spongiform change + synaptic/plaque PrP	kuru plaques synaptic/plaque PrP
Iatrogenic CJD GH recipients	spongiform change + synaptic perineuronal PrP	spongifrom change ++ synaptic/plaque PrP	spongiform change ++ synaptic/plaque PrP
Variant CJD PRNP 129 MM	florid plaques ++ plaque/perineuronal PrP	spongiform change ++ perineuronal/axonal PrP	florid plaques ++ plaque/perineuronal PrP

Table 13: Summary of some of the key pathological differences that are seen in the various subtypes of human CJD. Special reference to spongiform change and PrP deposition.
(Table courtesy of James W. Ironside).

In order to study the extent to which each of these individual factors influences terminal CNS pathology it would be necessary to set up further, much larger experiments than have been described in this thesis involving multiple strains of inbred mice infected by multiple peripheral routes with a variety of strains of scrapie. This was certainly not feasible within the time frame of this project.

4.6 Can Mice Devoid of Endogenous PrP Transport Scrapie Infectivity?

It is reported in the literature that that the presence of endogenous PrP in the central nervous system is required in order to facilitate the transport and propagation of scrapie infectivity such that the disease can spread throughout the brain (Bueler et. al., 1993; Sailer et. al, 1994; Weissmann et. al., 1994; Brandner et. al., 1996; Brandner et. al., 1997). The spread of the disease is explained, in the terms of the protein-only hypothesis, as a process of sequestration and alteration of the host encoded, endogenous, PrP into the pathogenic, disease-associated form (PrP^{SC}). The alteration which takes the form of a conformational change is what gives the agent its unusual physico-chemical properties. In the case of acquired disease (such as experimentally induced scrapie) the conformational change is driven by exogenous 'prions' which consist of the abnormal form of the protein. Once this process starts it becomes self-catalysing such that the limiting factor is the amount of available normal PrP. In accordance with this model mice that are devoid of endogenous PrP are resistant to infection with the scrapie agent; however, the actual transport of infectivity is also thought to be PrP dependant. The results gathered from this project suggest that this is not necessarily the case.

Although the numbers involved are very small it is interesting to note that three bioassay animals (C57BL mice) that had been injected with material from the visual systems of PrP-null animals previously injected intraocularly with ME7 scrapie developed disease, but this was not seen in any of the recipients of PrP-null tissue. The affected bioassay animals were injected with preparations of tissue harvested from the PrP-null mice 24hours post intraocular injection with ME7 scrapie.

Twenty-seven (27) bioassay animals were separated into three equally sized groups. Each of these groups was the recipient of either optic nerve, superior colliculus or dorsal lateral geniculate nucleus homogenates which were prepared

from a pool of six PrP-null mice sacrificed 24hours post injection. Of the nine animals who received the optic nerve preparation, two exhibited signs of scrapie infection and were sacrificed at 304 d.p.i. One of the animals that received the superior colliculus preparation also developed scrapie with an incubation period of 316 days. These three animals were confirmed as having scrapie caused by the ME7 strain of the agent by experienced staff at the Neuropathogenesis Unit. None of the animals that received the dLGN preparation developed or exhibited any sign of disease.

The most immediate concern surrounding this result was that it could be the consequence of contamination with extraneous, infective material not derived solely from the PrP-null tissue donors. However, there is no readily identifiable source of this type of contamination. The most likely source would be residual inoculum in the globe of the eye but care was taken not to rupture the globe whilst the tissues were harvested. Furthermore, if the inoculum pool had been contaminated in some way then it is likely that more of the bioassay animals would go on to develop scrapie. This is not the case.

A particularly interesting feature of this result rests in the comparison with the control group. The control animals received similarly prepared and pooled inoculum, but in this case the donor animals were PrP expressing 129/Ola mice. Groups of these animals were sacrificed in parallel with the PrP-null animals. The tissues harvested from the control group at 24 hours post infection only produced disease in three of the bioassay mice injected with the optic nerve preparation. This may indicate that the rate of trafficking of infectivity was actually quicker in the PrP-null mice than in the wild-type as indicated by the transmission of disease from the superior colliculus fraction.

This result indicates that there could be a degree of transport of infectivity in the CNS of PrP-null animals. The fact that the incubation periods were relatively longer in the recipients of PrP-null tissue coupled with the observation that only

tissues harvested 24 hours post-injection are infective may be indicative of a diluting effect. The discrepancy in incubation periods may be explained in terms of infectivity titre. In the wild-type where replication of the agent is assumed, the titre of infectivity rises and this may account for the shorter incubation period, if we assume that there is no replication of infectivity in PrP-null mice. The observation that only tissues harvested very early after initial injection with the agent are capable of transmitting the disease indicates that the level of infectivity in these visual system areas at the later timepoints is not as high. This could be the result of transport of a finite amount of infectivity through the CNS, the result of which is sub-infective levels of the agent over a wider area of the visual system. It may be a worthwhile exercise in the future to design an experiment that will enable not only regional assay of certain CNS nuclei but also whole brain infectivity assays in PrP-null mice. Proposals for worthwhile future work are considered at the end of this chapter.

The final feature of this result that is worth consideration concerns the pattern of disease appearance in the control group. The results show clearly that in animals infected with wild-type tissues harvested between 41 d.p.i. and 83 d.p.i. there is a noticeable trough in the number of animals that develop the disease. The reason for this is not clear, but it may represent a lag-phase in the donor animals during which the infectivity undergoes some form of processing and is not active in promoting disease (Kimberlin, 1979; Bruce and Dickinson, 1985) . This is conjecture at this time, and although there is always the possibility that the lack of scrapie-infections in animals in receipt of these tissues is the result of experimental error, this seems unlikely. However constraints of time, one of the main problems associated with TSE research, make it impossible to repeat this experiment during the course of this study.

What this experiment seems to show is that regardless of the PrP status of an animal, scrapie infectivity can be transported in the CNS. The speed at which infectivity is found in the superior colliculus of the PrP-null animals would suggest that the transport process is active, this is in keeping with previous reports that

infectivity travels by axonal transport (Kim et. al., 1990). Of course the result also supports the view held in the literature that animals devoid of endogenous PrP cannot effect the replication of the infective agent and that by association PrP is closely associated with the agent itself.

4.7 Summary.

This thesis reports the results of a pathological investigation into the effect that establishing scrapie infection in mice by a variety of peripheral routes, including oral has on the pattern of pathology that subsequently develops in the CNS. The inclusion of the oral route of infection was considered especially pertinent considering the recent suggestion of a causal link between BSE in cattle and vCJD in humans. A further study was conducted in parallel with this study for the purpose of examining the possibility that mice devoid of endogenous PrP are capable of at least transporting scrapie infectivity in the CNS. This study was conducted inoculating PrP-null mice, and their wild-type (control) counterparts, with ME7 scrapie by the intraocular route. By this route pathology and infectivity are targeted in a well defined manner to the projections of the optic nerve. This facilitates the micro-dissection of discrete areas of the visual system and assay of these regions for the presence of scrapie infectivity. The results suggests that infectivity can be transported in the CNS of mice devoid of PrP although the degree of transport is limited and does not appear to be accompanied by any replication of the agent that would be denoted by amplification of the amount of infectivity and subsequent long incubation (consistent with low levels of infectivity) in the affected bioassay animals.

This result contradicts the report that endogenous PrP is necessary for the transport of scrapie infectivity in the CNS (Brandner et. al., 1997) and is the first time that such an observation has been made. The possibility that this observation was the result of a contamination event was fully considered. However, on review of the experimental procedure and scrutiny of the pathology in the affected bioassay animals, there is no reason to suspect that the result does not support the fact that

transport of infectivity has been demonstrated in animals previously thought to be incapable of doing so.

The investigation into the role that the route of infection plays on the development of pathology in experimental scrapie infection constituted the major part of the work presented in this thesis. By designing the experiment in such a way as to restrict the experimental infection to a single strain of agent in a genetically homogeneous population it was possible to attribute any differences in the observed pathology to the route of infection. It is possible that the increased infecting dose that was administered to the orally infected animals (five times the volume administered to the i.p., i.m. and i.c. infected mice) may have had an effect on the development of pathology that is dissociated from the influence exerted by route of infection alone. However, considering that the oral route is thought to be up to 100,000 times less efficient at establishing infection than the i.c. route (Kimberlin and Walker, 1988), it is unlikely that this is the case. The results of this study have shown that the oral route of infection is actually very efficient at establishing CNS disease in experimental mice. All of the animals infected orally succumbed to infection in a relatively constant period of time. The incubation period observed when infection is established by this route is longer than any of the other routes of infection but the standard error associated with the mean incubation period for the orally infected mice is very small. This is taken to indicate uniform and efficient processing of infectivity in the periphery prior to invasion of the CNS. This demonstrable efficiency of oral infection is complemented by recent studies of oral pathogenesis in hamsters using 263K scrapie (Diringer et. al., 1998; McBride and Beekes, 1999) although if anything this study suggests that mice infected with ME7 are even more susceptible to disease following oral challenge. Ultimately the pathology seen in the brains of orally challenged animals was more severe than was seen in animals dosed by the other routes in this study. However, the actual distribution and appearance of the pathology, in terms of the brain areas affected and the form of the PrP protein found in those areas, was indistinguishable at the terminal stages from the pathology seen in the brains of i.p. and i.m. infected animals. The

increased severity of the lesions in the CNS of orally infected animals is therefore probably due to the increased incubation period. The i.p. and i.m. infected mice had similar incubation periods and displayed broadly similar terminal pathology both in terms of distribution and severity. Where the results were different was in the early stages of the disease where there were route-dependant differences in the appearance, both spatial and temporal, of the initial pathological lesions. This suggests that the route of infection may influence the way in which infectivity is processed in the periphery, by directing it to certain areas of replication such as site associated lymphoid tissues, and the route of access to the CNS, however once infection has been established in the brain the other known governors of pathology and pathogenesis (agent strain and host genetics) are the controlling factors.

It was intended that the establishment of a murine model of oral and intramuscular scrapie (which may be expanded to include other experimental TSE infections) would provide an animal model to elucidate the disease process associated with iatrogenic CJD and new variant CJD in man. However, the marked differences that are seen in the pathological presentation of these human diseases are not mirrored in the animal system. This presents more questions regarding the strains of agent involved in human disease and the role of the human PrP gene in directing pathogenesis than it answers concerning the role of route of infection. However, it also suggests that further studies in animals using the oral route of infection and others may be useful in breaking down the control mechanism into its component parts in order to assess which is the most influential. This could be done with a combination of well characterised mouse strain/ scrapie strain models. Animal models afford researchers the opportunity to examine the disease process at all times through the incubation period, this is obviously not the case in human disease. If there are to be any intervention type therapies for the treatment of acquired human TSEs then it is important to know as much as possible about the disease process. Given that oral acquisition of disease is a prime candidate in vCJD, and there is epidemiological evidence that some sporadic CJD cases may actually be acquired (in a manner akin to i.p. infection; Collins et. al., 1999) then studies of this type in

animal models are potentially valuable tools to further the understanding of acquired TSEs, both in man and in other animal species.

5. Conclusion

The experiments described in this thesis were designed to test the hypothesis that the route of infection affects the development of pathology and thereby thephenotype in cases of experimental murine scrapie. The results of this study indicate that:

- The hypothesis is confirmed. There are measurable and identifiable differences in the development of pathology which, due to the controlled nature of the agent/host model, can be attributed to the route of infection.
- The degree of pathology observed throughout the brain following oral infection is greater than is seen in the i.m. or i.p. infected cases. It is very likely that this is a function of the increased incubation period seen in the orally infected animals, such that there is simply more time for pathological lesions to develop. However, this result raises questions regarding the critical event, or sequence of events, that eventually leads to death.
- There is a close relationship between PrP deposition and GFAP accumulation in the i.m. and i.p. infected mice that does not appear in the case of the orally infected animals. In the i.m. and i.p. cases GFAP accumulation mirrors PrP deposition in the thalamus, hippocampus and frontal cortex. In the orally infected animals the PrP profile in the hippocampus and frontal cortex is very different from the GFAP profile. The reason for this is unclear and further work may be required to clarify the reason for this observation.
- The oral route of infection has been demonstrated to be an extremely efficient method of establishing disease in the murine model examined here. This is demonstrated by the very narrow incubation period range and the small standard error associated with the mean incubation period. The efficiency of the oral route of infection in mice may have implications for human disease, especially vCJD. vCJD is acquired orally and is caused by the same agent that is responsible for BSE in cattle. To date all reported cases of vCJD share a common *prn-p*

genotype. This is analogous to the agent strain/host strain controlled murine model that has been studied and may allow for the construction of a more accurate model of the likely size and duration of any future vCJD epidemic.

- It appears from these results that the application of a semi-quantitive method of assessing vacuolar degeneration in scrapie infected mouse brains is feasible. The close correlation obtained between the results obtained from a computerised image analysis system and those reported by experienced assessors of spongiform change suggest this. Employment of such a system may allow for more meaningful exchange of information between different laboratories and generate a uniform standard for assessing vacuolation. However, because the automated system is actually slower than an experienced pathologist, it will be some time before the technology is in place to make this a widespread and feasible option.
- It is difficult to draw any direct comparisons between the murine models and human diseases. Although disappointing in terms of this study it does produce more questions and suggests that further experiments should be designed in order to examine the influence that each component of the disease process, including agent strain, host strain and route of infection play in the development of a pathological phenotype.
- In addition to the development of CNS pathology following infection by alternate routes, there is an indication that peripheral processing of infectivity may also be affected by the route of infection. This is based on very few observations because the spleens were not routinely harvested from animals at the earlier stages of their incubation periods. Further experiments to examine more closely the involvement of the lymphoreticular system in acquired TSE infections are required.
- The results of the bioassay experiment indicate that scrapie infectivity can undergo limited transport in the CNS of animals devoid of endogenous PrP. This is, to the best of the author's knowledge the first time that this has been demonstrated.

The results of this study have presented a number of new questions that ought to be addressed. However, the nature of TSE infections, in particular their length, and the number of additional animals that would be required to address these

questions (and the associated difficulty of getting ethical approval for their use) meant that it was not possible to investigate these questions as a part of this project. This is unfortunate in terms of developing these questions but it is an unavoidable feature of working with such time-intensive agents.

Appendix I.

Details of pathogens excluded from spf animal facilities including NPU.

Category	Excluded Organisms
1*	all salmonellae and shigellae; Mycobacterium tuberculosis; Pasturella pseudotuberculosis; pathogenic skin fungi; Scabies mite; LCM; Leptospira; Listeria; Streptobacillus moniliformis
2*	all diseases listed under 1* plus :- Intermediate stages of cestodes; All parasitic arthropods; Ectromelia; Tyzzer's disease.
3*	Same as category 2* plus they must be free from:- Bordetella; All Pasturellas; All mycoplasmas; All coccidia; All pathogenic helminths.
4*	same as category 3* but must also be free from :- All pneumococci; Klebsiella; All helminths; All pathogenic protozoa; All common murine viruses.

Category 4* are what are generally regarded as spf.
Information for table kindly provided by Irene Mc Connell (NPU)

Appendix II.

Standard dose response curves from i.c. titration of ME7 scrapie in C57Bl mice.

Figure 46.

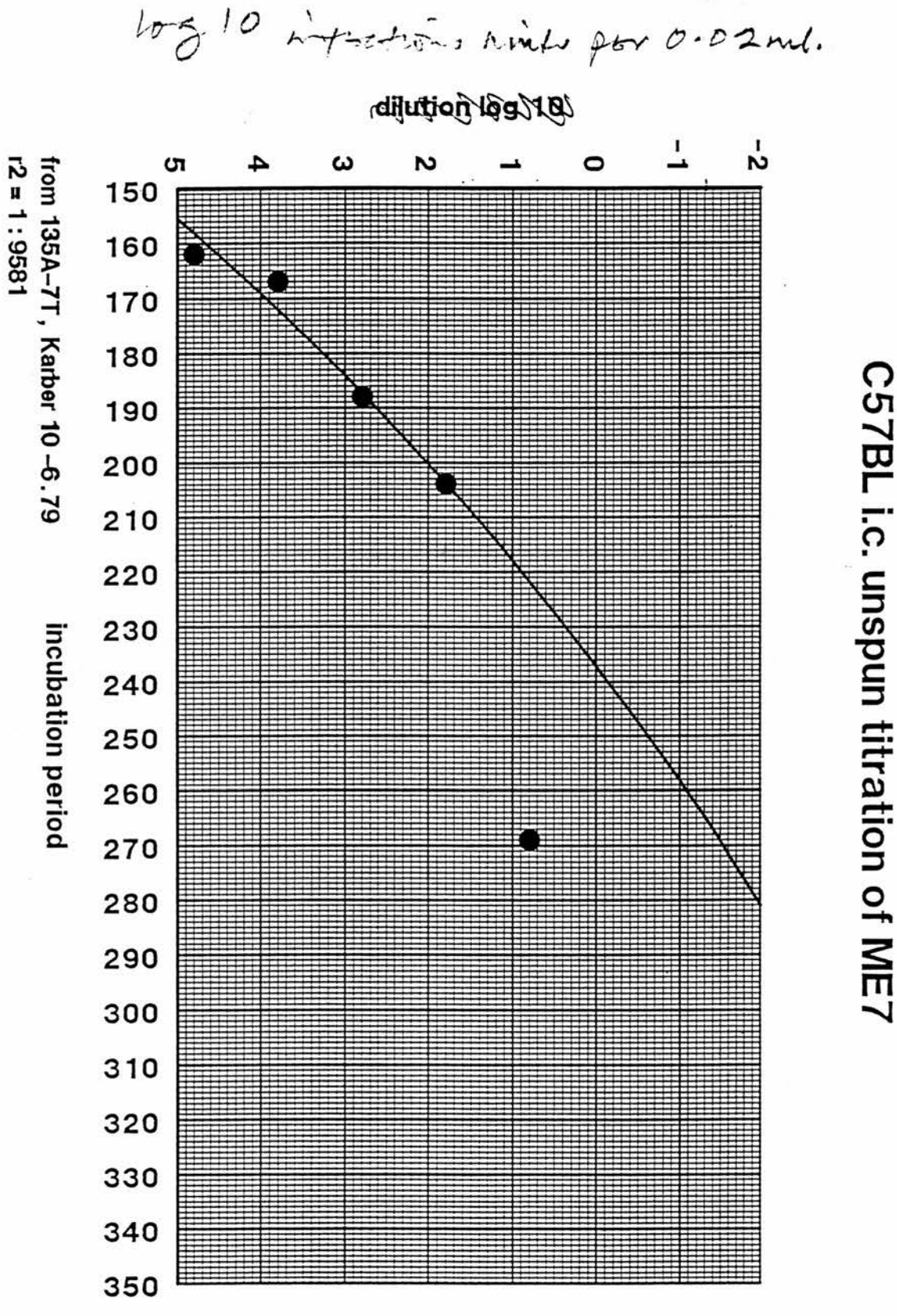

Figure 46 and 47 show dose response curves for a titration of unspun ME7 scrapie in C57BL mice. These curves makes it possible to determine the infecting dose (log_{10} infectious units per unit volume) of agent based on the incubation time (Courtesy of Dr Jan Fraser).

Figure 47.

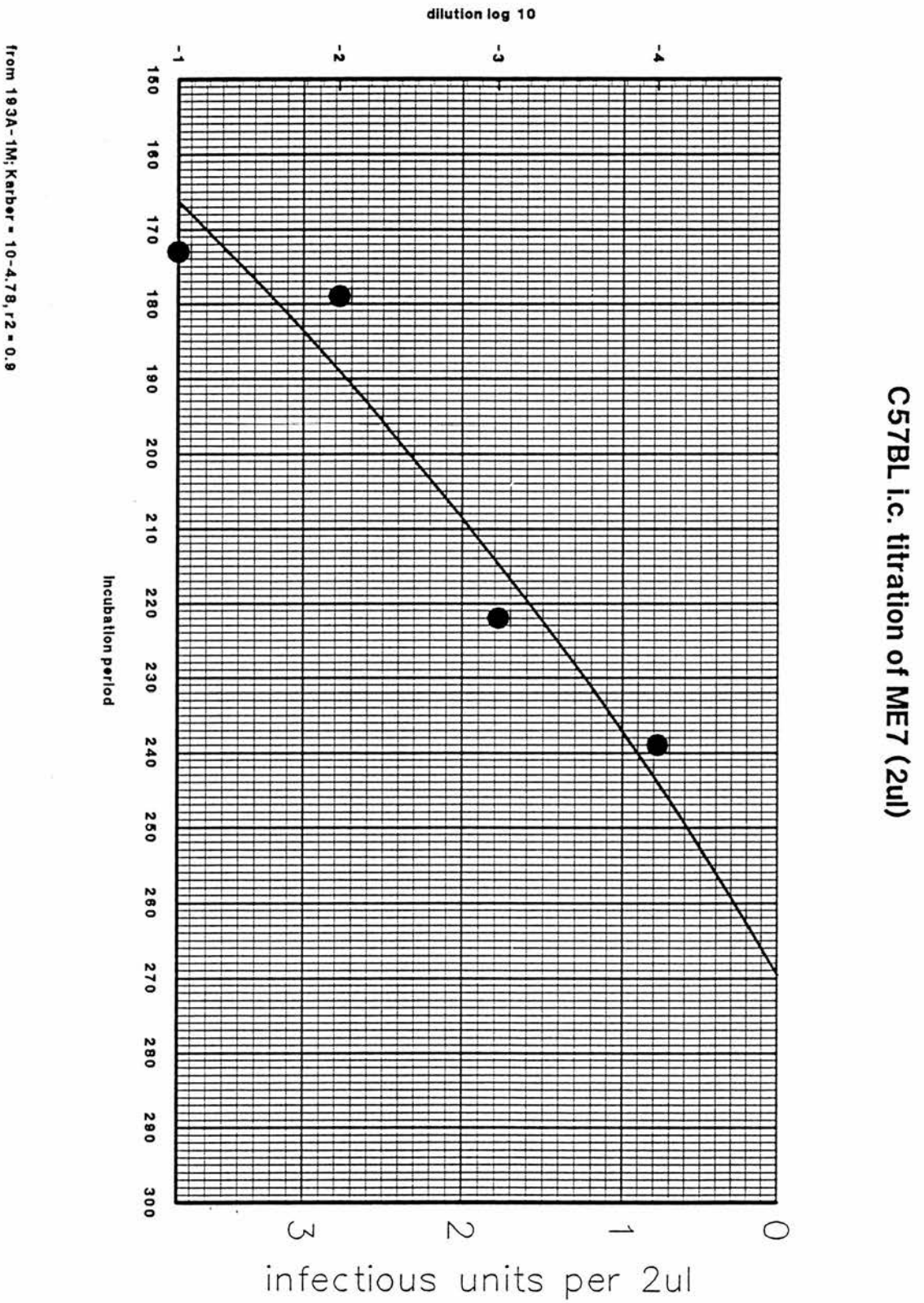
C57BL i.c. titration of ME7 (2ul)
from 193A-1M; Karber = 10-4.78, r2 = 0.9
dilution log 10
-1
-2
-3
-4
Incubation period
150
160
170
180
190
200
210
220
230
240
250
260
270
280
290
300
3
2
1
0
infectious units per 2ul

Appendix III.

Brain regions affected by PrP and GFAP following peripheral challenge with ME7 scrapie.

Oral Route of Infection

First PrP must develop between 186 and 221 days post injection; first positive immunostaining is seen in sections from 221 days post injection.

Astrocytes would appear to be upregulating within the same time interval.

221 d.p.i.

PrP seen in

Ventral Pontine reticular nucleus
Central grey matter
Central grey matter, medial
Dorsal cortex of the inferior colliculus very slight
Median eminence
Ventral tegmental area
Intrapeduncular nucleus
Pontine reticular nuc;eus oral
Supramamillary nucleus
Interposed cerebellar nucleus posterior
Locus coeruleus
Central inferior colliculus
Red nucleus
Subincertal Nucleus – encircled neurons.
Anterodorsal thalamic nucleus
some early lesion in the cerebral cortex
some early lesion in CA3 of hippocampus
Ventrolateral thalamic nucleus
Lateral posterior thalamic nucleus
basal cerebral peduncle
Substantia nigra compact
lateral hypothalamic area

250 d.p.i.

PrP also seen in

Frontal cerebral ctx
cental medial thalamic nucleus
mediodorsal thalamic nucleus
Gustatory thalamic nucleus
Dorsal tegmental nucleus
Dorsal raphe nucleus
Caudal linear raphe nucleus
Raphe pontis nucleus
Supramamillary nucleus
reticulotegmental nuc. [slight]
ventral tegmental area
Cortex
CA3 more pronuonced
CA1 diffuse
Sup' Colliculus
retrorubral fields
Hilus dentate gyrus
superior cerebellar peduncle

279d.p.i.	Cerebellar grey matter regions.
	Hypoglossal nucleus
	corpus callosum
	median preoptic nucleus
	intermediate lateral septal nucleus
	ventromedial hypothalamic nucleus
	medial spetal nucleus
	more evidence throughout cerebral ctx
	Superior vestibular/lateral vestibular nuclei
	Ventral pallidum
	Plaques in hippocampus
	Zona limitans
302d.p.i. terminal	Whole of hippocampus plaques limited to CA4
	Banding through Ctx, limited to certain layers (define)
	Posterior pretectal nucleus
	Hippocampal fissure
	Subiculum
	Vagus nerve
	Throughout hippocampal structure/dentate gyrus

GFAP upregulation observed during same time interval.

221d.p.i	
	Brainstem, possibly white matter structural type astrocytes
	ventral tegmental area
	caudal interstitial nucleus
	Ctx
	Pontine nucleus
	predorsal bundle
	ventral hip commissure
	anteroventral thalamic nuc' dorsomedial
	Deep mesencephalic nucleus
	Reticular thalamic nuc'
	Stria medullaris
250 d.p.i	
	Hypoglossal nuc'
	Area postrema
	Central grey matter
	rostral interpedunclar nuc'
	Antereior paraventricular nuc'
	Polymorph layer of Dentate gyrus V..slight.
	CA2
	cut off at ventral tegmental decussation
	red nucleus
	interstitial nuc'
	central grey matter
	mediodorsal thalamic nucleus

sup' colliculus
lateral thalamic nuclei
bed nu stria ter,med division
cerebellar nuclei
central inferior colliculus
pedunculopontine tegmental nuc'
lateral vestibular nuc'
epirubropinal nuc'
lateral lemniscuc

279d.p.i.

Widespread throughout Ctx
Thalamic nuclei
CA3
Lateral septal nuc'
Paramedian Raphe
hypoglossal
solitary tract
CA4

302 d.p.i.

Fimbria Hippocampus

Intramuscular Route of Infection

First PrP must develop between 102 and 140 days post injection; first positive immunostaining is seen in sections from 140 days post injection.

Astrocytes would appear to be upregulating after the appearance of PrP. First signs of reactive astrocytes seen in 166 d.p.i. Perhaps the GFAP run including tissues from 140 d.p.i. should be repeated.

140 d.p.i.

PrP seen in

Medial cerebellar nucleus
Central Grey Matter (Small deposits)
Anterior commissure
Stria Medullaris Thalamus
Paramedian Reticula nucleus
Solitary tract nucleus
Paramedian Raphe
Anterior tegmental nucleus
Caudal Linear Nucleus Raphe
Ventral Pontine Nucleus
Interposed cerebellar nuclei (Anterior and Posterior)
Lateral hypothalamic area
Red nucleus
Deep mesencephalic nucleus (Same region as red nuc')
Retrorubral fields
Medial vestibular nuclei
Intermediate reticular nucleus
Facial nucleus and it's nerve

perifacial zone
Locus coeruleus
Anteroventral thalamic nuclei
Lateral dorsal/posterior thalamic nuclei
Centrolateral thalamic nucleus
Fields of forel
Inferior colliculus
Hippocampus (CA3)- very early
Cerebral cortex – some discrete deposits within a single layer
Substantia Nigra
Reticular thalamic nucleus.

166 d.p.i.

PrP also seen in

Dorsal hypothalamic nucleus
Paraventricular thalamic nucleus
Paratenial thalamic nucleus
Some small signs in olfactory system
Hippocampus CA3/CA4
More cortical PrP – still apparently within a layer.
Dorsal Lateral Geniculate Nucleus.
Ventral cochlear nucleus

189d.p.i.

PrP also seen in

Widespread in cerebral cortex but still appears limited to discrete layer
Corpus callosum
Reunions and rhomboid thalamic nuclei
Posterodorsal tegmental nucleus
intermediodorsal thalamic nucleus
Gelatinosus thalamic nucleus
Medial septal nucleus
Accumbens nucleus
Hilus dentate gyrus
Plaques in posterior thalamic nuclear group
Medial tuberal nucleus
Paques in cerebral Ctx – dorsal regions
Medullary reticular field
Ventral Pallidum
substantia innominata
Globus pallidus
trigeminal nuc
K- Nucleus
Presubiculum

221d.p.i.

PrP also seen in

Ventromedial hypothalamic nucleus
Caudal linear nucleus raphe
septofimbrial nucleus
Detectable PrP Through the CA1 & CA2 region of hippocampus
Encircled neurons in Zona Limitans
Plaques ansa lenticularis

Superior cerebellar peduncle
Some PrP seen in higher layers of frontal region of Cerebral Ctx.

231 d.p.i.

PrP also seen in

Pontine nucleus
Supramamillary nucleus
Medial septal nucleus
Trapezoid body
Pyramidal tract
Reticulotegmental nucleus pons
PrP in several layers of the superior colliculus
Claustrum

Terminal 250 d.p.i.

Medial Mammillary nucleus
Some in grey matter of cerebellum
Throughout the cortex including many plaques.
Diffuse PrP throughout hippocampus with more
discrete deposits in the CA4 region; includes plaques.

GFAP upregulation observed at the 166 days post injection.

166 d.p.i

These appear to be very early signs of astrocytic upregulation
and as such do not appear to be widespread.
Medial cerebellar nucleus
Pontine reticular nucleus
Appears to be brainstem involvement that is not
mirrored in the observed PrP deposition.

189 d.p.i

More GFAP in brainstem
Gigantocellular reticular nuclei
Raphe obscurus
Paramedian reticular nucleus
Mediodorsal thalamic nucleus
Trapezoid body
Pontine nucleus
Predorsal bundle
Dorsal cortex of inferior colliculus
Lateral septal nucleus
Dorsal central grey matter
Foci in many thalamic nuclei
Medioventral periolivary nucleus
Some in CA1 region of hippocampus
Subsoeruleus nucleus
Discrete band in cerebral cortex similar to PrP deposition.

Pedunculopontine tegmental nucleus
Motor trigeminal nucleus
Interposed cerebellar nuclei.
CA3 & CA2
Spinal trigeminal nucleus, caudal/interpolar

221d.p.i.

Extension of band in the Cerebral cortex to frontal region of brain
Septofimbrial nucleus
Widespread GFAP deposition in the thalamic nuclear group
Dorsal cochlear nucleus
Superior vestibular nucleus
Facial nucleus
Superior colliculus
Extended deposition in the inferior colliculus
Sparing of much of the deep mesencephalic nucleus

231 d.p.i.

Central white matter structure of cerebellum
Anterior paraventricular thalamic nucleus
subfornical organ
Dorsal medullary reticular field
Spinal trigeminal nerv

Terminal 250 d.p.i.

Astrocytosis throughout the brain.
Hippocampus is very involved.
Band through the Caudate Putamen. This region is relatively spared as is the case with PrP.
Fimbria
Ventral pallidum
Medila tuberal nucleus
Heavy foci in central nuclei of thalamus
Corpus callosum
Some evidence of astrocytosis in grey mattey of cerebellar lobules.

Intraperitoneal Sequence of Events.

First appearance of PrP is seen in the 140 dpi group. But only in a single animal.

140 dpi.

Solitary tract nucleus
Deep Mesencephalic Nucleus
Intercolliculur nucleus
Dorsal Cortex, Inferior colliculus
Exterior Cortex, Inferior colliculus
Central Nucleus Inferior colliculus
Ventrolateral thalamic nucleus
Posterior thalamic nuclear group
Cuneiform nucleus
Dorsal medullary reticular field
Anterior Interposed cerebellar nucleus
Posterior Interposed cerebellar nucleus
Dorsal cochlear nucleus
Acoustic stria
Spinal vestibular nucleus
Lateral vestibular nucleus
Olivocochlear bundle
Alpha parvocellular reticular nucleus
Reticular substantia nigra
Restricted layers of cerebral cortex

166 dpi.

External cuneate nucleus
Arbor vitem of the cerebellum
Very early signs of PrP in the CA4 region of the hippocampus.
Posterior thalamic nuclear group
ventrolateral thalamic nucleus
Laterodorsal thalamic nucleus.

189 dpi.

Mesencephalic trigeminal nucleus
Parvocellular reticular nucleus
Ambiguus nucleus
Facial nerve root (facial nucleus)
Zonal layer superior colliculus
Superficial Grey layer, superior colliculus
CA3 & CA4 of hippocampus
Some CA1 involvement.
Evidence of PrP in the Caudate Putamen
Angular thalamic nucleus
antreoventral thalamic nucleus, dorsomedial
anteroventral thalamic nucleus, ventrolateral.
Reticular thalamic nucleus

Bed nucleus stria terminalis
Reticular Substantia Nigra
ansa lenticularis
Caudate putamen
Corpus callosum
Substantia Innominata
Lateral Preoptic area
Stria medullaris nucleus
Ventral Pallidum
Ethmoid thalamic nucleus
Lateral Hypophysial area
Cerebral cortex shows much more involvement.
Caudal Pontine reticular nucleus
Oral Pontine nucleus
Dorsal Cortex Iferior coliculus
superior cerebellar peduncle
Supragenual Nucleus
Tegmental nucleus
Paratenial thalamic nucleus
Anterior paravebtricular thalamic nucleus
Central grey matter
Parabrachial pigmented nucleus
Retrochiasmatic area
ventromedial hypophyseal area
Dorsal hypophyseal area
Posterior hypophyseal area

221 dpi

Corpus callosum
CA1
Laterodorsal thalamic nuc
Lateral Posterior thalamic nuc.
Medial tuberal nuceus
Nuc horizontal limb diagonal band
Zonal layer sup col
Optic nerve layer sup col
Intermediate grey matter sup col
Accumbens nucleus
Medial cerebelllar nucleus
medial longitudinal fasciculus
Gigantocellular reticular nucleus
Retrorubral fields
red nucleus

231 dpi.

Superior vestibular nucleus
Medial parabrachial nucleus
Mesencephalic trigeminal nucleus
Lateral hypophyseal magnocellular nucleus

CA1
Subiculum
Anteromedial thalamic nucleus
Mediodorsal thalamic nucleus
Central medial thalamic nucleus
parafascicular thalamic nucleus
posterior paraventricular thalamus nucleus
precommissural nucleus

246 dpi.

Pedunculopontine tegmental nucleus
basal cerebral peduncle
Ventromedial thalamic nucleus
Ventral posteromedial thalamic nucleus
Angular thalamic nucleus
dorsal/ventral posterior pretectal nucleus
Fields of Forel
Reticular thalamic nucleus
Ventral Pallidum
posterior anterior commisure
bed nucleus terminalis stria
Lateroanterior hypophyseal nucleus
pericentral dorsal tegmental nucleus
Dorsal paragigantocellular nucleus
Medial vestibular nucleus
intercalated nucleus
Supragenual nucleus
Gelatinosus thalamic nucleus
Rhomboid thalamic nucleus
reuniens thalamic nucleus (and Ventral reuniens)
parafascicular thalamic nucleus.

First appearance of GFAP is seen in the 140 dpi group.

140 dpi.

Small focal deposit in cerebral cortex
Dorsal cortex of inferior colliculus
External cortex of inferior colliculus
Central nucleus of inferior colliculus
Interposed cerebellar nuclei (posterior & anterior)
Fields of Forel
Zona Limitans
Medial tuberal nucleus
dorsal medullary reticular field
Spinal vestibular nucleus
Mesencephalic trigeminal nucleus
Lateral vestibular nucleus
olivocochlear bundle

parvocellular reticular nucleus
Evidence in all layers of the superior colliculus
Medial parabrachial nucleus
Supratrigeminal nucleus

166 dpi.

Hippocampus (CA1,2 & 3)
Dentate gyrus
corpus callosum
Internal capsule
Endopeduncular nucleus
Subthalamic nucleus
Dorsal cochlear nucleus

189 dpi.

Cortex frontal and occipital
Hippocampal fissure
Arbor vitem of cerebellum
solitary tract nucleus
Parvocellular reticular nucleus
dorsomedial spinal trigeminal nucleus
Facial nerve.
rhinal cortex near forebrain.
Oral Pontine reticular nucleus
Medial vestibular nucleus
Dorsal Paragigantocellular nucleus
Ventral pontine reticular nucleus
Gigantocellular reticular nuclei.
Abducens nucleus

221 dpi.

Arbor Vitem of cerebellum
Pontine Nuclei
longitudinal fasciculus pons
Medioventral periolivary nucleus
Lateral superior olive
Rostral periolivary region
Retro rubral fields
Red Nucleus
Basal cerebral peduncle
Substantia nigra
rubrospinal tract
epirubrospinal nucleus
Accumbens nucleus
Lateral Preoptic area
Zona Incerta
Ventromedial thalamic nucleus
Ventral posteromedial thalamic nucleus
Facial nucleus

ventral subcoeruleus nucleus
dorsal/ventral anterior pretectal nuclei
Optic tract nucleus
posterior pretectal nucleus
subparafascicular thalamic nucleus
Angular nucleus
Posterior Thalamic nuclear group
bed nucleus stria terminalis lateral division
Reticular thalamic nucleus
substantia innominata
Lateral septal nucleus, intermediate
Dorsal lateral septal nucleus
Anterior paraventricular thalamic nucleus
anterior commisural nucleus
Reuniens thalamic nucleus
Intermediate grey and white matter, sup colliculus
Dorsal cortex inferior colliculus
genu corpus callosum
fornix
Lots of cortical involvement..
Anteromedial thalamic nucleus
anteroventral preoptic nucleus
medial preoptic nuleus, central.
dorsomedial hypophysis
medial mammillary nucleus

231 dpi.

Claustrum
Caudate putamen
Spinal Vestibular nucleus
parvocellular reticular nucleus
dorsomedial spinal trigeminal nucleus
solitary tract nucleus
Lateroseptal nucleus, dorsal
dorsal fornix
septofimbrial nucleus
Anterior commissural nucleus
striohypothalamic nucleus
Anterior tegmental nucleus
ventral tegmental nucleus
paramedian raphe
septohypothalamic nucleus

246 dpi.

Intermediate grey and white matter of the Superior colliculus
Dorsal medullary reticular field
caudal spinal trigeminal nucleus
caudal gelatinous layer of the spinal trigeminal
rostroventerolateral reticular nucleus
Caudalventerolateral reticular nucleus

facial nucleus
hypoglossal nucleus
Roller nucleus
pyramidal decussation
Inferior Olive
ventral gigantocellular reticular nucleus

Appendix IV.

Data relating to non-disease associated tissue degradation in non-infected animals.

Vacuolation

Brain Area	1		2		3		4		5		6		7		8		9
	Mean	S.E.	Mean	S.E.	Mean	S.E.	Mean	S.E.	Mean	S.E.	Mean	S.E.	Mean	S.E.	Mean	S.E.	Mean
Timepoint																	
321 dpi	716	195	1396	124	521	38	406	110	266	28	369	32	288	46	501	164	620
249 dpi	1102	304	1966	78	740	36	517	191	617	69	327	31	420	114	723	120	1289
221 dpi	778	245	1551	371	472	73	237	29	623	48	349	19	713	54	681	162	877
166 dpi	1783	329	3423	170	994	232	302	63	738	26	1337	134	636	131	1579	153	1825

GFAP

Brain Area	1		2		3		4		5		6		7		8		9
	Mean	S.E.	Mean	S.E.	Mean	S.E.	Mean	S.E.	Mean	S.E.	Mean	S.E.	Mean	S.E.	Mean	S.E.	Mean
Timepoint																	
321 dpi	3	3	1285	210	1812	240	72	65	146	68	236	117	150	87	420	135	3657
249 dpi	65	42	2957	1204	1278	173	177	121	224	40	142	99	2	2	402	79	3617
221 dpi	57	30	2637	1567	1380	148	170	69	175	59	296	121	54	25	351	124	2910
166 dpi	15	8	604	111	1175	151	598	243	419	154	355	179	66	33	252	127	1452

All measurements of area are in μm^2

Details of measurements made in the brains of uninfected animals. These measurements provided information regarding the normal state of the murine brain against which the diseased brain could be compared.

References.

Aguzzi, A., Raeber, A., Blattler, T., Flechsig, E., Klein, M., Weissmann, C., and Brandner, S. (1997). Neurotoxicity and neuroinvasiveness of prions. Journal Of Neurovirology *3*, S23-S24.

Almond, J. W., Brown, P., Gore, S. M., Hofman, A., Wientjens, D. P. W. M., Ridley, R. M., Baker, H. F., Roberts, G. W., and Tyler, K. L. (1995). Creutzfeldt-Jakob disease and bovine spongiform encephalopathy: any connection? The British Medical Journal *311*, 1415-1421.

Alper, T., Cramp, W. A., Haig, D. A., and Clarke, M. C. (1967). Does the agent of scrapie replicate without nucleic acid?, Science *214*, 764-766.

Alper, T., Haig, D. A., and Clarke, M. C. (1966). The exceptionally small size of the scrapie agent. Biophysical research Communications *22*, 278-284.

Alpers, M. (1968). Kuru: Implications of its transmissibility for the interpretation of its changing epidemiological pattern. In The Central Nervous System, Some Experimental Models of Neurological Disease, International Academy of Pathology Monograph No 9, O. T. Bailey and D. E. Smith, eds. (Baltimore, London, Sydney: Williams and Wilkins), pp. 234-251.

Anderson, R. M., Donnelly, C. A., Ferguson, N. M., Woolhouse, M. E. J., Watt, C. J., Udy, H. J., Mawhinney, S., Dunstan, S. P., Southwood, T. R. E., Wilesmith, J. W., Ryan, J. B. M., Hoinville, L. J., Hillerton, J. E., Austin, A. R., and Wells, G. A. H. (1996). Transmission Dynamics and Epidemiology Of BSE In British Cattle. Nature *382*, 779-788.

Baldauf, E., Beekes, M., and Diringer, H. (1997). Evidence for an alternative direct route of access for the scrapie agent to the brain bypassing the spinal cord. Journal of General Virology *78*, 1187-1197.

Bateman, D., Hilton, D., Love, S., Zeidler, M., Beck, J., and Collinge, J. (1995). Sporadic Creutzfeldt-Jakob disease in a 18-year old in the UK. Lancet *346*, 1155-1156.

Beekes, M., McBride, P.A., and Baldauf, E. (1998). Cerebral targeting indicates vagal spread of infection in amsters infected with scrapie. Journal of General Virology *79*, 601-607.

Bell, J.E., and Ironside, J.W. (1993). Neuropathology of spongiform encephalopathies in humans. British Medical Bulletin *49*, 193-197.

Bernoulli, C., Seigfried, J., Baumgartner, G., Regli, F., Rabinowicz, T., Gajdusek, D. C., and Gibbs jr, C. J. (1977). Danger of accidental person-to-person transmission of Creutzfeldt-Jakob disease by surgery. Lancet, 478-479.

Betmouni, S., and Perry, V.H. (1999). The acute inflammatory response in CNS following injection of prion brain homogenate or normal brain homogenate. Neuropathology and Applied Neurobiology *25*, 20-28.

Blättler, T., Brandner, S., Raeber, A., Klein, M., Voigtlander, T., Weissmann, C., and Aguzzi, A. (1997). PrP-expressing tissue required for transfer of scrapie infectivity from spleen to brain. Nature *389*, 69-73.

Bolton, D. C., McKinley, M. P., and Prusiner, S. B. (1982). Identification of a protein that purifies with the scrapie prion. Science *218*, 1309-1311.

Bradley, R. (1997). Animal prion diseases. In Prion Diseases, J. Collinge and M. S. Palmer, eds. (Oxford: Oxford University Press), pp. 89-129.

Bradley, R. (1994). Bovine spongiform encephalopathy epidemiology: a brief review. Livestock Production Science *38*, 5-16.

Braig, H. R., and Diringer, H. (1985). Scrapie: concept of a virus-induced amyloidosis of the brain. Embo Journal. *4*, 2309-2312.

Brandner, S., Isenmann, S., Raeber, A., Fischer, M., Sailer, A., Kobayashi, Y., Marino, S., Weissmann, C., and Aguzzi, A. (1996a). Normal Host Prion Protein Necessary For Scrapie-Induced Neurotoxicity. Nature *379*, 339-343.

Brandner, S., Raeber, A., Blättler, T., Fischer, M., Weissmann, C., and Aguzzi, A. (1996b). Normal host prion protein (PrP^C) is required for scrapie spread within the central nervous system. Proceedings of the National Academy of Sciences of the USA *93*, 13148-13151.

Britton, T. C., Al-Sarraj, S., Shaw, C., Campbell, T., and Collinge, J. (1995). Sporadic Creutzfeldt-Jakob disease in a 16-year old in the UK. Lancet *346*, 1155.

Brown, D.R., Schulz-Schaeffer, W.J., Schmidt, B., and Kretzschmar, H.A. (1997). Prion protein-deficient cells show altered response to oxidative stress due to decreased SOD-1 activity. Experimental Neurology *146*, 104-112.

Brown, K.L., Stewart, K., Ritchie, D.L., Mabbott, N.A., Williams, A., Fraser, H., Morrison, W.I., and Bruce, M.E. (1999). Scrapie replication in lymphoid tissues depends on prion protein-expressing follicular dendritic cells. Nature Medicine *5*, 1308-1312.

Brown, P., Preece, M. A., and Will, R. G. (1992). "Friendly fire" in medicine: hormones, homografts, and Creutzfeldt-Jakob disease. Lancet *340*, 24-27.

Bruce, M. E. (1981). Serial studies on the development of cerebral amyloidosis and vacuolar degeneration in murine scrapie. Journal of Comparative Pathology *91*, 589-597.

Bruce, M. E. (1996). Strain Typing Studies of Scrapie and BSE. In Prion Diseases, H. Baker and R. M. Ridley, eds. (Totowa, New Jersey.: Humana Press Inc'), pp. 223--236.

Bruce, M. E., McBride, P. A., and Farquhar, C. F. (1989). Precise targetting of the pathology of the sialoglycoprotein, PrP, and vacuolar degeneration in mouse scrapie. Neuroscience Letters *102*, 1-6.

Bruce, M. E., McConnell, I., Fraser, H., and Dickinson, A. G. (1991). The disease characteristics of different strains of scrapie in Sinc congenic mouse lines: implications for the nature of the agent and host control of pathogenesis. Journal of General Virology *72*, 595-603.

Bruce, M.E., and Dickinson, A.G. (1985). Genetic control of amyloid plaque production and incubation period in scrapie infected mice. Journal of Neuroapthology and Experimental Neurology *44*, 285-294.

Bruce, M. E., Will, R. G., Ironside, J. W., McConnell, I., Drummond, D., Suttie, A., McCardle, L., Chree, A., Hope, J., Birkett, C., Cousens, S., Fraser, H., and Bostock, C. J. (1997). Transmissions to mice indicate that 'new variant' CJD is caused by the BSE agent. Nature *389*, 498-501.

Büeler, H., Aguzzi, A., Sailer, A., Greiner, R.-A., Autenried, P., Aguet, M., and Weissman, C. (1993). Mice Devoid of PrP Are Resistant to Scrapie. Cell *73*, 1339-1347.

Büeler, H., Fischer, M., Lang, Y., Bluethmann, H., Lipp, H. P., DeArmond, S. J., Prusiner, S. B., Aguet, M., and Weissman, C. (1992). Normal development and behaviour of mice lacking the neuronal cell-surface PrP protein. Nature *356*, 577-582.

Chandler, R.L. (1961) Encephalopathy in mice produced with scrapie brain material. Lancet ***i***, 1378.

Chou, S., M., Payne, W.M., Gibbs, C.J., and Gadjusek, D.C. (1980) Transmission and scanning electron microscopy of spongiform change in Creutzfeldt-Jakob disease. Brain *103*, 885-904.

Chretien, F., Dorandeu, A., Adle-Biasette, H., Ereau, T., Wingertsmann, L., Brion, F., and Gray, F. (1999). Programmed cell death as a mechanism of neuronal loss in prion diseases. Clinical and Experimental Pathology *7*, 181-191.

Cole, S. And Kimberlin, R.H. (1985). Pathogenesis of mouse scrapie: dynamics of vacuolation in brain and spinal cord after intraperitoneal infection. Neuropathology and applied Neurobiology *11*, 213-227.

Collee, J. G., and Bradley, R. (1997a). BSE: a decade on - part 1. The Lancet *349*, 636-641.

Collee, J. G., and Bradley, R. (1997b). BSE: a decade on - part 2. The Lancet *349*, 715-721.

Collinge, J., Brown, J., Hardy, J., Mullan, M., Rossor, M. N., Baker, H., Crow, T. J., Lofthouse, R., Poulter, M., Ridley, R., and al., e. (1992). Inherited prion disease with 144 base pair gene insertion. 2. Clinical and pathological features. Brain *115*, 687-710.

Collinge, J., and Palmer, M.S. (1997) Human Prion Diseases. In, Prion Diseases. Ed. Collinge, J., and Palmer, M.S. Oxford University Press, New York. 18-56.

Collinge, J., Whittington, M. A., Sidle, K. C. L., Smith, C. J., Palmer, M. S., Clarke, A. R., and Jeffreys, J. G. R. (1994). Prion protein is neccessary for normal synaptic function. Nature *370*, 295-297.

Collins, S., Law, M.G., Fletcher, A., Boyd, A., kaldor, J., and Masters, C.L. (1999) Surgical treatment and risk of sporadic Creutzfeldt-Jakob disease: A case-controlled study. Lancet *353*, 693-697.

Creutzfeldt, H. G. (1920). Über eine eigenartige herdförmige Erkrankung des Zentralnervensystems. Z. ges Neurol. Psychiat. *57*, 1-18.

Deslys, J. P., Lasmezas, C. I., Streichenberger, N., Hill, A., Collinge, J., Dormont, D., and Kopp, N. (1997). New variant Creutzfeldt-Jakob disease in France. Lancet *349*, 30-31.

Devillemeur, T. B., Deslys, J. P., Pradel, A., Soubrie, C., Alperovitch, A., Tardieu, M., Chaussain, J. L., Hauw, J. J., Dormont, D., Ruberg, M., and Agid, Y. (1996). Creutzfeldt-Jakob-Disease From Contaminated Growth-Hormone Extracts In France. Neurology *47*, 690-695.

Dickinson, A. G. (1976). Scrapie in sheep and goats. Frontiers of Biology *44*, 209-241.

Dickinson, A.G. (1975). Host-pathogen interactions in scrapie. Genetics *79*, 387-395.

Dickinson, A. G., MacKay, J. M. K., and Zlotnik, I. (1964). Transmission by contact of scrapie in mice. Journal of Comparative Pathology *74*, 250-254.

Dickinson, A. G., Meikle, V. M., and Fraser, H. (1968). Identification of a gene which controls the incubation period of some strains of scrapie agent in mice. Journal of Comparative Pathology. *78 (3)*, 293-299.

Dickinson, A. G., and Outram, G. W. (1988). Genetic aspects of unconventional virus infections: the basis of the virino hypothesis. Ciba Foundation Symposium *135*, 63-83.

Dickinson, A. G., Young, G. B., Stamp, J. T., and Renwick, C. C. (1965). An analysis of natural scrapie in Suffolk Sheep. Heredity *20*, 485-503.

Diedrich, J. F., Duguid, J. R., and Haase, A. T. (1991a). The role of astrocytes in the neuropathology of scrapie and Alzheimer's disease. Virology *2*, 233-238.

Diedrich, J. F., Minnigan, H., Carp, R. I., Whitaker, J. N., Race, R., Frey, W., 2d., and Haase, A. T. (1991b). Neuropathological changes in scrapie and Alzheimer's disease are associated with increased expression of apolipoprotein E and cathepsin D in astrocytes. Journal of Virology. *65*, 4759-4768.

Diringer, H., Beekes, M., and Oberdieck, U. (1994). The nature of the scrapie agent - the virus theory. Annals of the New York Academy of Sciences *724*, 246-258.

Diringer, H., Roehmel, J., and Beekes, M. (1998). Effect of repeated oral infection of hamsters with scrapie. Journal of General Virology *79*, 609-612.

Doi, T. (1991). Relationship between periodical organ distribution of Creutzfeldt-Jakob disease (CJD) agent and prion protein expression in CJD agent-infected mice. Nagasaki Igakkai Zasshi *66*, 104-114.

Duffy, P., Wolf, J., Collins, G., DeVoe, A. G., Streeten, B., and Cowen, D. (1974). Possible person-to-person transmission of Creutzfeldt-Jakob disease. New England Journal of Medicine *290*, 692.

Eklund, C.M., Kennedy, R.C., and Hadlow, W.J. (1967). Pathogenesis of scrapie infection in the mouse. Journal of Infectious Diseases *117*, 15-22.

Estibeiro, J. P. (1996). Multiple roles for PrP in the prion diseases. TINS *19*, 257-258.

Farquhar, C. F., Somerville, R. A., Dornan, J., Armstrong, D., Birkett, C., and Hope, J. (1994). A review of the detection of PrP^{sc}. In BSE Update. Proceedings of a Consultation on BSE with the Scientific Veterinary Committee of the Commission of the European Communities, 14-15th September 1993,Brussels, R. Bradley and B. Marchant, eds.: European Commission), pp. pp301-313.

Farquhar, C. F., Somerville, R. A., and Ritchie, L. A. (1989). Post-mortem immunodiagnosis of scrapie and bovine spongiform encephalopathy. Journal of Virological Methods. *24*, 215-221.

Ferguson, N. M., Ghani, A. C., Donnelly, C. A., Denny, G. O., and Anderson, R. M. (1998). BSE in Northern Ireland: epidemiological patterns past, present and future. Proceedings Of the Royal Society Of London Series B-Biological Sciences *265*, 545-554.

Field, E. J., and Raine, C. S. (1964). Acta Neuropathologica *4*, 200.

Fischer, M., Rulicke, T., Raeber, A., Sailer, A., Moser, M., Oesch, B., Brandner, S., Aguzzi, A., and Weissmann, C. (1996). Prion protein(PrP) with amino-proximal deletions restoring susceptibility of PrP knockout mice to scrapie. EMBO *15*, 1255-1264.

Forloni, G., Bugiani, O., Tagliavini, F., and Salmona, M. (1996). Apoptosis-Mediated Neurotoxicity Induced By Beta-Amyloid and Prp Fragments. Molecular and Chemical Neuropathology *28*, 163-171.

Foster, J., and Hunter, N. (1998). Transmissible spongiform encephalopathies: transmission, mechanism of disease, and persistence. Current Opinion in Microbiology *1*, 442-447.

Foster, J. D., Davies, D. J., and Fraser, H. (1986). Primary retinopathy in scrapie in mice deprived of light. Neuroscience Let. *72*, 111-114.

Fraser, H. (1982a). Neuronal spread of scrapie agent and targeting of lesions within the retino-tectal pathway. Nature *295*, 149-150.

Fraser, H. (1982b). The retino-tectal spread of scrapie producing asymmetrical infection and lesions in the superior colliculus contralateral to the injected eye in mice. Neuropath. Appl. Neurobiol. *8*, 242.

Fraser, H. (1979a). Scrapie: A transmissible degenerative CNS disease. Progress in Neurological Research, 194-210.

Fraser, H. (1979b). Scrapie: the precision of the lesions and their diversity. In Slow Transmissible Diseases of the Nervous System, S. B. Prusiner and W. J. Hadlow, eds. (New York: Academic Press), pp. 387-405.

Fraser, H. (1970). Scrapie: The experimental disease in inbred strains of mice. In Veterinary Pathology (University of Edinburgh: Edinburgh), pp. 95.

Fraser, H., and Dickinson, A. G. (1968). The sequential development of the brain lesions of scrapie in three strains of mice. Journal of Comparative Pathology *78*, 301-311.

Fraser, H., and Dickinson, (1973). Scrapie in mice. Aget strain differences in the distribution and intensity of grey matter vacuolation. Journal of Comparative Pathology *83*, 29-40.

Fraser, J.R., Brown, J., Bruce, M.E., and Jeffrey, M. (1997). Scrapie-induced neuron loss is reduced by treatment with basic fibroblast growth factor. NeuroReport *8*, 2405-2409.

Gerstmann, J. (1928). Über ein noch nicht beschriebenes Reflex-Phanomen bei einer Erkrankung des zerebellaren System. Wien. Med. Wochenschr. *78*, 906-908.

Giese, A., Groschup, M. H., Hess, B., and Kretzschmar, H. A. (1995). Neuronal cell-death in scrapie-infected mice is due to apoptosis. Brain Pathology *5*, 213-221.

Gilmour, J. S., Bruce, M. E. and MacKellar, A. (1986). Cerebrovascular amyloidosis in scrapie- affected sheep. Neuropathology and Applied Neurobiology *12*, 173-183.

Gomes, F.C.A., Paulin, D., and Moura-Neto, V. (1999). Glial fibrillary acidic protein (GFAP) modulation by growth factors and its implication in astrocyte differentiation. Brazilian Journal of Medical and Biological Research *32*, 619-631.

Gordon, W. S. (1946). Louping-ill, tick-borne fever and scrapie. The Veterinary Record *58*, 516.

Gordon, W. S. (1966). Review of work on scrapie at Compton, England 1952-1964. USDA report of scrapie seminar, ARD *91-53*, 19-40.

Griffiths, J. (1967). Self replication and scrapie. Nature *214*, 1043-1044.

Harris, D.A. (1999). Cellular biology of Prion Diseases. Clinical Microbiology Reviews *12*, 429-444.

Hartsough, G., and Burger, D. (1965). Encephalopathy of mink. I. Epizootilogic and clinical observations. Journal of Infectious Diseases *115*, 387-392.

Hill, A. F., Antoniou, M., and Collinge, J. (1999). Protease-resistant prion protein produced in vitro lacks detectable infectivity. Journal of General Virology *80*, 11-14.

Hill, A. F., Desbruslais, M., Joiner, S., Sidle, K. C. L., Gowland, I., Collinge, J., Doey, L. J., and Lantos, P. (1997). The same prion strain causes vCJD and BSE. Nature *389*, 448-450.

Hilton, D.A., Fathers, E., Edwards, P., Ironside, J.W., and Zajicek, J. (1998). Prion immunoreactivity in appendix before clinical onset of variant Creutzfeldt-Jakob disease. Lancet *352*, 703-704.

Hooper, M., Hardy, K., Handyside, A., Hunter, S., and Monk, M. (1987). HPRT-deficient Lesch-nyhan mouse embryos derived from germline colonization by cultured cells.

Hope, J., Multhaup, G., Reekie, L. J. D., Kimberlin, R. H., and Beyreuther, K. (1988). Molecular pathology of scrapie-associated fibril protein (PrP) in mouse brain affected by the ME7 strain of scrapie. European Journal of Biochemistry *172*, 271-277.

Horiuchi, M., Yamazaki, N., Ikeda, T., Ishiguro, N., and Shinagawa, M. (1995,). A cellular-form of prion protein (prpc) exists in many nonneuronal tissues of sheep. Journal of General Virology. *76, No.Pt10,*, 2583-2587.

Hunter, N., Dann, J. C., Bennett, A. D., Somerville, R. A., McConnell, I., and Hope, J. (1992). Are Sinc and the PrP gene congruent? Evidence from PrP gene analysis in Sinc congenic mice. Journal of General Virology. *73*, 2751-2755.

Ingrosso, L., Pisani, T., and Pocchiari, M. (1999). Transmission of the 263K scrapie strain by the dental route. Journal of General Virology *80*, 3043-3047.

Jakob, A. (1923). Spatische Pseudosklerose. In Monographien aus dem Gesamtegebiete der Neurologie und Psychiatrie, Die Extrapyramidalen Erkrankungen, O. Foester and K. Wilmanns, eds. (Berlin: Springer), pp. 212-245.

Jakob, A. (1921). Über eigenartige Erkrankungen des Zentralnervensystems mit bemerkenswertem anatomischen Befunde. Z. ges Neurol. Psychiat. *64*, 147-228.

Jeffrey, M,. Goodbrand, I.A., and Goodsir, C.M. (1995) pathology of the transmissible spongiform encephalopathies with special emphasis on ultrastructures. Micron *26*, 277-298.

Jeffrey, M., and Halliday, W.G. (1994). Numbers of neurons in vacuolated and non-vacuolated neuroanatomical nuclei in bovine spongiform encephalopathy-affected brains. Journal of Comparative Pathology *110*, 287-293.

Jeffrey, M., and Wells, G. A. H. (1988). Spongiform encephalopathy in a nyala (tragelaphus-angasi). Veterinary Pathology *25*, 398-399.

Kim, Y.S., Carp, R.I., Callahan, S.M., and Wisniewski, H.M. (1990). Pathogenesis and pathology of scrapie after sterotactic injection of strain 22L in intact and bisected cerebella. Journal of Neuropathology and Experimental Neurology.

Kimberlin, R. H. (1976a). General introduction to some slow virus diseases. Frontiers of Biology *44*, 3-13.

Kimberlin, R. H. (1976b). Experimental scrapie in the mouse: a review of an important model disease. Science Progress *63*, 461-481.

Kimberlin, R.H. (1979). Early ebents in pathogenesis of scrapie in mice: biological and biochemical studies. In, Slow transmissible diseases of the nervous system. Eds. Hadlow, W.J. and Prusiner, S.B. Academic Press, New York.

Kimberlin, R. H. (1994). A scientific evaluation of research into bovine spongiform encephalopathy (BSE). In Transmissible Spongiform Encephalopathies (Proceedings of a consultation on BSE wth the Scientific Veterinary Commission of the European Communities held in Brussels, 14-15 September 1993). eds. Bradley, R. and Marchant, B. (Brussels: CEC), pp. 455-477.

Kimberlin, R. H., and Walker, C. A. (1979). Pathogenesis of scrapie: agent multiplication in brain at the first and second passage of hamster scrapie in mice. J. Gen. Virol. *42*, 107-117.

Kimberlin, R.H., and Walker, C.A. (1988). Pathogenesis of experimental scrapie. In, Novel infectious agents and the central nervous system (Ciba Foundation Symposium 135). Eds. Bock, G., and Marsh, J. Wiley, Chichester. 37-62.
Knezevic, N., and Jovanovic, M. (1986). The first incidence of scrapie in Yugoslavia. Acta Veterinaria-Beograd *36*, 31-38.

Koch, T. K., Berg, B. O., DeArmond, S. J., and Gravina, R. F. (1985). Creutzfeldt-Jakob disease in a young adult with idiopathic hypopituarism. New England Journal of Medicine *313*, 731-733.

Korth, C., Stierli, B., Streit, P., Moser, M., Schaller, O., Fischer, R., Schulz-Schaeffer, W., Kretzschmar, H., Raeber, A.R., Billeter, M., Wuethrich, K., and Oesch, B. (1997). Prion (PrP^{Sc}) specific epitope defined by a monoclonal antibody. Nature *390*, 74-77.

Kretzschmar, H. A., Giese, A., Brown, D. R., Herms, J., Keller, B., Schmidt, B., and Groschup, M. (1997). Cell death in prion disease. Journal Of Neural Transmission Supplement, 191-210.

Kubo, M., Kimura, K., Yokoyama, T., and Kobayashi, M. (1995). Distribution of prion protein in scrapie-affected mice using inoculation and immunohistochemistry. Bulletin of the National Institute of Animal Health, 25-29.

Lantos, P. L. (1992). From slow virus to prion: a review of transmissible spongiform encephalopathies. Histopathology *20*, 1-11.

Macdonald, S. T., Sutherland, K., and Ironside, J. W. (1996). A Quantitative and Qualitative-Analysis Of Prion Protein Immunohistochemical Staining In Creutzfeldt-Jakob-Disease Using 4 Anti Prion Protein Antibodies. Neurodegeneration *5*, 87-94.

MacKay, J.M.K., and Smith, W. (1961). A case of scrapie in an uninoculated goat - a natural occurence or a contact infection. The Veterinary Record *73*, 394-395.

McBride, P.A., Eikelenboom, P., Kraal, G., Fraser, H and Bruce, M.E. (1992). PrP protein is associated with follicular dendritic cells of spleens and lymph nodes in uninfected and scrapie infected mice. Journal of Pathology *168*, 413-418.

McBride, P.A., and Beekes, M. (1999). Pathological PrP is abundant in sympathetic and sensory ganglia of hamsters fed with scrapie. Neuroscience Letters *265*, 135-138.

McGowan, J. (1922). Scrapie in Sheep. Scottish Journal of Agriculture *5*, 365-375.

McGowan, J. P. (1914). Scrapie. Bulletin of the Edinburgh and East Scotland College of Agriculture, 278.

McLean, C. A., Ironside, J. W., Alpers, M. P., Brown, P. W., Cervenakova, L., Anderson, R., and Masters, C. L. (1998). Comparative neuropathology of kuru with the new variant of Creutzfeldt-Jakob disease: Evidence for strain of agent predominating over genotype of host. Brain Pathology *8*, 429-437.

Maignien, T., Lasmezas, C.I., Beringue, V., Dormont, D., and Deslys, J.P. (1999). Pathogenesis of the oral route of infection of mice with scrapie and bovine spongiform encephalopathy agents. Journal of General Virology *80*, 3035-3042.

Manson, J., West, J. D., Thomson, V., McBride, P., Kaufman, M. H., and Hope, J. (1992). The prion protein gene - a role in mouse embryogenesis. Development *115*, 117-122.

Manson, J. C., Clarke, A. R., Hooper, M. L., Aitchison, L., McConnell, I., and Hope, J. (1994). 129/ola mice carrying a null mutation in PrP that abolishes messenger-RNA production are developmentally normal. Molecular Neurobiology *8*, 121-127.

Manuelidis, L. (1997). The viral face of the coin in transmissible encephalopathies. Journal Of Neurovirology *3*, S22.

Manuelidis, L., Sklaviadis, T., Akowitz, A., and Fritch, W. (1995). Viral particles are required for infection in neurodegenerative creutzfeldt-jakob-disease. Proceedings of the National Academy of Sciences of the USA *92*, 5124-5128.

Medori, R., Tritschler, H. J., Leblanc, A., Villare, F., Manetto, V., Chen, H. Y., Xue, R., Leal, S., Montagna, P., Cortelli, P., Tinuper, P., Avoni, P., Mochi, M., Baruzzi, A., Hauw, J. J., Ott, J., Lugaresi, E., Autiliogambetti, L., and Gambetti, P. (1992). Fatal familial insomnia, a prion disease with a mutation at codon-178 of the prion protein gene. New England Journal of Medicine *326*, 444-449.

Merz, P. A., Somerville, R. A., Wisniewski, H. M., and Iqbal, K. (1981). Abnormal fibrils from scrapie-infected brain. Acta Neuropathol. *54*, 63-74.

Millson, g.C., Hunter, G.D., and Kimberlin, R.H. (1976). The physico-chemical nature of the scrapie agent. In, Slow virus disease of animals and man. Ed. Kimberlin, R.H. Amsterdam. 243.

Moore, R. C., Hope, J., McBride, P. A., McConnell, I., Selfridge, J., Melton, D. W., and Manson, J. C. (1998). Mice with gene targetted prion protein alterations show that Prnp, Sinc and Prni are congruent. Nature Genetics *18*, 118-125.

Moser, M., Colello, R. J., Pott, U., and Oesch, B. (1995). Developmental expression of the prion protein gene in glial cells. Neuron *14*, 509-517.

Murdoch, G. H., Sklaviadis, T., Manuelidis, E. E., and Manuelidis, L. (1990). Potential retroviral RNAs in Creutzfeldt-Jakob disease. Journal of Virology. *64*, 1477-1486.

Nathanson, N., Wilesmith, J., and Griot, C. (1997). Bovine spongiform encephalopathy (BSE): Causes and consequences of a common source epidemic. American Journal Of Epidemiology *145*, 959- 969.

O'Rourke, K.I., Huff, T.P., Leathers, C.W., Robinson, M.M., and Gorham, J.R. (1994). SCID mouse spleen does not support scrapie agent replication. Journal of General Virology *75*, 1511-1514.

Outram, G. W. (1976). The pathogenesis of scrapie in mice. Frontiers of Biology *44*, 325-357.

Outram, G. W., Fraser, H., and Wilson, D. T. (1973). Scrapie in mice. Some effects on the brain lesion profile of ME7 agent due to genotype of donor, route of injection and genotype of recipient. Journal of Comparative Pathology *83*, 19-28.

Parker, R.C. (1959) Methods of tissue culture. 3rd Edition, Pitman Medical Publishing Ltd. London, 245-266.

Parry, H. B. (1964). Natural scrapie in sheep: its occurrence and dissemination in the field. III. The effect of the introduction of scrapie affected sheep into flocks and premises free of the disease and the question of residual contamination. In Scrapie Seminar (Washington D.C.: U.S. Department of Agriculture), pp. 125-135.

Parry, H. B. (1962). Scrapie: A transmissible and hereditary disease of sheep. Heredity *17*, 75-105.

Pattison, I. H. (1988). Fifty years with scrapie: a personal reminiscence. Vet. Rec. *123*, 661-666.

Pattison, I.H., and Jones, K.H. (1967). The astrocyte reaction in experimental scrapie in the rat. Research in Veterinary Science *8*, 160-165.

Pattison, I. H., Hoare, M. N., Jebbett, J. N., and Watson, W. A. (1974). Further observations on the production of scrapie in sheep by oral dosing with foetal membranes from scrapie-affected sheep.

Pattison, I. H., and Millson, G. C. (1961). Scrapie produced experimentally in goats with special reference to the clinical syndrome. Journal of Comparative Pathology *71*, 101-108.

Prusiner, S. (1982). Novel Proteinaceous Infections Particles Cause Scrapie. Science *216*, 136-144.

Prusiner, S. B. (1993). Genetic and infectious prion diseases. Archives of Neurology *50*, 1129-1153.

Prusiner, S. B., Cochran, S. P., Baringer, J. R., Groth, D., Masiarz, F., McKinley, M., Bildstein, C., Garfin, D., Hadlow, W. J., Race, R. E., and Eklund, C. M. (1980). Slow viruses: molecular properties of the agents causing scrapie in mice and hamsters. Progress in Clinical & Biological Research *39*, 73-89.

Puchtler, H., Sweat, F., and Levine, M. (1962). On the binding of congo red by amyloid. Journal of Histochemistry and Cytochemistry *10*, 355.
Sailer, A., Bueler, H., Fischer, M., Aguzzi, A., and Weissmann, C. (1994). No propagation of prions in mice devoid of prp. Cell *77*, 967-968.

Race, R. E., and Ernst, D. (1992). Detection of proteinase K-resistant prion protein and infectivity on mouse spleen by 2 weeks after scrapie inoculation. Journal of General Virology *73*, 3319-3323.

Sailer, A., Bueler, H., Fischer, M., Aguzzi, A., and Weissmann, C. (1994). No propagation of prions in mice devoid of PrP. Cell *77*, 967-968.

Sakaguchi, S., Katamine, S., Yamanouchi, K., Kishikawa, M., Moriuchi, R., Yasukawa, N., Doi, T., and Miyamoto, T. (1993). Kinetics of infectivity are dissociated from PrP accumulation in salivary glands of Creutzfeldt-Jakob disease agent-inoculated mice. Journal of General Virology *74*, 2117-2123.

Sato, Y., Ohta, M., and Tateishi, J. (1980). Experimental transmission of human subacute spongiform encephalopathy to small rodents. II Ultrastructural study of spongy state in grey and white matter. Acta Neuropathologica *51*, 135-140.

Scott, J. R., and Fraser, H. (1987). The central projections of the retina as a simple scrapie model. Neuropathology and Applied Neurobiology *13*, 237.

Sefton, A.J., and Dreher, B. (1985). Visual system. In, Forebrain and Midbrain. Ed. Paxinos, G. Academic Press, Australia. 169-221.

Selvaggini, C., Degioia, L., Cantu, L., Ghibaudi, E., Diomede, L., Passerini, F., Forloni, G., Bugiani, O., Tagliavini, F., and Salmona, M. (1993). Molecular characteristics of a protease-resistant, amyloidogenic and neurotoxic peptide homologous to residues-106-126 of the prion protein. Biochemical and Biophysical Research Communications *194*, 1380-1386.

Sigurdsson, B. (1954). Observations of three slow infections of sheep. I Maedi, IIJohne's disease, III Rida, chronic encephalitis of sheep with general remarks on infections which develop slowly and some of their special characteristics. The British Veterinary Journal *110*.

Somerville, R. A. (1991). The transmissible agent causing scrapie must contain more than protein. Reviews in Medical Virology *1*, 131-139.

Somerville, R.A., Birkett, C.R., Farquhar, C.F., Hunter, N., Goldmann, W., Dornan, J., Grover, D., Henion, R.M., Percy, C., Foster, J., and Jeffrey, M. (1997). Immunodetection of PrP^{Sc} in spleens of some scrapie-infected sheep but not BSE-infected cattle. Journal of General Virology *78*, 2389-2396.

Somerville, R. A., and Dunn, A. J. (1996). The Association Between Prp and Infectivity In Scrapie and Bse Infected-Mouse Brain. Archives Of Virology *141*, 275-289.

Stamp, J.T., Brotherston, J.G., Zlotnik, I., Mackay, J.M.K., and Smith, W. (1959). Further studies on scrapie. Journal of Comparative Pathology *69*, 268.

Sutherland, K., Macdonald, S. T., and Ironside, J. W. (1996). Quantification and Analysis Of the Neuropathological Features Of Creutzfeldt-Jakob-Disease. Journal Of Neuroscience Methods *64*, 123-132.

Taylor, D. M. (1992). Bovine spongiform encephalopathy (BSE): a stimulus to wider research. Medical Laboratory Sciences *49*, 334-339.

Taylor, D. M., Fernie, K., McConnell, I., Ferguson, C. E., and Steele, P. J. (1998). Solvent extraction as an adjunct to rendering: the effect on BSE and scrapie agents of hot solvents followed by dry heat and steam. Veterinary Record *143*, 6-9.

Thadani, V., Penar, P. L., Partington, J., Kalib, R., Janssen, R., Schonberger, L. B., Rabkin, C. S., and Prichard, J. W. (1988). Creutzfeldt-Jakob disease probably acquired from a cadaveric dura mater graft. Journal of Neurosurgery *69*, 766-769.

Tobler, I., Gaus, S. E., Deboer, T., Achermann, P., Fischer, M., Rülicke, T., Moser, M., Oesch, B., McBride, P. A., and Manson, J. C. (1996). Altered circadian rhythms and sleep in mice devoid of prion protein. Nature *380*, 639-642.

Toumazos, P. (1988). First report of ovine scrapie in Cyprus. British Veterinary Journal *144*, 98-100.

van Keulen, L.J., Schreuder, B.E., Meloen, R.H., Mooij Harkes, G. Vromans, M.E., and Langeveld, J.P. (1996). Immunohistochemical detection of prion protein in lymphoid tissue of sheep with natural scrapie. Journal of Clinical Microbiology *34*, 1228-1231.

Vassar, P. S., and Culling, C. F. A. (1959). Fluorescent stains, with special reference to amyloid and connective tissue. Archives of Pathology *68*, 487-498.

Weissmann, C., Bueler, H., Sailer, A., Fischer, M., Aguet, M., and Aguzzi, A. (1993). Role of PrP in prion diseases. British Medical bulletin *49*, 995-1011.

Weller, R.O., Steart, P.V., and Powell-Jackson, J.D. (1986). Pathology of Creutzfeldt-Jakob disease associated with pituitery-derived human growth hormone administration. Neuropathology and Applied Neurobiology *12*, 117-129.

Wells, G. A. H., Scott, A. C., Johnson, C. T., Gunning, R. F., Hancock, R. D., Jeffrey, M., Dawson, M., and Bradley, R. (1987). A novel progressive spongiform encephalopathy in cattle. Vet. Rec. *121*, 419-420.

Wilesmith, J. W. (1991). Origins of BSE. The Veterinary Record. *128*, 310.

Wilesmith, J. W., Wells, G. A. H., Cranwell, M. P., and Ryan, J. B. M. (1988). Bovine spongiform encephalopathy - epidemiological-studies. The Veterinary Record. *123*, 638-644.

Will, R. G., Ironside, J. W., Zeidler, M., Cousens, S. N., Estibeiro, K., Alperovitch, A., Poser, S., Pocchiari, M., Hofman, A., and Smith, P. G. (1996). A New Variant Of Creutzfeldt-Jakob-Disease In the UK. Lancet *347*, 921-925.

Williams, A. E., Ryder, S., and Blakemore, W. F. (1995). Monocyte recruitment into the scrapie-affected brain. Acta Neuropathologica *90*, 164-169.

Williams, A. E., Vandam, A. M., Manahing, W. K. H., Berkenbosch, F., Eikelenboom, P., and Fraser, H. (1994). Cytokines, prostaglandins and lipocortin-1 are present in the brains of scrapie-infected mice. Brain Research. *654*, 200-206.

Williams, E., and Young, S. (1980). Chronic wasting disease of captive mule deer: a spongiform encephalopathy. Journal of Wildlife Diseases *16*, 89-98.

Wilson, D. R., Anderson, R. D., and Smith, W. (1950). Studies in scrapie. Journal of Comparative Pathology *60*, 267-282.

Wootton, R. (1995). Introduction to histological image processing. In Image analysis in histology. Coventional and confocal microscopy, R. Wootton, D. R. Springall and J. M. Polak, eds. (Cambridge: Cambridge University Press), pp. 3-18.

Wyatt, J. M., Pearson, G. R., Smerdon, T., Gruffyddjones, T. J., and Wells, G. A. H. (1990). Spongiform encephalopathy in a cat. Vet. Rec. *126*, 513.

Zanusso, G., Liu, D. C., Ferrari, S., Hegyi, I., Yin, X. H., Aguzzi, A., Hornemann, S., Liemann, S., Glockshuber, R., Manson, J. C., Brown, P., Petersen, R. B., Gambetti, P., and Sy, M. S. (1998). Prion protein expression in different species: Analysis with a panel of new mAbs. Proceedings of the National Academy of Sciences of the United States of America *95*, 8812-8816.

Zeidler, M., Johnstone, E. C., Bamber, R. W. K., Dickens, C. M., Fisher, C. J., Francis, A. F., Goldbeck, R., Higgo, R., JohnsonSabine, E. C., Lodge, G. J., McGarry, P., Mitchell, S., Tarlo, L., Turner, M., Ryley, P., and Will, R. G. (1997a). New variant Crutzfeldt-Jakob disease: psychiatric features. Lancet *350*, 908-910.

Zeidler, M., Stewart, G. E., Barraclough, C. R., Bateman, D. E., Bates, D., Burn, D. J., Colchester, A. C., Durward, W., Fletcher, N. A., Hawkins, S. A., Mackenzie, J. M., and Will, R. G. (1997b). New variant Creutzfeldt-Jakob disease: neurological features and diagnostic tests. Lancet *350*, 903-907.

Zigas, V., and Gadjusek, D.C. (1957). Kuru: clinical study of a new syndrome resembling paralysis agitans in the natives of the eastern highlands of Australian New Guinea. Medical Journal of Australia *2*, 745-754.

Zlotnik, I., and Rennie, J.C. (1962). The pathology of the brain of mice inoculated with tissue from scrapie sheep. Journal of Comaprative Pathology *72*, 360.

Zlotnik, I., and Rennie, J.C. (1963). Further observations on the experimental transmission of scrapie from sheep and goats to laboratory mice. Journal of Comparative Pathology *73*, 150-162.